Paleogene integrative stratigraphy, biotas, and paleogeographical evolution of the Qinghai-Tibetan Plateau and its surrounding areas

Jia LIU[1,2*], Ai SONG[1,3], Lin DING[4], Tao SU[1] & Zhekun ZHOU[1,2†]

[1] *CAS Key Laboratory of Tropical Forest Ecology, Xishuangbanna Tropical Botanical Garden, Chinese Academy of Sciences, Mengla 666303, China;*
[2] *State Key Laboratory of Palaeobiology and Stratigraphy, Nanjing Institute of Geology and Palaeontology, Chinese Academy of Sciences, Nanjing 210008, China;*
[3] *Institute of Paleontology, Yunnan University, Kunming 650500, China;*
[4] *State Key Laboratory of Tibetan Plateau Earth System, Environment and Resources (TPESER), Institute of Tibetan Plateau Research, Chinese Academy of Sciences, Beijing 100101, China*

Abstract   The Paleogene is a crucial period when terrestrial and marine ecosystems recovered from major disruptions and gradually approached their modern states. In the Qinghai-Tibetan Plateau and its surrounding regions, the Paleogene also represents a significant phase of tectonic evolution in the Qinghai-Tibetan Plateau-Himalaya orogeny, reorganization of Asian climates, and evolution of biodiversity. Due to limitations in research conditions and understanding, there are still many controversies regarding stratigraphic divisions in the Qinghai-Tibetan Plateau and its surrounding regions. In recent years, extensive studies on sedimentary petrology, magnetostratigraphy, and isotope dating have been conducted in the region. Numerous fossils have been discovered and reported, contributing to a more systematic understanding of biostratigraphy. These studies have laid a solid foundation for the comprehensive investigation of the stratigraphy, biotas and paleogeographic evolution of the Qinghai-Tibetan Plateau and its surrounding regions during the Paleogene. In this paper, we integrate recent research on fossils, isotopic dating, magnetostratigraphy, and geochemistry to refine the stratigraphic divisions and correlation framework of different tectonic units in the region, building upon previous studies. Since the Second Tibetan Plateau Scientific Expedition and Research, the knowledge of Paleogene floras has gradually expanded. This paper discusses the biostratigraphic significance of extinct and newly appeared taxa based on the latest dating results of these plant species. The new understanding of fossil species such as the "*Eucalyptus*" and Arecaceae establishes connections between the Paleogene flora of the Qinghai-Tibetan region and the biotas of Gondwana, specifically Oceania and South America. The evolutionary history of key taxa near the Yarlung Zangbo suture zone indicates that the collision between the Indian and Eurasian plates occurred approximately 65–54 Ma. Paleoelevation reconstructions, based on plant fossils, suggest that the Hengduan Mountain had already formed their current topographic pattern prior to the Early Oligocene. The warm and humid lowlands adjacent to the main suture zones in the Paleogene Qinghai-Tibetan Plateau served as the primary pathway for biota exchanges. The relatively low elevation of the Himalaya during the Paleogene did not effectively block the moisture from the Indian Ocean.

Keywords   Qinghai-Tibetan Plateau, Fossils, Biostratigraphy, Paleoenvironment, Paleogeography, Paleogene

* Corresponding author (email: liujia@xtbg.ac.cn)
† Corresponding author (email: zhouzk@xtbg.ac.cn)

1.   Introduction

The Cretaceous-Paleogene mass extinction event is one of the significant biotic extinction events in Earth's history, with over 75% of species disappearing near this boundary (Raup and Sepkoski Jr, 1982). Subsequently, during the Paleogene period (66–23.03 Ma), both terrestrial and marine ecosystems underwent a recovery (Lyson et al., 2019; Carvalho et al., 2021) and gradually approached their modern status (Ni et al., 2016; Linnemann et al., 2018; Benton et al., 2022; Wu M X et al., 2022).

The term Paleogene was first proposed by German geologist C.F. Naumann in 1866 (Zhang and Li, 2000; Wang Y Q et al., 2019). The stratigraphic units and epochs under the Paleogene have undergone multiple changes, and since 1976, the International Commission on Stratigraphy has divided the Cenozoic Era into the Paleogene, Neogene, and Quaternary (Zhang and Li, 2000; Wang Y Q et al., 2019). In China, the term Old/Early Tertiary has been used in academia (Wang Y Q et al., 2021). In 1999, the China Stratigraphy Committee decided to adopt the classification scheme of the "1989 Global Stratotype Section and Point" of the International Union of Geological Sciences, renaming the Old/Early Tertiary as the Paleogene (Zhang and Li, 2000). With the advancement of global Cenozoic research, the Paleogene is further divided into three series and nine stages based on marine stratigraphy, including the Paleocene with the Danian, Selandian, and Thanetian stages; the Eocene with the Ypresian, Lutetian, Bartonian, and Priabonian stages; and the Oligocene with the Rupelian and Chattian stages (Speijer et al., 2020). Except for the Bartonian stage in the Early Eocene, the Global Stratotype Sections and Point have been established for the remaining eight stages (Speijer et al., 2020).

The Paleogene witnessed a series of significant geological and climatic events. Factors such as the positions and topography of continents, the opening and closing of ocean gateways, and volcanic activity had a profound impact on the climate and environment during the Paleogene (Lyle et al., 2008; Scher et al., 2015; Carvalho et al., 2021). Although the global environment experienced drastic changes during the Cretaceous-Paleogene transition, the climate still maintained a warm pattern similar to the Cretaceous (Westerhold et al., 2020). In the early Paleogene, global temperatures notably increased, followed by a prolonged cooling process that gradually shifted from a greenhouse climate to an icehouse climate (Westerhold et al., 2020). In the Qinghai-Tibetan Plateau and its surrounding regions, the Paleogene period was marked by the collision between the Indian and the Eurasian Plate, leading to the formation and evolution of the Qinghai-Tibetan Plateau-Himalaya orogen, the closure of the Neo-Tethys Ocean, reorganization of the Asian climate, establishment of the modern monsoon system, and in-

tensification of inland arid environments; this period was also crucial for the formation and evolution of the central valley in the plateau and the generation of biodiversity hotspots (Molnar and Tapponnier, 1975; Su et al., 2019a, 2020; Fang et al., 2021; Spicer et al., 2021; Ding et al., 2022; Wu F et al., 2022; Xiong et al., 2022; Zhou et al., 2023).

Early stratigraphic divisions in the Qinghai-Tibetan Plateau and its surrounding regions have primarily relied on biostratigraphy, and significant achievements have been made in stratigraphy and the study of major geological events. However, due to limitations in research conditions and knowledge, there are still many controversies regarding stratigraphic divisions (Hu et al., 2017; Xi et al., 2020; Li J G et al., 2020). In recent years, researchers have conducted extensive work in sedimentary petrology, magnetostratigraphy, isotope dating, and other fields in the Qinghai-Tibetan Plateau and its surrounding regions. They have discovered and reported various types of fossils, further deepening the study of biostratigraphy (Hu et al., 2017; Su et al., 2019b; Xi et al., 2020; Zhou et al., 2023), providing a solid foundation for unraveling the integrative stratigraphy, biotas, and paleogeographic evolution of this region during the Paleogene.

This article, based on lithostratigraphy and biostratigraphy, integrates recent research in isotope dating, magnetostratigraphy, and chemical stratigraphy. It attempts to propose a stratigraphic division and correlation framework for different tectonic units in the Qinghai-Tibetan Plateau and its surrounding regions, building upon previous work (Zhang et al., 2010; Hu et al., 2017; Wang Y Q et al., 2019, 2021; Li J G et al., 2019, 2020; Xi et al., 2020; Li, 2021). The study of marine strata is well-developed, and recent review studies have provided detailed summaries of various fossil groups, comparing them with international standards (Hu et al., 2017; Li et al., 2019; Xi et al., 2020; Li, 2021). On the other hand, in recent years, significant progress has been made in the study of terrestrial strata dating and paleobiology, but a systematic review and summary are yet to be conducted. This article provides a brief introduction to relevant marine strata research, focusing on important terrestrial paleobiota and exploring the Paleogene paleogeographic evolution in the Qinghai-Tibetan region.

2.   Stratigraphic framework

Zhang et al. (2010) systematically compiled geological mapping and published literature related on the Qinghai-Tibetan Plateau and its surrounding regions. Based on basin types, tectonic backgrounds, sedimentary characteristics, biostratigraphy, and chronological studies, they divided the region into five stratigraphic realms: Tarim-Western Kunlun, Qaidam-Qilian-Western Qinling, Qiangtang-Western Si-

chuan, Western Margin of Yangtze, and Gangdise-Himalaya-Ganga (Zhang et al., 2010). These realms were further subdivided into 13 stratigraphic subrealms (Zhang et al., 2010; Figure 1). Apart from the Tarim-Western Kunlun and Gangdise-Himalaya-Ganga stratigraphic realms, which have marine sedimentary deposits during the Paleogene, the other realms are predominantly characterized by terrestrial deposits. The marine strata contain abundant foraminifera, radiolarians, calcareous nannofossils, diatoms, bivalves, and gastropods (Hao and Wan, 1985; Xi et al., 2020). The terrestrial strata are mainly represented by plant fossils (Su et al., 2020; Zhou et al., 2023), pollen (Miao et al., 2016; Li et al., 2019), ostracods (Xia, 1982), fish (Wu et al., 2017), and a small amount of phytoliths (Zhang et al., 2022) have been reported. Mammal fossils are mainly found in the northern, eastern, and southern parts of the plateau (Zong, 1987; Wang et al., 2007; Deng and Ding, 2015; Deng et al., 2021; Ni et al., 2023). Based on the division and subdivision of the tectonic-stratigraphic units by Zhang et al. (2010), as well as recent advancements in biostratigraphy and chronological studies, this article revises and improves the Paleogene stratigraphic framework of the Qinghai-Tibetan Plateau and its surrounding regions.

3. Integrative stratigraphy of the Qinghai-Tibetan Plateau and its surrounding regions in the Paleogene

3.1 Tarim-Western Kunlun stratigraphic realm

The Tarim-Western Kunlun stratigraphic realm is divided into the Tarim and the Western Kunlun-Karakoram stratigraphic subrealm, based on the characteristics of basin types and sedimentary sequences (Figure 2) (Zhang et al., 2010).

3.1.1 Tarim stratigraphic subrealm

In the western region of the Tarim stratigraphic subrealm, marine deposits dominate. It is subdivided, from older to younger, into the Tuyiluoke, Aertashi, Qimugen, Gaijitage, Kalataer, Wulagen, Bashibulake, and Keziluoyi Formations (Zhang et al., 2010; Xi et al., 2020). The Tuyiluoke Formation mainly consists of reddish sandy mudstone and claystone with continental saline marsh and lagoon facies (Yong et al., 1989; Xi et al., 2020). The Cretaceous-Paleogene boundary is generally placed within or above the Tuyiluoke Formation (Hao et al., 2001; Xi et al., 2016). Xi et al. (2020) reviewed the research results of marine biota in the western Tarim Basin, and concluded that fossil preservation in this formation is poor, and current evidence is insufficient to determine the precise location of the boundary. The Aertashi Formation is parallel or at a slight angle of unconformity with the underlying Tuyiluoke Formation. It is characterized by white and grayish-white thick gypsum

layers interbedded with gray and grayish-white marl, chalk, and gypsified chalk. It represents coastal brackish lagoon deposits with few fossils, but shows the early Paleocene age (Xi et al., 2020). The Qimugen Formation represents normal shallow marine deposits, primarily composed of gray-green mudstone interbedded with sandstone and grayish shale. The upper part consists of gray-green and light red marl (Jiang T et al., 2018; Xi et al., 2020). The Qimugen Formation contains abundant foraminifera, calcareous nannofossils, dinoflagellates, and bivalve fossils, dating from the late Paleocene to the early Eocene (late Selandian to early Ypresian) (Lan and Wei, 1995; Yang et al., 1995; Cao et al., 2018; Jiang T et al., 2018; Xi et al., 2020). It also exhibits the characteristic calcareous nannofossil *Rhomboaster-Discoaster* assemblage and negative carbon isotope excursion associated with the Paleocene-Eocene Thermal Maximum (Cao et al., 2018). The zircon U-Pb dating of volcanic ash at the base of the Qimugen section is 57.58±0.49 Ma (Zhang S et al., 2018). The Gaijitage Formation primarily consists of intertidal facies reddish mudstone, claystone interbedded with gray-green mudstone and gypsum layers (Xi et al., 2020). It contains early Eocene shallow-water benthic foraminifera assemblages, including *Nonion-Cibides-Anomalinoides* (Hao et al., 1982), as well as ostracods such as *Cytheridea aspera* and *Haplocytheridea* (Yang et al., 1995), and bivalve fossils (Xi et al., 2020). The Kalataer Formation is in conformable contact with the underlying Gaijitage Formation. The lower part consists of a small amount of gray-green mudstone, while the upper part is primarily composed of gray limestone or marl with oyster shells, indicating a carbonate platform depositional environment (Xi et al., 2020). The foraminiferal assemblages are similar to those of the Gaijitage Formation (Hao et al., 1982), and common ostracods include *Cytheridea* and *Cytherura* (Yang et al., 1995). The gastropod fossils indicate an early Middle Eocene Lutetian stage, specifically the *Ostrea* (*Turkostrea*) *strictiplicata-O.* (*T.*) *cizancourt* assemblage (Bosboom et al., 2014a; Xiong, 2019). The Wulagen Formation represents open carbonate platform and coastal sedimentation (Xi et al., 2020). The lower part is primarily composed of gray-green mudstone with thin layers of bioclastic limestone, while the upper part consists of gray-green and dark red mudstone interbedded with fine sandstone and gypsum layers (Xi et al., 2020). The foraminifera (Fan, 2018; Xi et al., 2020), ostracods (Yang et al., 1995), dinoflagellate assemblages, and calcareous nannofossil zone NP16 (Xi et al., 2020) indicate a middle to late Middle Eocene age. The bivalve assemblage *Sokolowia buhsii-Kokanostrea kokanensis* corresponds to the late Middle Eocene of the regional Turkestan stage in Central Asia (Bosboom et al., 2014a; Xiong, 2019). The Bashibulake Formation is mainly distributed in the foreland of the Tianshan Mountain and represents bay-lagoon deposition. It is characterized by purplish-red, reddish-gray
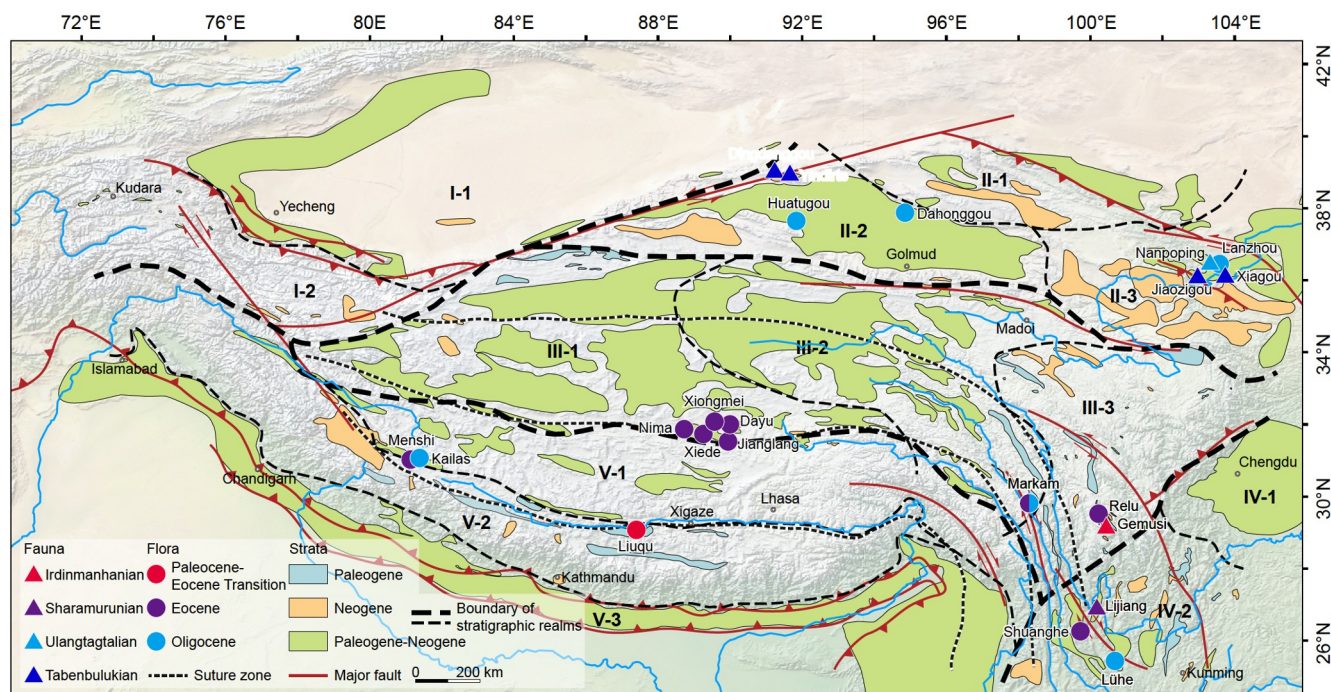
Figure 1 Distribution and stratigraphic realms of Cenozoic basins in the Qinghai-Tibetan Plateau and its surrounding regions (modified from Zhang et al., 2010), as well as the locations of Paleogene flora and fauna. I Tarim-Western Kunlun stratigraphic realm: I-1, Tarim stratigraphic subrealm; I-2, Western Kunlun-Karakoram stratigraphic subrealm. II Qaidam-Qilian-Western Qinling stratigraphic realm: II-1, Jiuquan-Zhangye stratigraphic subrealm; II-2, Qaidam stratigraphic subrealm; II-3, Lanzhou-Xining stratigraphic subrealm. III Qiangtang-Western Sichuan stratigraphic realm: III-1, Qiangtang stratigraphic subrealm; III-2, Hoh Xil-Yushu stratigraphic subrealm; III-3, Western Sichuan-Eastern Xizang stratigraphic subrealm. IV Western Margin of Yangtze stratigraphic realm: IV-1, Chengdu stratigraphic subrealm; IV-2, Western Yunnan stratigraphic subrealm. V Gangdise-Himalaya-Ganga stratigraphic realm: V-1, Gangdise stratigraphic subrealm; V-2, Yarlung Zangbo-Himalaya stratigraphic subrealm; V-3, Ganga stratigraphic subrealm.

mudstone, siltstone interbedded with gray-green siltstone, mudstone, and gypsum layers, with a thick gypsum layer at the base (Xi et al., 2020). The age of the Bashibulake Formation is determined as the Bartonian-Priabonian of the Eocene (Bosboom et al., 2014a), but it does not exclude the possibility of the uppermost part extending into the early Rupelian of the Oligocene (Zhang, 2017; Xi et al., 2020). The deposition of the Wulagen and Bashibulake Formations in the Tarim Basin coincided with the Tethys regression event, which has received significant attention. Numerous studies have been conducted on sedimentary facies, biostratigraphy, and magnetostratigraphy, revealing differences in the depositional ages of the highest marine strata (e.g., Bosboom et al., 2011, 2014b; Sun et al., 2016). The seawater diachronous retreat from the Tarim Basin (Sun et al., 2016). The Keziluoyi Formation is in parallel unconformable or slightly angular unconformable contact with the underlying Bashibulake Formation. It is primarily composed of terrestrial purplish-red sandstone, calcareous mudstone, dark red mudstone interbedded with gray-green sandstone, and thin layers of gypsum. It contains ostracods such as *Cyprideis*, *Daruwinula*, *Hemicyprideis*, *Hemicyprinotus*, and *Mediocypris* (Zhang et al., 2010). The age of the Bashibulake Formation is assigned to the Oligocene to early Miocene (Xi et al., 2020).

In the Shache Basin, the Paleogene is primarily characterized by terrestrial deposition, and its stratigraphic division is similar to that of the Western Tarim Basin. The strata in this basin contain abundant pollen fossils (Wang et al., 1986). In the early to middle Paleocene Aertashi Formation, the pollen assemblage is dominated by *Classopollis*, and there is a significant presence of angiosperm species closely related to modern plants (Wang et al., 1986). Normapolles pollen is commonly found, including *Nudopollis*, *Trudopollis*, *Oculopollis*, and *Extratriporopollenites* (Wang et al., 1986). In the late Paleocene to early Eocene, the pollen assemblage of the Qimugen Formation is dominated by angiosperm pollen from the Fagaceae, with a higher content of pollen associated with the Ulmaceae, Betulaceae, and Juglandaceae (Wang et al., 1986). Normapolles and *Proteacidites* still play an important roles in the assemblage (Wang et al., 1986). In the early Eocene, the pollen assemblage of the Gaijitage Formation shows a significant increase in tropical and subtropical components; Normapolles pollen is virtually absent, and common Paleogene genera such as *Sapotaceoidaepollenites*, *Beaupreaidites*, and *Proteacidites* are reduced; the content of drought-tolerant *Ephedripites* pollen increases (Wang et al., 1986). In the middle Eocene, the Kalataer Formation is dominated by pollen from tropical and subtropical genera such as *Rutaceoipollis*, *Symplocoipolle-*

Figure 2　Stratigraphic comparison between the Tarim-West Kunlun stratigraphic realm and the Gangdise-Himalaya-Ganga stratigraphic realm (based on Hu et al., 2017 and Xi et al., 2020).

nites, and *Engelhardtioipollenites* (Wang et al., 1986). In the middle Eocene, the pollen assemblage of the Wulagen Formation is characterized by dominant genera such as *Quercoidites* and *Meliaceoidites*; the diversity of tropical and subtropical components increases; such as *Pentapollenites*, commonly found in the Paleocene, are occasionally observed (Wang et al., 1986). In the late Oligocene to early Miocene, the pollen assemblage of the Bashibulake Formation is characterized by a high diversity and abundance of drought-tolerant *Ephedripites*; the dominant pollen remains *Quercoidites*, while the tropical and subtropical components decrease; the content of herbaceous taxa such as *Chenopodipollis* increases (Wang et al., 1986). In the Oligocene, the lower part of the Kiziluoyi Formation has a pollen assemblage dominated by *Pinus*, *Piceapollis*, and *Ephedripites*; *Quercoidites* and *Ulmipollenites* are commonly observed (Wang et al., 1986).

In the Kuqa Basin, the Paleogene strata are primarily characterized by alternating deposition of bay-lagoon facies. During the Oligocene, the depositional environment gradually shifted from a mixed marine-continental salt lake facies to an inland salt lake depositional environment (Sun et al., 1999). The Paleogene is divided into the Talake Formation (Paleocene), Xiaokuzibai Formation (Eocene), and Suweiyi Formation (Oligocene), which preserve abundant pollen and a small amount of charophyte fossils (Sun et al., 1999). In the lower part of the Talake Formation, the pollen assemblage is characterized by a high content of *Schizaeoisporites*, accounting for approximately 18% of the assemblage; *Ephedripites* and *Parcisporites* represent 26% and 16% of the assemblage, respectively; angiosperm pollen is dominated by *Ulmipollenites* and *Quercoidites*, with frequent occurrences of *Proteacidites* and Normapolles (Wang et al., 1986). In the middle part of the Talake Formation, gymnosperm pollen increases significantly, while the abundance of angiosperm pollen, including *Ulmipollenites*, *Quercoidites*, and Normapolles, decreases; a large number of marine planktonic algae are also observed (Wang et al., 1986). In the upper part of the Talake Formation, the abundance of *Polypodiaceoisporites* is high, while gymnosperm pollen decreases; there is an increase in the diversity and abundance of Normapolles (Wang et al., 1986). In the upper part of the Xiaokuzibai Formation, the genus *Taxodiaceaepollenites* increases to 13%; the dominant angiosperm family is Fagaceae, and tropical and subtropical components such as *Retitricolpites*, *Rutaceoipollis*, and *Sapotaceoidaepollenites* are common, with occasional occurrences of Normapolles (Wang et al., 1986). In the Suweiyi Formation, all Normapolles disappear, and there is a significant decrease in tropical components; drought-tolerant herbaceous taxa, such as *Chenopodipollis*, appear (Wang et al., 1986). The Paleogene strata also yield charophyte fossils including *Maedlerisphaera chinensis*, *Sphaerochara minuscula*, *Charites* sp.,

Gyrogona sp., and *Obtusochara* sp. (Zhao, 2011).

3.1.2 Western Kunlun-Karakoram stratigraphic subrealm

The Western Kunlun-Karakoram stratigraphic subrealm mainly includes the Yarkant River and the Tianshuihai-Aksayqin Lake Basins, which are two intermountain depression sag-faulted basins (Zhang et al., 2010). In the Paleogene, this region experienced significant uplift, resulting in the erosion of the Paleogene Kashgar Group. The Kashgar Group is sporadically distributed only in the areas north of Kudara, Longmu Co, and south of Mahuangshan. The predominant sedimentary environments are alluvial fan deposits from mountain front rivers and debris flow fans, with some areas exhibiting a coastal bay-lagoon environment. The Kashgar Group, named after its occurrence near Wuqia County, has a stratigraphic division consistent with that of the Tarim Basin. It is divided from bottom to top into the Aertashi Formation, Qimugen Formation, Gaijitage Formation, Kalataer Formation, Wulagen Formation, and Bashibulake Formation (Xinjiang Uygur Autonomous Region Regional Stratigraphic Compilation Group, 1981). However, research on the Kashgar Group in this stratigraphic subrealm is limited, with only a few reports of marine fossils such as *Nummulites* (Xi et al., 2020). Recent research suggests that the Tielongtan Group is the latest marine stratum in the Western Kunlun region (Gao et al., 2023). Planktonic foraminifera indicate that the end of deposition age is no earlier than 76–66 Ma (Gao et al., 2023).

3.2 Qaidam-Qilian-Western Qinling stratigraphic realm

The Qaidam-Qilian-Western Qinling stratigraphic realm is divided into three subrealms based on the characteristics of basin types and sedimentary sequences. These subrealms are the Jiuquan-Zhangye, Qaidam, and Lanzhou-Xining stratigraphic subrealms (Figure 3) (Zhang et al., 2010).

3.2.1 Jiuquan-Zhangye stratigraphic subrealm

In the Jiuquan-Zhangye stratigraphic subrealm, the Paleogene sequence in the Jiuquan Basin is relatively complete. It is divided from bottom to top into the Eocene Huoshaogou Formation and the Oligocene Baiyanghe Formation. The depositional age of the Huoshaogou Formation is determined to be 40.2–33.4 Ma based on magnetostratigraphy and mammalian fossil researche (Dai et al., 2005), while the Baiyanghe Formation is dated to 31–24 Ma (Song, 2006). The Huoshaogou Formation unconformably overlies the underlying Cretaceous Xinminbao Group or Chijinbao Formation and mainly represents piedmont-fluvial-lacustrine deposition. The lithology consists of conglomerate, reddish-orange and white sandstone, mudstone interbedded with conglomerate, conglomeratic sandstone, and fine conglom-

Figure 3 Stratigraphic comparison among the Qaidam-Qilian-Western Qinling stratigraphic realm, the Qiangtang-Western Sichuan stratigraphic realm and the western margin of Yangtze stratigraphic realm.

erate (Dai et al., 2005; Song, 2006; Zhang et al., 2010). The pollen assemblages of the Huoshaogou Formation are dominated by *Ephedripites*, *Chenopodipollis*, and *Nitrariadites* (Ma, 1993). The assemblages also contain a large number of bisaccate pollen grains from the Pinaceae, which overall represent the dry and hot vegetation landscape of the northern subtropical desert-semidesert (Miao et al., 2008). The Oligocene Baiyanghe Formation primarily consists of fan-delta and shallow-lake facies with intercalated salt lake deposits (Dai et al., 2005). It is in parallel unconformity or angular unconformity contact with the underlying Huoshaogou Formation (Dai et al., 2005). The main lithology includes red, reddish-brown conglomeratic sandstone, sandstone, and mudstone interbedded with gypsum layers (Dai et al., 2005). The Baiyanghe Formation yields mammalian fossils such as *Mimolagus rodens*, *Anagalopsis kansuensis*, *Tataromys grangeri*, *T. sigmoden*, *Leptotataromys minor*, *Parasminthus* cf. *asiae-centralis*, *P. tangingili*, *P. parvulus*, *Eucricetodon asiaticus*, *Desnatolagus* sp., *Sinolagomys*? sp., and *Amphechinus* sp. (Dai et al., 2005; Song, 2006; Miao et al., 2008). It is a typical Tabenbulukian fauna and can be correlated with the Paoniuquan Formation in the Danghe-Xorkol Basin (Wang B Y et al., 2003; Wang Y Q et al., 2019). The Neogene Shulehe Formation unconformably overlies the Baiyanghe Formation (Song, 2006).

3.2.2   Qaidam stratigraphic subrealm

The Qaidam stratigraphic subrealm includes three basins: the Qaidam Basin, the Danghe-Xorkol Basin, and the Ayakkum Lake Basin.

In the Qaidam Basin, the Paleogene sequence is divided from bottom to top into the Lulehe Formation, Xiaganchaigou Formation, and Shangganchaigou Formation. Magnetostratigraphy studies indicate that the depositional ages of these three formations are 52–44.2 Ma, 44.2–34.2 Ma, and 34.2–23 Ma, respectively (Sun et al., 2005; Ji et al., 2017; Zhang, 2021). However, different researchers have different interpretations regarding the depositional sequences, ages and boundaries between these formations (Nie et al., 2020; Wang W et al., 2022). The Lulehe Formation is unconformably overlain by the underlying strata. It is primarily composed of purple-red conglomerates interbedded with sandstones, along with siltstones and mudstones. During its early stage, the depositional environment was dominated by piedmont alluvial fan and fluvial sediments. In the middle stage, it transitioned to a marginal shallow lake and delta front environment, while in the late stage, it represented delta plain sedimentation. The Lulehe Formation contains a charophyte assemblage of *Sphaerochara parvula-Aclistocahara nuguishanensis* (Ma, 2014). The presence of ostracods is limited and characterized by the *Candon-Candoniella-Ilyocypris* assemblage (Zhang, 2021). The

pollen assemblage is dominated by *Quercoidites*, *Chenopodipollis*, and *Nitrariadites* (Lu et al., 2010). The Xiaganchaigou Formation is mainly composed of reddish-brown mudstone interbedded with silty sandstone in the western part of the basin. In the eastern part, it consists of yellow-green and gray-white conglomerates, gravelly sandstones, and purple-red sandy mudstones. Ostracods in this formation include *Austrocypris* sp., *Eucypris mutilis*, *Cyprinotus giganto-triangulatus*, and *Qaibeigouia reniformis*, which belong to the late Eocene-early Oligocene (Sun et al., 2005). The lower part of the formation contains a charophyte assemblage of *Croftiella shimenqiaoensis-Obtusochara jianglingensis*, while the upper part contains *Maedlerisphaera chinensis-Grovesichara yangii* (Ma, 2014). The lower part of the Xiaganchaigou Formation has a pollen assemblage dominated by the assemblage of *Quercoidites-Piceapollis-Nitrariadites*, while the middle-upper part is characterized by *Ephedripites-Qinghaipollis-Nitrariadites* (Lu et al., 2010). The Shangganchaigou Formation exhibits lithological similarities with the Xiaganchaigou Formation. The charophyte fossils are similar to those found in the upper part of the Xiaganchaigou Formation (Ma, 2014). The pollen assemblage is characterized by *Ephedripites-Chenopodipollis-Nitrariadites* (Lu et al., 2010). Ostracods from this formation include *Hemicyprinotus* sp., *H. valvaetumidus*, *Mandelstam*, *Mediocypris*, *Candonaeformis*, and *Cyprinotus*, which belong to the Oligocene-early Miocene (Sun et al., 1999; Sun et al., 2005; Zhang, 2021). In the Huatugou area, the lower part of the Shangganchaigou Formation (early Early Oligocene) contains rich plant fossils known as the Huatugou flora, which includes abundant *Podocarpium* (Yan et al., 2018). Fossilized fruits of *Ailanthus confucii* and leaves of the *Ailanthus* sp. were also reported in the same layer (Yang et al., 2021a), along with the discovery of the fish *Paleoschizothorax qaidamensis* (Yang et al., 2021b). In the Dahonggou area, the upper part of the Shangganchaigou Formation (30.8 Ma) contains a flora known as the Dahonggou flora, dominated by *Populus* sp. and *Podocarpium podocarpum*, with occurrences of *Glyptostrobus* sp. and *Cyclocarya* sp., etc. (Han et al., 2020; Song et al., 2020). In the Lulehe area, the Shangganchaigou Formation has yielded fish fins, teeth, and bones belonging to Cyprinidae and Barbinae, known as the Lulehe fish fauna (Wang et al., 2007).

In the Danghe-Xorkol Basin, the Paleogene exhibit distinct lithological differences from the neighboring Hexi Corridor Basin, specifically the Huoshaogou Formation and Baiyanghe Formation (Wang B Y et al., 2003). Wang B Y et al. (2003) designated a set of reddish-brown mudstone, sandy mudstone, and conglomerate-dominated strata on the northern margin of the Danghe South Mountain as the Paoniuquan Formation. The lower and upper boundaries of the Paoniuquan Formation are through faults contact with the

Precambrian and Middle Miocene Tiejianggou Formation, respectively (Wang B Y et al., 2003). The lower part of the Paoniuquan Formation yields the Dingdanggou fauna from the late Early Oligocene, including taxa such as *Desmatolagus gobiensis*, *D. pusillus*, *Tataromys* cf. *sigmodon*, *Cyclomylus* sp., *Amphechinus*? sp., *Sivameryx* cf. sp., *Phyllotillon* sp., *Aprotodon*? sp., etc. (Wang B Y et al., 2003). The Paoniuquan Formation also yields the Yindirte fauna, which representing a typical Late Oligocene Tabenbulukian assemblage (Wang B Y et al., 2003; Wang Y Q et al., 2019). In the Xorkol Basin, an unnamed stratum of red mudstone interbedded with calcareous nodules and paleosols was discovered. Paleomagnetic dating suggests an age range of 51–39 Ma (Li J X et al., 2018). In the upper part of this formation, fossils of middle Eocene small mammal, *Yuomys altunensis*, have been found (Li J X et al., 2018).

In the Ayakkum Lake Basin, the lower part of the Shimagou Formation is composed of shallow gray and light brown sandstone, coarse-grained sandstone with gravel, and reddish-brown calcareous siltstone, which are interbedded with reddish-brown calcareous silty mudstone. The upper part consists of interbedded reddish-brown calcareous sandstone and calcareous silty mudstone, with lenses of sandstone and conglomerate (Zhang et al., 2010). The lower part of the Shimagou Formation represents alluvial fan and fluvial deposits, while the upper part represents deltaic deposits. Fossils, including the ostracods (*Eucypris paraserrata* and *E. mutilis*) and pollen, indicate a sedimentary age of the Oligocene (Zhang et al., 2010).

In the Kumkol Basin, the lower part of the Shimagou Formation (equivalent to the Huatiaoshan Formation) may have started depositing in the Oligocene (Li Q et al., 2020). The gray-green silty mudstone of the Shimagou Formation contains ostracods such as *Eucypris paraserrata*, *E. mutilis*, *E.* cf. *lenghuensis*, *Limnocythere* cf. *hubeiensis*, *Qaibeigouia reniformis*, *Cyprinotus reniformis*, *C. subquadratus*, *Candona bicompressa*, *Candoniella* sp., etc. (Zhang et al., 1996). The dominant ostracod genera are *Cyprinotus* and *Eucypris*, indicating an age of the Oligocene (Zhang et al., 1996). Fossil evidence of small mammals and magnetostratigraphy at the top of the Shimagou Formation suggest an age around the late Middle Miocene, approximately 12.5 Ma (Li Q et al., 2020). The lower part of the Shimagou Formation contains pollen assemblage of *Chenopodipollis-Tubulifloridites-Pinus* (Xiao et al., 2003).

3.2.3 *Lanzhou-Xining stratigraphic subrealm*

The Paleogene strata of the Lanzhou-Minhe Basin are divided from bottom to top into the Xiliugou Formation, Yehucheng Formation, and Xianshuihe Formation. Through studies of paleomagnetism and mammal fossils, the deposition ages of the Xiliugou Formation were determined to be late Paleocene to early Early Eocene (58–51 Ma), the Ye-

hucheng Formation to be late Early Eocene to early Oligocene (51–31.5 Ma), and the Xianshuihe Formation to be early Oligocene to early Miocene (31.5–20 Ma) (Yue et al., 2001). The Xiliugou Formation consists of brick-red conglomerates and sandstone at the basin margin, transitioning to brick-red blocky sandstones interbedded with mudstones, representing a deltaic to lacustrine deposition in the central basin (Yue et al., 2001). The Yehucheng Formation is characterized by purple-red mudstones, siltstones, and sandstone interbeds with abundant gypsum layers (Xie, 2004). The lower part of the Xianshuihe Formation consists of yellow sandstones interbedded with lacustrine clays, while the middle and upper parts represent Neogene deposits (Yue et al., 2001). The lower part of the Xianshuihe Formation contains ostracods, fish, amphibians, charophytes, and plants (Geng et al., 2001). Among the plant fossils, *Populus* is the dominant genus (Geng et al., 2001). The presence of *Rhus turcomanica* in the fossil flora indicates that the deposition age is middle to late Paleogene (Geng et al., 2001). The lower part of the Xianshuihe Formation yields the Nanpoping fauna, which includes various records such as *Desmatolagus pusillus*, Ochotonidae indet., *Ordolagus teilhardi*, Aplodontidae indet., *Tsaganomys altaicus*, *Tataromys plicidens*, *Tataromys sigmodon*, *Tataromys minor*, *Eucricetodon asiaticus*, *Parasminthus tangingoli*, *Parasminthus parvulus*, *Yindirtemys grangeri*, *Bounomys bohlini*, *Bounomys ulantatalensis*, *Monosaulax* sp., *Anomoemys lohiculus*, *Karakoromys* sp., *Steneofiber* sp., *Allacerops* cf. *turgaica*, *Paraceratherium huangheense*, *Schizotherium ordosium*, *Aprotodon lanzhouensis*, and *Paraentelodon* sp. In the upper of the lower part of Xianshuihe Formation, the red mudstones yield the Xiagou fauna, which includes *Amphechinus* sp., *A.* cf. *rectus*, *A.* cf. *minimus*, Soricidae indet., *Desmatolagus* cf. *gobiensis*, *Ordolagus* sp., *Sinolagomys kansuensis*, *S.* cf. *major*, *Tsaganomys altaicus*, Tataromyindae indet., *Tataromys plicidens*, *Tachyoryctoides* sp., *Eucricetodon* sp., *Heterosminthus lanzhouensis*, *Parasminthus* sp., *P. asiaecentralis*, *P. tangingoli*, *P. parvulus*, *Sinosminthus* sp., *Yindirtemys xiningensis*, *Y. ambiguous*, *Y. grangeri*, *Litodonomys huangheensis*, *Didymoconus berkeyi*, and *Aprotodon* sp. (Qiu and Wang, 1999; Xie, 2004; Zhang P et al., 2016, 2018). The ages of the Nanpoping fauna and Xiagou fauna are constrained to approximately 31–30 Ma and 26–25 Ma, respectively, based on magnetostratigraphic results (Zhang P et al., 2018).

In the Xining Basin, the Paleogene is divided from bottom to top into the Qijiachuan Formation, Honggou Formation, Mahalagou Formation, and Xiejia Formation. Integrated studies of stratigraphy, paleontology, and geochronology indicate that the deposition ages of these formations are approximately 54.0–51.8 Ma for the Qijiachuan Formation, 51.8–43.0 Ma for the Honggou Formation, 43.0–34.0 Ma for the Mahalagou Formation, and 34.0–24.0 Ma for the Xiejia

Formation (Fang et al., 2019). The Qijiaquan Formation mainly consists of alluvial fan and fan-delta to shallow lake deposits. At the basin margins, it is characterized by alluvial fan and fan-delta with interbedded conglomerate and sandstone deposits. In the central part of the basin, the lower part contains pebbly to coarse sandstones, while the middle to upper part consists of mudstone and gypsum, indicating shallow lake sedimentation as the primary environment. The pollen assemblage in the lower part of Qijiachhuan Formation is dominated by angiosperms, with high content of Ulmaceae pollen, and small content of Normapolles and *Schizaeoisporites*; in the upper part, the content of *Ephedripites* increases, and a significant amount of *Polypodiaceaesporites* occurs sporadically in some layers (Sun et al., 1980). The Honggou Formation exhibits conglomerate, sandstone, and gypsum-bearing rocks at the basin margins, while mudstone intercalated with gypsum dominates in the central part of the basin. The Honggou Formation lacks Normapolles, while tricolpate and tricolporate type pollen are abundant; the upper part of the formation shows an increase in *Ephedripites* content (Sun et al., 1980). The Mahalagou Formation in the Xining Basin consists of intercalations of clayey mudstone, mudstone with gypsum, conglomerate at the basin margins. In the central part of the basin, it is characterized by interbedded mudstone and gypsum. The deposition environment of the formation can be divided from the basin center to the margin into saline deep lake, saline shallow lake, lacustrine, and alluvial fan deposition. The pollen assemblage of the Mahalagou Formation is dominated by *Ephedripites* and *Nitrariadites*, and there is a sudden increase in the content of *Piceapollis* and *Abiespollenites* pollen in the late Eocene (36.6 Ma) (Dupont-Nivet et al., 2008; Abels et al., 2011; Hoorn et al., 2012). The Xiejia Formation is characterized by alternating beds of sandy mudstone and clayey gypsum intercalations in its lower part, with lenses of conglomerate at the base. The upper part is composed of brownish-yellow, sandy, and calcareous mudstone. It represents a transition from saline to freshwater lacustrine environment (Dai et al., 2006). The upper part of the Xiejia Formation is known for the Xiejia fauna (Li et al., 1980), and its age has been revised to the late Oligocene, approximately 25 Ma (Fang et al., 2019). In the Linxia Basin, the Paleogene is represented by the Tala Formation and Jiaozigou Formation (Qiu et al., 2004). The lower part of the Tala Formation consists of fluvial deposits of purple-red conglomerate; the middle part is primarily composed of fluvial-lacustrine purple-red sandstone and interbedded mudstone; the upper part is characterized by lacustrine purple-red mudstone, which contains fossils of bivalves and tree trunks (Fang et al., 1997). The lower part of the Jiaozigou Formation is composed of conglomerate, while the upper part is dominated by purple-red mudstone of fluvial-lacustrine facies (Deng, 2004). The conglomerates at the

base of the Jiaozigou Formation contain a significant assemblage of giant rhinoceros fauna, represented by *Dzungariotherium orgosense* (Deng, 2004; Deng et al., 2021). Other known species include *Tsaganomys altaicus*, *Megalopterodon* sp., *Schizotherium ordosium*, Hyracodontidae indet., *Ardynia altidentata*, *A*. sp., *Aprotodon lanzhouensis*, *Paraentelodon macrognathus*, *Allacerops* sp., *Paraceratherium linxiaense*, *Ronzotherium* sp., *Aprotodon lanzhouensis*, and others (Deng, 2004; Qiu et al., 2004; Qiu et al., 2023). The pollen assemblages indicate a sparse woodland and steppe environment, dominated by herbaceous taxa such as *Chenopodipollis*, Polygonaceae, and Asteraceae, and the common tree species include Cupressaceae, *Quercoidites*, *Betulaepollenites*, and *Fraxinoipollenites* (Ma et al., 1998). The Tala Formation and Jiaozigou Formation are assigned to the Oligocene (Fang et al., 2003; Qiu et al., 2004; Fang et al., 2016). The most recent magnetostratigraphic and mammalian biostratigraphic studies have revised the ages of the Tala Formation and Jiaozigou Formation to approximately 33.8–31.0 Ma and 27.0–22.5 Ma, respectively (Sun et al., 2023). There may be a sedimentary hiatus of approximately 4 Ma between the Tala Formation and Jiaozigou Formation, and the age of the Jiaozigou *Paraceratherium* fauna is estimated to be around 27 Ma (Sun et al., 2023) or 29 Ma (Zheng et al., 2023). Recently, the strata, which dominated by red coarse clastic conglomerates and sandstones, have also been discovered in the western part of the Linxia Basin (Feng et al., 2022). The strata represent the oldest Paleogene strata found in the Basin. Although no mammalian fossils have been found, lithology and sedimentary facies can be compared with those of neighboring Guide and Lanzhou Basins (Feng et al., 2022). Magnetostratigraphic studies have constrained the lower part of the strata to an approximate depositional age of 54–40 Ma (Feng et al., 2022).

The eastern part of the Xunhua-Hualong Basin is connected to the contemporaneous Linxia Basin during the Paleogene. The Paleogene strata in this region are represented by the Tala Formation (Zhang et al., 2013). The Tala Formation is in angular unconformity contact with the underlying formations and represents a fluvial-alluvial fan depositional environment. The lower part of the Tala Formation consists of thick layers of medium to coarse conglomerates interbedded with pebbly sandstones; in the middle part, conglomerates decrease, and alternations of conglomerates and sandstones are observed; the upper part consists of fine-grained sandstones interbedded with purple mudstones (Zhang et al., 2013), with occasional gypsum layers (Lease et al., 2012). The Tala Formation yields abundant pollen fossils in the mudstone layers, and the common genera include *Pinuspollenites*, *Piceapollis*, *Ephedripites*, *Chenopodipollis*, and Asteraceae (Luo et al., 2010). The lower part of the Tala Formation is characterized by a pollen assemblage of Pinaceae-*Chenopodipollis*-*Nitrar-*

iadites-*Ephedripites*, indicating a sparse shrub-grassland environment; the upper part of the formation is characterized by a pollen assemblage of Pinaceae-*Chenopodipollis*-*Nitrariadites*-*Ephedripites*-*Quercoidites*, with an increased representation of broad-leaved trees, represented by *Quercoidites*, suggesting a transition to a forest-steppe environment (Xu, 2015).

In the Guide Basin, the Paleogene is divided into the Gepiza Formation and the Xiagarang Formation from bottom to top (Song, 2006). The Gepiza Formation is equivalent to the Xining Group and is in angular unconformity contact with the underlying formations. Regionally, it can be correlated with the Qijiachuan Formation in the Xining Basin and the Xiliugou Formation in the Lanzhou Basin (Song, 2006). The lithology of the Gepiza Formation is predominantly reddish-brown conglomerates, sandstones, and siltstones (Song, 2006). The Xiagarang Formation is conformably overlain by the Gepiza Formation and is unconformably overlain by the Middle Miocene Guidemen Formation (Song, 2006). The lower part of the Xiagarang Formation consists of thick layers of purple mudstone interbedded with yellow-brown siltstone; the middle part contains purple mudstone interbedded with bluish-gray mudstone, grayish-green sandstone, and gypsum layers; the upper part consists of thick layers of purple mudstone with thin interbeds of mudstone and sandstone (Song, 2006).

3.3   Qiangtang-Western Sichuan stratigraphic realm

The Qiangtang-Western Sichuan stratigraphic realm includes the Qiangtang stratigraphic subrealm, the Hoh Xil-Yushu stratigraphic subrealm, and the Western Sichuan-Eastern Xizang stratigraphic subrealm (Figure 3) (Zhang et al., 2010).

3.3.1   Qiangtang stratigraphic subrealm
In this subrealm, the Paleogene is generally referred to as the Niubao Formation, the Dingqinghu Formation (also known as the Dingqing Formation), the Kangtuo Formation, and the Suonahu Formation.

In the Lunpola Basin, the lower part of the Niubao Formation is predominantly composed of reddish-brown sandstone and conglomerate, while the middle and upper parts are dominated by gray and grayish-green mudstone, interbedded with mudstone, oil shale, and tuffaceous limestone (Ma et al., 2013). The middle to upper parts of the Niubao Formation contain ostracod assemblages of *Cypris*-*Limnocythere* and *Cypris*-*Candona* (Xia, 1982), as well as a charophyte assemblage of *Obtusochara jingzhouensis*-*Grambastichara tornata* (Xia, 1986). The lower part of the Niubao Formation is characterized by a pollen assemblage dominated by tricolpate and tricolporate angiosperm pollen, with high diversity; gymnosperms are represented mainly by *Ephedripites*, while Pinaceae pollen is extremely rare (Song

and Liu, 1982). The upper part of the Niubao Formation has a similar pollen assemblage to the lower part but with an increased abundance of Pinaceae pollen and the presence of *Chenopodipollis* (Song and Liu, 1982). The mudstone and shale of the middle part of the Niubao Formation have yielded abundant plant, insect, and fish fossils. Some reported fossil species include *Sabalites tibetensis* (Su et al., 2019a), *Koelreuteria lunpolaensis* (Jiang et al., 2019; Chen et al., 2022), *Limnobiophyllum pedunculatum* (Low et al., 2019), *Ailanthus maximus* (Liu et al., 2019), *Cedrelospermum tibeticum* (Jia et al., 2019), *Eoanabas thibetana* (Wu et al., 2017), *Aquarius lunpolaensis* (Cai et al., 2019), and a large number of plant thorn fossils (Zhang et al., 2022). This fossil flora is referred to as the Dayu flora (Liu et al., 2019; Su et al., 2019a) and is dated to the late Eocene, approximately 39 Ma (Fang et al., 2020; Xiong et al., 2022). In the western part of the Lunpola Basin, the late Eocene Xiongmei flora has also been discovered, and the fossilized fruits of *Podocarpium tibeticum* have been reported (Li et al., 2022). Biostratigraphic, magnetostratigraphic, and isotopic dating results indicate that the deposition age of the Niubao Formation is from the Eocene to the early Oligocene, approximately 50–29 Ma (Han et al., 2019; Fang et al., 2020; Xiong et al., 2022). The Dingqinghu Formation is mainly composed of lacustrine grayish-green mudstone interbedded with oil shale, mudstone, and tuffaceous limestone, with lower and upper parts characterized by red mudstone and paleosols. The lower part of the Dingqinghu Formation contains ostracod assemblages of *Austrocypis*-*Cyprinotus* and *Ilyocypris*-*Limnocythere* (Xia, 1982), and the pollen assemblage includes *Pinuspollenites*-*Ephedripites*-*Chenopodipollis*-*Quercoidites* (Sun et al., 2014; Xie et al., 2021a). Plant, insect, and fish fossils have been reported, including *Marsilea* sp. (Xie et al., 2021b) and *Aquarius lunpolaensis* (Cai et al., 2019). Based on the combined evidence of animal and plant fossils, paleomagnetic data, and zircon U-Pb dating of volcanic ash, the lower part of the Dingqinghu Formation is interpreted to be from the late Early Oligocene (Sun et al., 2014; Fang et al., 2020; Xiong et al., 2022).

In Bangor Basin, the Dingqinghu Formation is absent, and the Paleogene is represented by the Niubao Formation, mainly distributed along the northern margin of the basin. The lithology mainly consists of purple-red coarse clastic rocks, with interbedded grayish-blue, brownish-yellow mudstones, siltstone, and sandstone in the middle part. The middle part of the Niubao Formation in the Bangor Basin is rich in plant, insect, and fish fossils. Bai et al. (2017) first reported some plant fossils. Currently, several plant fossils have been systematically identified and published, including *Ailanthus maximus* (Liu et al., 2019), *Lagokarpos tibetensis* (Tang et al., 2019), *Firmiana* sp. (Del Rio et al., 2022), *Craigia* sp. (Del Rio et al., 2022), *Illigera eocenica* (Wang T X et al., 2021), and *Koelreuteria allenii* (Chen et al., 2022).

This plant assemblage is referred to as the Jianglang flora (Liu et al., 2019; Su et al., 2020). The Jianglang flora exhibits a rich diversity, with 70 identified taxa, and represents a subtropical warm and humid dense forest environment, and detrital zircon U-Pb ages constrain the age of flora to the Middle Eocene (~47 Ma) (Su et al., 2020).

The Paleogene strata in the southern part of the Nima Basin has a thickness of up to 4 km, primarily consisting of fluvial, lacustrine, deltaic, and alluvial red bed deposits (DeCelles et al., 2007). In the Xiabiecuo area in the northern part of basin, it is interbedded with multiple layers of gray to grayish-black oil shale (Li et al., 2010). Paleomagnetic research, volcanic ash zircon U-Pb dating, and biostratigraphy constrain the deposition age to the late Oligocene to early Miocene, approximately 27 to 22 Ma (Meng et al., 2017; Wu et al., 2019). The pollen assemblage is dominated by *Piceapollis*, *Pinuspollenites*, and *Abiespollenites* (Wu et al., 2019). In the southern part of the basin, near Cozheluoma Town, plant and animal fossils have been discovered and reported in the interbedded gray siltstone of the Niubao Formation (Liu et al., 2019). Described in detail are *Ailanthus maximus* (Liu et al., 2019), *Cedrelospermum tibeticum* (Jia et al., 2019), *Equisetum oppositum* (Yang et al., 2016), *Tchunglinius tchangii* (Wang and Wu, 2015), and *Aquarius lunpolaensis* (Cai et al., 2019). This fossil flora is referred to as the Nima flora (Liu et al., 2019). The plant, insect, and fish fossils discovered in the Nima flora can be compared to the Dayu flora in the Lunpola Basin, indicating a similar age (Liu et al., 2019). In the eastern part of the Nima Basin, in the Niubao Formation of the Xiede area, abundant plant and animal fossils have also been discovered. Currently reported are thorn fossils (Zhang et al., 2022) and *Nangamostethos tibetense* (Xu et al., 2022). This flora is referred to as the Xiede flora, which shows similarities in plant composition and lithology to the Dayu flora and likely represents a similar age (Zhang et al., 2022).

In the Amdo Basin, the Niubao Formation is primarily composed of lacustrine purplish-red and grayish-green mudstone interbedded with siltstone and gypsum. The fossil assemblage indicates a depositional age from the Paleocene to the early Eocene (Cai and Fu, 2003). The ostracod assemblage consists of *Cypris decaryi-Limnocythere hubeiensis-Sinocypris reticulata*; the charophyte assemblage includes *Lamprothamnium lanpinensis-Chara banyueshanensis*; and insect fossils include *Hammaptergx* sp., *Scolypopites* sp., Blattidae, Fulgoridiidae, Elcanidae, Orthoptera, Homoptera, and others (Cai and Fu, 2003).

In the northern Qiangtang region, the Paleogene is divided into the Kangtuo Formation and the Suonahu Formation from bottom to top in the Heihuling, Tucuo, Jiangaidarina, Duogecuoren region. The volcanic rocks in the upper and lower parts of the Kangtuo and Suonahu Formations have been dated using zircon U-Pb dating, which constrains their depositional age to the Paleocene to Oligocene (Ding et al., 2000; Shen, 2020). Initially, the Kangtuo Formation and Suonahu Formation were considered as the Neogene (Shen, 2020). Comparative studies with the Hoh Xil Basin have shown that the Kangtuo Formation and Suonahu Formation are roughly contemporaneous with the Fenghuoshan Formation and Yaxicuo Formation, respectively (Li L et al., 2018; Dai et al., 2020). The Kangtuo Formation consists of purplish-red conglomerates interbedded with sandstones, pebbly sandstones, siltstones, and mudstones. Fossil charophytes of the Paleogene, including *Obtusochara* sp., *O. lanpingensis*, and *Gyrogona qianjiangica*, have been found in the formation, and the dominant pollen taxon is *Ephedripites* (Yue et al., 2006). The zircon U-Pb dating of the bentonite in the Qixiangcuo Basin indicates an age range of 43.8 to 45.4 Ma (Zhao et al., 2020). Combined with the age of the underlying andesite, the depositional age of the Kangtuo Formation is constrained to the Paleocene to Eocene. In the Gerze Basin, the Kangtuo Formation has some ostracods, with *Heterocypris igneus* being the main species, along with *Heterocypris* sp., *Limnocythere* sp., *Cyprinotus* sp., *Austrocypris posticaudata*, and others (Jiang G L et al., 2014; Wei et al., 2016). Charophytes such as *Obtusochara qianjiangica*, *O. jianglingensis*, and *O. lanpingensis* have also been found, which are consistent with the Eocene assemblages in North China, Bohai Bay, and the Jianghan Basin (Jiang G L et al., 2014; Wei et al., 2016). The Suonahu Formation is in unconformable contact with the underlying Kangtuo Formation or the Mesozoic strata (Shen, 2020). The lower part of the formation represents braided river deposits, characterized by conglomerates and pebbly sandstones; the middle to upper part consists of lacustrine deposits, including purplish-red and gray mudstones, siltstones, and gypsum layers (Shen, 2020). Fossils of freshwater gastropods and bivalves are found in the formation (Shen, 2020). The zircon U-Pb dating of the underlying andesite in the Suonahu Formation indicates an age of 46.6 Ma (Wang J et al., 2019), suggesting a depositional age of the Eocene to Oligocene.

3.3.2   Hoh Xil-Yushu stratigraphic subrealm
The northern part of this subrealm is characterized by the development of Paleogene sedimentary formations, including the Fenghuoshan Formation, the Tuotuohe Formation, and the Yaxicuo Formation. The Fenghuoshan Formation is predominantly composed of purplish-red conglomerates; the lower part of the formation contains abundant pollen assemblages with common elements from the Cretaceous (Li and Yuan, 1990; Staisch et al., 2014; Li et al., 2015). Based on zircon U-Pb dating of volcanic ash layers in the middle part of the Fenghuoshan Formation (62.5 Ma) and paleomagnetic data, the age of the Fenghuoshan Formation is determined to be Cretaceous to early Eocene, predating 51 Ma (Staisch et al., 2014; Jin et al., 2018). The Tuotuohe

Formation represents a fluvial-delta-lacustrine depositional environment. It is primarily composed of rhythmic layers consisting of purplish-red and brick-red conglomerates, gray sandstones, siltstones, and bioclastic limestone. Fossil assemblages found in the formation including ostracods such as *Cypris decaryi*, *Gautheir* sp., *Candoniella albicans*, *Darwinula* sp., and charophytes such as *Peckichara serialis* (Zhang et al., 2010). Miao et al. (2016) identified a pollen assemblage dominated by *Ephedripites* (*Distachyapites*) and *Ephedripites* (*Ephedripites*) in the red beds of the Tanggula Mountain, with high contents of *Chenopodipollis* and *Nitrariadites*, and low content of Pinaceae pollen (Miao et al., 2016). Li et al. (2019) suggested a late Oligocene to Miocene age based on the relatively high content of *Chenopodipollis*. However, Duan et al. (2007, 2008) and Li (2015) reported pollen assemblages dominated by coniferous pollen in the upper part of the Tuotuohe Formation and the Yaxicuo Formation, which have similar lithologies. The Miocene Wudaoliang Formation, characterized by gray lacustrine mudstone deposits, is considered to be above the Tuotuohe Formation. Therefore, the pollen assemblages mentioned above are likely to be found in the lower part of the Tuotuohe Formation. The pollen assemblages in the upper part of the Tuotuohe Formation are dominated by angiosperm, with an increased abundance of bisaccate pollen of Pinaceae (Duan et al., 2007). The Yaxicuo Formation consists of purplish-red and grayish-purple clayey fine-grained sandstones, as well as light grayish-green sandstone. It represents a delta-lacustrine depositional environment, and contains pollen, charophytes, and ostracods. The lower part of the Yaxicuo Formation is characterized by the ostracod assemblage of *Austrocypris* cf. *posticaudata-Candoniela albicans-Leucocythere tropis*, while the upper part contains the assemblage of *Ilyocypris errabundis-Darwinula stenimpudica* (Song et al., 2019). Late Eocene bivalves such as *Pisidium* sp. and *P. amnicum* have been found in the formation (Wang J X et al., 2003). Charophytes present include *Obtusochara brevicylindrica*, *Tectochara houi*, *Amblyochara svbeiensis*, and *Hornichara qinghaiensis* (Zhou, 2007). The pollen assemblages in the Yaxicuo Formation are dominated by bisaccate pollen of Pinaceae, with significant variations in the abundance of *Picea* and *Pinus* in different regions (Duan et al., 2008; Li, 2015). Studies on detrital zircons and biostratigraphy indicate that the deposition of the Yaxicuo Formation in the Tuotuohe sub-basin occurred after 36 Ma, placing its age in the late Eocene to Oligocene (Lin et al., 2020).

The eastern and southern parts of this region also contain other Paleogene sedimentary units, such as the Gongjue Formation, Zongbai Formation, Ranmugou Formation, Lawula Formation, and Seru Formation. The basins in this region were formed as strike-slip pull-apart basins within the Lancangjiang fault zone, Bangong-Nujiang fault zone, and parallel sub-fault zones, under a compressional tectonic setting. The Paleogene deposits in these basins are primarily characterized by fluvial-lacustrine sedimentation, with thick and widespread coarse clastic rocks. They are unconformably overlain by the underlying formations.

The Gongjue Basin is characterized by a thick layer of red terrestrial clastic rocks, known as the "Gongjue Red Beds", predominantly composed of braided river sandstone and conglomerate, and the uppermost part consists of lacustrine sandstone interbedded with gypsum and mudstone (Wei, 1985). It is divided into the Gongjue Formation and the Ranmugou Formation from bottom to top (Xiong et al., 2020). There is some disagreement among different researchers regarding the start and end deposition ages of the Paleogene formations in the Gongjue Basin (Li et al., 2020b; Xiong et al., 2020; Xiao et al., 2021; Wang L et al., 2022). The lower part of the Gongjue Formation is characterized by thick layers of purple-red conglomerate and medium-grained sandstone, while the upper part is dominated by fine-grained sandstone and siltstone. The sedimentary environment transitioned from an alluvial fan to fluvial deposition (Tang, 2015), with intermittent aeolian dune deposition (Xiong et al., 2020). The upper part of the Gongjue Formation contains dark brown and gray-black mudstone with a pollen assemblage dominated by angiosperms (Song and Li, 1982). *Ephedripites* (*Distachyapites*) is commonly present, while pollen from the Pinaceae and Podocarpaceae is absent, indicating an Eocene age (Song and Li, 1982). The upper part of the Gongjue Formation also reported a pollen assemblage dominated by *Momipites*, indicating an Eocene age (Studnicki-Gizbert et al., 2008). Fossilized plant remains of *Sabalites* sp. and *Plibinia* sp. have also been found in the red beds (He et al., 1983; Li et al., 2020b). The Ranmugou Formation can be divided into two parts from bottom to top: purplish-gray conglomerate part, and a purple-red sandstone part. It represents typical fluvial depositional environments with the development of floodplain and multiple paleosol layers (Tang, 2015; Xiong et al., 2020). Fossilized palm leaves have been discovered in the lower part of the Ranmugou Formation (Xiong et al., 2020). The upper part is characterized by a pollen assemblage including *Celtispollenites-Caryapollenites-Tricolpites-Tricolporopollenites*, with low abundance of *Ephedripites*, *Nitrariadites*, and Pinaceae (Wang L et al., 2022).

The Paleogene strata in the Nangqian Basin are similar to those in the Changshagongma Basin, mainly consisting of alluvial fan, fluvial, and lacustrine deposits. The lower part is composed of sandstone and conglomerate, while the upper part consists of mudstone and sandstone (Dai et al., 2013). The overlying volcanic rocks have been dated using zircon U-Pb dating to be around 37–38 Ma, and intrusive rocks within the stratigraphic sequence have been dated to be around 49–51 Ma (Deng et al., 1999). Based on these results and fossil evidence, the age of the deposits is determined to

be the Eocene (Deng et al., 1999). Among the ostracod fossils in the Gongjue Formation, *Eucypris hengyangensis* is the most abundant species, followed by species such as *Cypris* sp., *Cyprinotus* sp., and *Ilyocypris* sp.; other common species include *Cypridopsis* sp., *Herpetocypris* sp., *Cypria* sp., *Subulacypris* sp., and *Darwinula* sp. (Wei, 1985). The ostracod assemblages are dominated by species commonly found in the Eocene in China (Wei, 1985). Other fossils found in the formation include mollusks such as *Hippeutis* sp., *Negulus* sp., *Cinima* sp., and *Bithynia* sp. (Zhang et al., 2010). The pollen assemblage is dominated by *Ephedripites-Nitrariadites-Quercoidites*, with the occasional presence of coniferous species (Yuan et al., 2020). Based on the pollen assemblage, the deposition age of the Gongjue Formation in the Nangqian Basin is estimated to be the late Eocene, around 41.2–37.8 Ma (Yuan et al., 2020). Zircon U-Pb dating of volcanic rocks and paleomagnetic studies indicate that the deposition age of the Gongjue Formation in the Nangqian Basin is from 52.5 to 35 Ma (Zhang et al., 2020). Similar rift basins adjacent to the Nangqian Basin include the Qumalai, Yuejiamake, Shanglaxiu, and Xialaxiu Basins (Horton et al., 2002; Yuan et al., 2020; Zhang et al., 2020).

The Markam Basin is a narrow and elongated rift basin located on the southeastern margin of the Qinghai-Tibetan Plateau. The Tertiary deposits in this basin are referred to as the Lawula Formation, which unconformably overlies the underlying Cretaceous strata (Tao and Du, 1987; Zhang et al., 2005). The lower part of the Lawula Formation consists of gray-yellow conglomerate and breccia. The middle part is characterized by extensive basalt flows intercalated with volcanic ash layers. The upper part primarily comprises fluvial-lacustrine and swamp deposits, including brown-yellow mudstone, gray-black carbonaceous mudstone, and shale interbedded with brown-yellow siltstone, fine sandstone, and coal seams. Multiple layers of plant fossils are found within the mudstone, siltstone, and sandstone, collectively referred to as the Markam flora (Tao and Du, 1987; Su et al., 2019b). Based on the plant fossils, the Lawula Formation was originally considered to have been deposited during the late Miocene (Tao and Du, 1987). However, more recent studies using methods such as ^{40}Ar-^{39}Ar dating of volcanic ash and high-potassium volcanic rocks, zircon U-Pb dating of trachyte have constrained the deposition age of the Lawula Formation to the late Eocene to early Oligocene (Zhang et al., 2005; Ma et al., 2016; Su et al., 2019b). In addition to the plant assemblages dominated by the Betulaceae reported by Tao and Du (1987), new taxa have been reported in recent years. These include *Equisetum oppositum* (Ma et al., 2012), *Elaeagnus tibetensis* (Su et al., 2014), *Quercus tibetensis* (Xu et al., 2016), *Hemitrapa alpina* (Su et al., 2018), *Tsuga asiatica* (Wu et al., 2020), *Alnus* cf. *ferdinandi-coburgii* (Xu H et al., 2019), *Berhamniphyllum junrongiae* (Zhou et al., 2020), and *Quercus* cf. *presenescens*

(Chen et al., 2021), etc. Several plant taxa within the Lawula Formation represent some of the earliest fossil records in the Qinghai-Tibetan Plateau and even globally, with their nearest living relatives distributed along the southeastern margin of the plateau since the late Eocene (Su et al., 2014, 2018; Wu et al., 2020; Chen et al., 2021). The lower layers of the Markam flora are dominated by Fagaceae and Betulaceae, the middle layers are predominantly composed of Betulaceae, and the upper fossil layers are primarily characterized by Salicaceae and Rosaceae (Tao and Du, 1987; Su et al., 2019b; Deng W et al., 2020). There has been a significant shift in the vegetation from the late Eocene to the early Oligocene, transitioning from a mixed forest of medium-sized, evergreen deciduous broad-leaved trees to alpine shrubland dominated by small-leaved species (Su et al., 2019b; Deng W et al., 2020).

In the Leiwuqi Basin, the Paleogene strata are divided into three units from bottom to top: the Dongriga Formation, the Ranmugou Formation, and the Seru Formation (Wang, 2022). The Dongriga Formation mainly consists of purple-red sandstone, interbedded with gypsum layers and coarse conglomerates. The Ranmugou Formation can be correlated with the adjacent Gongjue Basin and is assigned to the Eocene. The lower part of the Seru Formation is dominated by purple-red fine sandstone and siltstone with interbedded mudstone, while the upper part mainly comprises yellow-greenish sandstone, mudstone, and thin coal seams (Wang, 2022). Fossil flora, primarily represent taxa from the Betulaceae and Salicaceae, was found in the upper part of the Seru Formation, which are consistent with the early Oligocene MK1 fossil layer of Markam flora (Tao and Du, 1987; Su et al., 2019b; Deng W et al., 2020). The lower part of the Seru Formation contains a pollen assemblage dominated by Pinaceae, with *Abies* and *Picea* accounting for over 20% of the assemblage (Wang, 2022).

3.3.3 Western Sichuan-Eastern Xizang stratigraphic subrealm

In the Relu Basin, the Paleogene strata are divided into the Changzong Formation and the Relu Formation. The ages of these formations have been determined based on fossil assemblages and volcanic ash, with the Changzong Formation ranging from 50 to 45 Ma and the Relu Formation ranging from 45 to 34 Ma (He et al., 2022). The Changzong Formation is characterized by purple-red conglomerates, sandstones interbedded with mudstones, and occasional aeolian sand dune deposits, indicating typical alluvial fan deposition (He et al., 2022). The lower part of the Relu Formation consists of conglomerates, sandstones, and mudstones with interbedded mudstone and limestone, representing alluvial fan-delta-lacustrine deposition. The upper part is dominated by purple-red conglomerates, sandstones interbedded with mudstones, and paleosols (He et al., 2022). The lower part of the Relu Formation contains plant fossils such as *Palibinia*

pinnatifida, *Eucalyptus relunensis*, *Banksia puryearemsis*, *Hemiptelea paradavidii*, *Comptonia* sp., *Viburnum* sp., *Pistacia* sp., etc. (Chen et al., 1983; Guo, 1986). It also contains ostracods like *Heterocypris* sp., *Cypridopsis* sp., *Australorbis* sp., and *Kosmogyra* sp. (He et al., 2022), as well as charophytes like *Gyrogona gianjiangica* and *Kosmogyra* sp. (Wei and Luo, 2005; Zhang et al., 2010). The upper part of the Relu Formation in the Changshagongma Basin has a pollen assemblage of *Lycopodiumsporites-Ephedripites* (*Distachyapites*), indicating a deposition age in the Eocene (Wei and Luo, 2005). The Relu Formation in Gemusi region yields abundant mammal fossils (Zong et al., 1996). The discovery of *Yuomys dawai* and *Y. gemuensis* in Gemusi region indicates a deposition age during the Irdinmanhan (the early Middle Eocene, 49–45 Ma), suggesting a low-altitude forest environment (Ni et al., 2023).

The Zongbai Formation has a wide distribution. The lower part consists of gray, gray-yellow, and gray-brown thick layers of conglomerate and sandstone, while the upper part is composed of gray claystone, mudstone, black shale interbedded with gray-yellow medium to fine-grained sandstone, siltstone, and oil shale. In the Rechang area, gastropods such as *Planorbarius subdiscus*, *Pingiella dengqenensis*, and *Guraulus* sp. have been found (Zhang et al., 2010). In the Bangda area, the plant fossil *Equiselum* sp. has been discovered (Zhang et al., 2010). In the Zongbai area, gastropods such as *Viviparus* sp., *Lymnaea* sp., *Pingiella dengqenensis*, *Gyraulus* sp., *Planorbarius* sp., *Amnicola* sp., *Pseudamnicola* sp., *Physa* sp., as well as ostracods like *Stenocypris* sp., *Cyprois* sp., *Eucypris* sp., and insects like *Erotylidae incertae*, have been identified (Zhang et al., 2010). Based on the fossil assemblage, the Zongbai Formation is assigned to the Eocene (Zhang et al., 2010). In these regions, the Lawula Formation is composed of gray-white, yellow-green sandstone, conglomerate, mudstone, and siltstone, locally containing tuff and thin coal seams. In the middle part, there are porphyritic rocks, quartz porphyritic rocks, and biotite quartz porphyritic rocks intercalated with conglomerate. Plant fossils such as *Equisetum* sp., *Betula mankongensis*, *B*. cf. *utilis*, *B*. cf. *vera*, *Carpinus* cf. *fargesiana*, and *C. grandis* have been found (Zhang et al., 2010). Ostracods like *Stenocypia fischeri*, *Candoniella donschanensis*, gastropods like *Australorbis* cf. *pseuduammonius*, and charophytes like *Obtusochara* sp. have also been identified (Zhang et al., 2010). The lithology and plant fossils of the Lawula Formation in Rechang, Bangda, and Zongbai can be compared with the Markam Basin, indicating a deposition age of late Eocene to early Oligocene (Su et al., 2019b).

3.4 Western Margin of Yangtze stratigraphic realm

3.4.1 Chengdu stratigraphic subrealm

The Chengdu stratigraphic subrealm is limited to the Chengdu Basin. The Paleogene strata in the basin constitute a large-scale fluvio-lacustrine clastic deposition. The Paleogene sequence from older to younger consists of the Mingshan Formation and the Lushan Formation, which have continuous sedimentation with the underlying Cretaceous Guankou Formation (Jiang Z F et al., 2014). The Mingshan Formation is composed of reddish-brown sandstone, siltstone, mudstone interbedded with conglomerates and evaporite layers. The upper part of this formation yields the ostracod assemblage of *Sinocypris funingensis-Limnocythere hubeiensis-Ilyocypris dungshanensis* (Wang et al., 2006). The paleomagnetic dating indicates an age range of 65 to 45 Ma (Wang et al., 2006). The Lushan Formation is characterized by reddish-brown mudstone interbedded with reddish-brown and yellow-green muddy sandstone. It yields the ostracod assemblage of *Pinnocypris postacuta-Limnocythere jiangsuensis-Cyprinotus formalis* (Wang et al., 2006).

3.4.2 Western Yunnan stratigraphic subrealm

In this subrealm, which includs the Xichang, Yanbian, Yanyuan, Ninglang, and Lijiang Basins, the Paleogene strata are mainly characterized by alluvial fan and fluvio-lacustrine clastic deposition. The Paleogene strata in this region are referred to as the Lijiang Formation (Zong, 1987), the Leidashu Formation (Jiang L et al., 2018), the Baoxiangsi Formation (Ma et al., 2021), and the Ninglang Formation (Zhu, 2022). In the Lijiang Basin, amount of mammalian fossils has been discovered, forming the Lijiang fauna (Zong et al., 1996; Bai, 2022). The fauna includes species such as Metatelmatheriinae indet., *Lophialetes*? sp., *Breviodon lumeiyiensis*, *Diplolophodon xiangshanensis*, *D. similis*, Amynodontidae indet., *Prohyracodon major*, *P. meridionale*, *Lijiangia zhangi*, *Lunania youngi*, *Eomoropus minimus*, and *Grangeria cania*, representing the Sharamurunian of the Middle Eocene (Bai, 2023). Fossil records of the genera "*Eucalyptus*" and *Palibinia*, as well as ostracod assemblages *Sinocyporis-Cypris* (*Cristocypris*)-*Parailyocypris*, have also been reported in Lijiang and Weixi areas (Shen et al., 2017). In the Ninglang Basin, the age of the upper part of the Ninglang Formation is constrained by detrital zircon and intrusive rock dating, suggesting an older age limit of approximately 34 Ma (Zhu, 2022). This age is consistent with the occurrence of the late Eocene charophytes *Cyrogona qianjiangica*, *Obtusochara brevalis*, *O. subcylindrica*, as well as the ostracod assemblages indicating the same age (Zhu, 2022).

In the Chuxiong Basin, the Cenozoic sedimentary strata in the Nanhua area, originally thought to belong to the Upper Miocene, has been revised to the Late Eocene-Early Oligocene based on absolute zircon U-Pb dating of volcanic ash, plant fossils, and magnetostratigraphic results (Linnemann et al., 2018; Liu, 2019; Li et al., 2020a). The lower part of the

strata, representing the Late Eocene, consists primarily of braided fluvial deposits of conglomerates, sandstones, and siltstones; the middle-upper part, representing the Oligocene, is characterized by lacustrine and swamp deposits of grayish-black mudstones, coal seams, siltstones, and fine-grained sandstones, interbedded with multiple layers of volcanic ash (Liu, 2019). The sediments have yielded abundant plant leaf, fruit, wood, and pollen fossils (Linnemann et al., 2018; Tang et al., 2020; Wu et al., 2021, 2022; Deng et al., 2022). The Oligocene pollen assemblage is dominated by *Quercoidites*, with common occurrences of *Pinuspollenites* and *Piceapollis* (Tang et al., 2020). The plant fossils were named to the Lühe flora, dominated by *Quercus* subgenus *Cyclobalanopsis*, *Carpinus*, and *Betula* (Wu M X et al., 2022). Reported plant fossil taxa include *Dipteronia brownii* (Ding et al., 2018a), *Cryptomeria yunnanensis* (Ding et al., 2018b), *Tsuga asiatica* (Wu et al., 2020), *Fraxinus zlatkoi* (Wu et al., 2021), and *Taxodioxylon* sp. (Deng et al., 2022).

In the Lanping Basin, the Cenozoic strata comprise a series of piedmont-lacustrine to fluvial-lacustrine clastic deposits, including the development of coal seams in lacustrine and swamp environments. These deposits are in continuous sedimentation with the underlying Cretaceous terrestrial strata. The rock sequence in the basin, from older to younger, consists of the Yunlong Formation, the Guolang Formation, and the Baoxiangsi Formation (Zhu et al., 2011). The Yunlong Formation is in conformable contact with the underlying Upper Cretaceous Hutousi Formation, and primarily consists of red sandy mudstones in a saltwater lake facies (Shen et al., 2017). It contains a semi-saline water ostracod assemblage of *Sinocypris-Parailyocypris-Eucypris* (Shen et al., 2017). In the Wenshui River area, a late Paleogene charophytes assemblage of *Obtusochara-Peakichara* is present in the Yunlong Formation, including species such as *Peakichara varians*, *Obtusochara lanpingensis*, *Tectochara* sp., and *Charites* cf. *angustior* (Shen et al., 2017). Ostracod assemblages found near Jinding Town include *Limnocythere yunlongensis*, *Eucyris* cf. *anlunensis*, *Sinocypris* sp., *Cypinotus* cf. *leotus*, and *Sinocypris subovata*, which exhibit characteristic of the late Paleocene *Sinocypris-Eucyris* assemblage in South China (Shen et al., 2017). The sedimentary deposits equivalent to the Yunlong Formation in the Simao Basin are referred to as the Mengyejing Formation, with its depositional age revised to the Late Cretaceous to early Paleocene (Yan et al., 2021). Therefore, the possibility of the lower part of the Yunlong Formation being Late Cretaceous cannot be ruled out. The Lower Eocene Guolang Formation is in conformable contact with the underlying Yunlong Formation and consists of purple-red and brick-red fine sandstones, siltstones, mudstone, and sandy mudstone, with the presence of ostracod (*Limnocythere* sp.) (Zhu et al., 2011). The Eocene Baoxiangsi Formation is characterized by alluvial fan deposits of conglomerate and sandstone (Zhu et al., 2011).

In the Jianchuan Basin, the Cenozoic strata consist of a series of piedmont-lacustrine to fluvial-lacustrine clastic rock deposits with volcanic rocks. The Paleogene strata in the Jianchuan Basin are divided from old to young into the Yunlong Formation, Baoxiangsi Formation, Jinsichang Formation, Shuanghe Formation, and Jianchuan Formation. The Yunlong Formation in the Jianchuan Basin is sometimes referred to as the Mengyejing Formation. It has a relatively small outcrop and is predominantly composed of purple-red sandstones in a fluvial-lacustrine environment. The depositional age of the Yunlong Formation is Late Cretaceous to Paleocene (Shen et al., 2017; Gourbet et al., 2017; Zheng et al., 2022). The Baoxiangsi Formation is widely developed in the Jianchuan Basin. It consists of a red, coarse clastic terrestrial deposits, locally interbedded with aeolian sand dune deposits. The depositional age of the Baoxiangsi Formation has been constrained to the Eocene based on magnetostratigraphy and the age of overlying strata, although the end of its deposition is still somewhat debated (Fang et al., 2021; Zheng et al., 2022). The Jinsichang Formation is characterized by medium to thick-bedded, purple-red conglomerates and sandstones. The intrusion of volcanic rocks in the Jinsichang Formation has a zircon U-Pb age of approximately 35 Ma (Lu et al., 2012). Furthermore, the Jinsichang Formation is angular unconformable with the underlying Baoxiangsi Formation, and its deposition age is assigned to the middle Eocene (Wang et al., 2020). The Shuanghe Formation is only exposed near the Shuanghe Coal Mine in the Jianchuan Basin. It is primarily composed of dark gray coal seams, light gray to gray, medium to thick-bedded sandstones, and grayish-white siltstone and mudstone. Fossils found in the Shuanghe Formation include late Eocene ostracods such as *Austrocypris* sp., *Homoeucypris* sp., *Heterocypris* sp., *Candona* sp., *Cyprinotus* sp., *Eucypris* sp., *Limnocythere* sp., *Clinocypris* sp. (Shen et al., 2017), as well as mammal fossils like *Zaisanamynodon* sp. (Gourbet et al., 2017). The coal seams contain abundant plant fossils, with dominant species belonging to the sub-tropical evergreen species of Lauraceae, which are collectively referred to as the Shuanghe flora (Writing Groupe of Cenozoic Plant Compilation, 1978). Based on the stratigraphic contacts and zircon U-Pb dating of volcanic rocks, the deposition age of the Shuanghe Formation is determined to be in the late Eocene. However, different researchers have disputed the beginning of deposition for the Shuanghe Formation (Wang et al., 2020; Fang et al., 2021; Zheng et al., 2022). The Jianchuan Formation is in conformable contact with the underlying Shuanghe Formation. It mainly consists of volcanic breccias, tuffaceous rocks interbedded with gray-green and gray-yellow conglomeratic sandstones, fine sandstones, and shales, as well as carbonaceous shales. The Jianchuan Formation contains plant fossils such as *Beryophyllum yunna-*

nense, *Palaeosinomenium hengduanensis*, *Quercus* sp., *Pinus* sp., and others in its sandstones and shales (Writing Groupe of Cenozoic Plant Compilation, 1978; Zhou, 1996; Wu et al., 2023). The zircon U-Pb dating of volcanic rocks in the Jianchuan Formation has constrained its deposition to the late Eocene (Wang et al., 2020).

3.5 Gangdise-Himalaya-Ganga stratigraphic realm

Based on the characteristics of basin types and basin sedimentary, the Gangdise-Himalaya-Ganga realm is divided into the Gangdise, the Yarlung Zangbo-Himalaya, and the Ganga stratigraphic subrealms (Figure 2) (Zhang et al., 2010).

3.5.1 Gangdise stratigraphic subrealm

The Gangdise stratigraphic subrealm includes the Gangdise volcanic arc of the sedimentary basins distributed on both sides of this volcanic arc and overlain by it. The Paleogene sedimentary formations that have developed in this subrealm include the Niubao Formation, the Qiuwu Formation, the Rigongla Formation, and the Kailas Formation.

The Paleogene formation near Gegyai County is called the Niubao Formation. The lower part consists of conglomerates, sandstones interbedded with purple, brown, and gray-green siltstones, while the upper part consists of sandstones, conglomerates, siltstones, as well as purple and gray-green mudstones. Fossils within this formation include gastropods like *Pyrazus montensis*, *Batillaria* (*Vicinocerithium*) *inopinata*, *Harrisianella* (*Teliostomopsis*) *regularicostata*, *Thericium* (*Pseudoaluco*) cf. *dejaeri*, *T.* (*Chondrocerithium*) cf. *koeneni*, and *Bittium versigranulum*, indicating its age to be Paleogene (Zhang et al., 2010). In areas like Pulan, Angren, and Xigaze, the Paleogene Qiuwu Formation represents fluvial-fan delta-lacustrine environments (Zhang et al., 2010). The lower part of this formation consists of gray-green conglomerates, conglomeratic sandstones, and sandstones interbedded with siltstones and silty mudstones; the middle part consists of gray sandstones interbedded with siltstones and mudstones; the upper part consists of dark gray sandstones, gray-black muddy siltstones, and siltstone interbedded with silty mudstone and coal seams (Li, 2004; Zhang et al., 2010). The Qiuwu flora, found in Jisong Coal Mine in Angren County, is dominated by the genus "*Eucalyptus*" and includes common tropical and subtropical taxa such as *Ficus* (Tao, 1981). The pollen assemblage from the Qiuwu Formation in Dongga Coal Mine primarily consists of *Quercoidites*, as well as pollen-types with pore or tricolpate (Li, 2004). Presence of *Graminidites* and *Tsugaepollenites* suggests a deposition age from the late Oligocene to early Miocene (Li, 2004). Detrital zircon U-Pb dating studies have constrained the oldest sedimentation age of the Qiuwu Formation in the Xigaze area to be late Oligocene to early

Miocene (26–21 Ma) (Ding et al., 2017c). The fossil flora discovered in Dongga Coal Mine in Xigaze, named the Qiabulin flora, is dated to the early Miocene, approximately 21–19 Ma (Ding et al., 2017c). The Rigongla Formation, located in the Zhongba area, is characterized by reddish-brown conglomerates interbedded with purple-red conglomeratic sandstones, sandy mudstones, and calcareous mudstones. It contains Paleogene gastropod fossils *Bithynia* sp. (Zhang et al., 2010). The lower part of the formation has a K-Ar age of 35.5 Ma for the tuff, and based on fossils and isotope ages, its sedimentation age is inferred to be Oligocene (Zhang et al., 2010). Fossil plants, mainly belonging to *Alnus*, are found in the Rigongla Formation near Shiquanhe Town (Xizang Autonomous Region Geological Survey Institute, 2003). The Kailas Formation, located near Kailas Mountain, comprises interbedded mudstones and sandstones, and it yields the Kailas flora dominated by the genus *Populus* (Ai et al., 2019). The zircon U-Pb age of the tuff is determines the age of the flora to be the latest Late Oligocene, approximately 23.3 Ma (Ai et al., 2019).

3.5.2 Yarlung Zangbo-Himalaya stratigraphic subrealm

In this subrealm, the Paleogene sedimentary basins are predominantly characterized by marine strata in southern Tibet. The Paleogene marine strata include the Jidula Formation, Zongpu Formation, Enba Formation, Zhaguo Formation, Denggang Formation, Sangdanlin Formation, Zheya Formation, Zongzhuo Formation, Jiachala Formation, Quxia Formation, and Jialazi Formation. The Paleogene terrestrial strata are mainly represented by the Liuqu Formation, which consists of conglomerates interbedded with sandstones.

The Paleogene marine deposits in southern Tibet are spread across a vast region to the south of the Gangdise magmatic arc. Due to the uplift and detachment from the marine environment since the late Eocene, most of the Paleogene residual marine sediments have been eroded and exhausted. Currently, only scattered remnants of Paleogene marine strata can be observed in areas like Gyantse, Gamba-Tingri, Zhongba, Saga-Guoyala, Sangmai, and Yadong. The Yarlung Zangbo-Himalaya stratigraphic subrealm exhibits distinct sedimentary facies in the Paleocene to Eocene marine strata. From north to south, the marine environment transitions from shallow sea to deep sea and back to shallow sea (Hu et al., 2017). The northern belt of shallow sea distribution is narrow and can be observed in Zhongba and Barga regions (Hu et al., 2017). In contrast, the southern belt has a wider distribution and can be seen in the Gamba-Tingri area (Hu et al., 2017). The stratigraphic sequence from bottom to top includes the Jidula Formation, Zongpu Formation and Zhepure Formation, mainly composed of near-shore bioclastic limestone rich in benthic foraminifera and calcareous fossils (Hu et al., 2017). The intermediate zone sandwiched between the two shallow sea belts, a semi-deep

sea to deep sea sedimentary environment prevails. From east to west, the semi-deep sea to deep sea sediments are distributed along the Gyantse-Saga-Guoyala-Sangmai area (Hu et al., 2017). In the eastern part of the intermediate zone, the strata are characterized by the slope fan deposition of a semi-deep sea in Gyantse, known as the Jiachala Formation (Hu et al., 2017). In the western part of the intermediate zone, radiolarian chert and mixed rocks represent a semi-deep sea to deep sea environment (Hu et al., 2017). Extensive research has been conducted on the comprehensive stratigraphic correlation and subdivision of the Paleogene marine sedimentary sequences (Figures 2 and 4) (Hu et al., 2017; Li J G et al., 2020; Li, 2021). The calcareous nannofossil zonation in this area is characterized by three assemblages corresponding to the calcareous nannofossil zones NP15, NP16, and NP17, ranging from the late Middle Eocene Bartonian to the early Priabonian (Li J G et al., 2020; Li, 2021). The foraminiferal assemblage consists of nine zones, including three planktonic zones and six benthic zones that can be correlated with international standard zones (Li J G et al., 2020; Li, 2021). The bivalve fossils are composed of three assemblages representing the Early Paleocene, Middle-Late Paleocene, and Early-Middle Eocene (Li J G et al., 2020; Li, 2021). The radiolarian assemblage includes seven fossil zones ranging from RP1 to RP7, corresponding to the international standard zones, with the latest possibly extending to the Early Eocene (Li J G et al., 2020; Li, 2021). The ostracod fossils are characterized by three assemblage zones (Li J G et al., 2020; Li, 2021).

The terrestrial deposits of the Liuqu Formation in the Lhaze area consist of purple-red, gray-yellow, and yellow-green conglomerates, sandstones, and silt mudstones. The plant fossils of the Liuqu flora mainly include taxa from the Myrtaceae, Lauraceae, Magnoliaceae, Moraceae, and Arecaceae, which are mainly distributed in tropical and subtropical regions (Tao, 1988). The genus "*Eucalyptus*" is also present (Tao, 1988; Fang et al., 2005; Ding et al., 2017c; Xu C L et al., 2019). Freshwater gastropod and bivalve fossils have been found (Tao, 1988). Based on volcanic ash dating, the sedimentation age of the Liuqu Formation is constrained to the Paleocene-Eocene, and the age of the Liuqu flora estimated at approximately 56 Ma (Ding et al., 2017c). However, based on regional stratigraphic correlations and detrital zircon analysis, some researchers suggest that the sedimentation age of the Liuqu Formation ranges from the late Oligocene to the early Miocene (Hu et al., 2017). However, based on the currently discoveries of Liuqu flora, the vegetation composition is significantly different from other late Paleogene flora found in the Qinghai-Tibetan Plateau. Therefore, the deposition age of the Liuqu Formation should be in the early Paleogene. The Liuqu flora represents a northernmost flora of the Indian Plate, and its species composition is closely related to the Paleogene flora of India. The Liuqu Formation has also reported pollen assemblages with a distinct Oligocene appearance (Wei et al., 2011). The vegetation indicated by these pollen assemblages differs significantly from the Liuqu flora, necessitating further investigation.

3.5.3   Ganga stratigraphic subrealm

The Paleogene succession in the Kashmir-Hazara region of the Himalayan foreland basin is divided into the Hangu Formation, Lockhart Formation, Patala Fomation, Margalla Hill Limestone and Chorgalli Formation, and Murree Formation. The Hangu Formation consists of coarse-grained sandstones, limestones, and carbonaceous shales. It contains the benthic foraminiferal Zone SBZ1, indicating an early Paleocene age (Danian) (Shah, 2009). The Lockhart Formation is characterized by the benthic foraminiferal Zone SBZ3, which correlates with planktonic foraminiferal Zone P4, suggesting a late Paleocene age (Thanetian) (Hanif et al., 2014). The upper part of the Patala Formation contains larger benthic foraminifera such as *Miscellanea* and *Ranikothalia*, indicating that the end of this formation is the late Paleocene to early Eocene (Hanif et al., 2013). The Margalla Hill Limestone and Chorgalli Formation are dated to approximately 55–53 Ma based on foraminiferal assemblages and the age of overlying Kuldana Formation volcanic ash (Baig and Munir, 2007; Ding et al., 2016). The Kuldana Formation is composed of shale, limestone, sandstone, and siltstone. The lower part of the formation is dated to 53.2 Ma and contains foraminiferal Zones SB12-14, indicating deposition age of the late Eocene from 53 to 43 Ma (Baig and Munir, 2007; Ding et al., 2016). The Murree Formation consists of a terrestrial sequence of mudstones interbedded with grayish-green sandstones and siltstones. The lower part of the formation contains animal fossils such as *Teleoceras* cf. *fatehjungensi*, *Palaeochoerus* sp., *Gonotelma* sp., *Leptomeryx* sp., *Primus microps*, *Menoceras* sp., and *Microbunodon* sp; the upper part of the formation includes the discovery of *Dinotherium pentapotamiae*; and the main fossil assemblage corresponds to the Bugti fauna of the Oligocene (Bhatia and Bhargava, 2006). The presence of Asteraceae species in the pollen assemblage indicates a deposition age of the Murree Formation in the Oligocene to early Miocene (Pradhan and Sharma, 2003). The Balakot Formation, characterized by red beds, was initially considered to be in conformable contact with the underlying Patala Formation, suggesting a deposition age from the late Paleocene to the Lutetian of the Eocene (Beck et al., 1995). However, subsequent studies revealed that these two formations were not continuously deposited (Najman et al., 2001). The age of the Balakot Formation, based on detrital mica ages, is concentrated in the range of 40–36 Ma, indicating a deposition age from the Oligocene to the Middle Miocene (Najman et al., 2001).

The Paleogene strata in Himachal Pradesh and western

Figure 4 Biostratigraphy of the Tarim-West Kunlun and Gangdise-Himalaya-Ganga stratigraphic realms, modified from references (Xi et al., 2020; Li J G et al., 2020; Li, 2021).

Nepal are divided into the Subathu Formation and the Dagshai Formation from bottom to top. The Subathu Formation is primarily composed of gray mudstone, and its deposition age has been constrained to be between 61.5 and 41.5 Ma based on foraminifera and paleomagnetic results (Srivastava et al., 2013). The Dagshai Formation consists mainly of fluvial deposits, including grayish-white sandstone interbedded with red mudstone. There is a stratigraphic hiatus between the Dagshai Formation and the underlying Subathu Formation (Lakshami et al., 2000). The youngest detrital mica age and paleomagnetic data suggest a deposition age ranging from the late Late Eocene to the Oligocene (Lakshami et al., 2000). The overlying formation is the Lower Miocene Kasauli Formation (Acharyya, 2007; Srivastava et al., 2011).

The Paleogene strata in the central part of Nepal are divided into the Amile Formation and the Bhainskati Formation from bottom to top. The Amile Formation consists mainly of fluvial and deltaic deposits, characterized by thick layers of white quartz sandstone and calcareous mudstone, interbedded with gray-black coal or lignite (DeCelles et al., 2004). Its deposition age is considered to range from the Late Cretaceous to the Early Eocene (Najman et al., 2005). The overlying marine Bhainskati Formation is in conformable contact with the Amile Formation. It is predominantly composed of black shale, and contains *Nummulit*e foraminiferal fauna (DeCelles et al., 2014). The deposition age of the Bhainskati Formation is interpreted as middle-late Eocene, equivalent to the Subathu Formation in the western region of Nepal, and its deposition may have started in the Late Paleocene (DeCelles et al., 2014). The Dumri Formation, a terrestrial deposit, unconformably overlies the Bhainskati Formation, and paleomagnetic dating suggests that its deposition began around 20 Ma (Ojha et al., 2009).

In summary, except for the Tarim-Western Kunlun and Gangdise-Himalaya-Ganga stratigraphic realms, the Paleogene strata in the Qaidam-Qilian-Western Qinling, Qiangtang-Western Sichuan, and Western Margin of Yangtze stratigraphic realms are predominantly characterized by terrestrial deposits. The distribution of marine deposits in the plateau and surrounding areas is influenced by the collision of the India and Eurasia plates, as well as global sea level changes (Hao and Zeng, 1984; Xi et al., 2020). The Tarim-Western Kunlun stratigraphic realm has witnessed multiple marine transgressions and regressions since the Late Cretaceous (Hao and Zeng, 1984; Xi et al., 2020). During the deposition of the Middle to Upper Eocene Wulagen Formation and Bashibulake Formation, the seawater retreat from this realm (Bosboom et al., 2011, 2014b; Sun et al., 2016). Extensive magnetostratigraphy and biostratigraphy studies indicate that the seawater retreat from the Tarim Basin around 47 to 41 Ma, with diachronous characteristics (Sun et al., 2016). The complete retreat of the Paratethys Sea from the Tarim Basin marked the cessation of marine sedimentation in the inland regions of China, leading to changes in the Asian marine-continent configuration and atmospheric circulation, intensifying the aridity of the Asian interior (Licht et al., 2016; Xi et al., 2020). Marine deposits in the southern Tibet region are widely distributed, and the highest marine strata are of particular interest due to their association with the collision between the India and Eurasia plates and the uplift of the Himalaya orogeny. Based on current researches, although the disappearance of marine deposits varies across different regions of this realm, most of the highest marine strata in the realm occurred between 45 and 40 Ma. During the late Paleocene to early Eocene, the collision between the India and Eurasia plates occurred, and the Gangdise-Himalaya-Ganga stratigraphic realm began to accumulate thick sequences of conglomerates and sandstones known as the Liuqu Formation. In the Qaidam-Qilian-Western Qinling stratigraphic realm of the northern plateau, the response to the India-Eurasia plate collision resulted in the deposition of coarse clastic sediments such as the Lulehe Formation, Qijiachuan Formation, Xiliugou Formation, and Gepiza Formation in regions like Qaidam, Linxia, Xining, Lanzhou, and Guide Basins (e.g., Fang et al., 2019; Feng et al., 2022). In the Qiangtang-Western Sichuan and Western Margin of Yangtze stratigraphic realms, widespread unconformities exist between the Upper Eocene and Lower Oligocene, possibly attributed to the intense uplift of the southeastern margin of the Qinghai-Tibetan Plateau during the Late Eocene to Early Oligocene (Su et al., 2019b).

4.   Comparison of the Paleogene strata in the Qinghai-Tibetan Plateau and its surrounding regions

The Paleogene marine strata in the Qinghai-Tibetan Plateau and its surrounding regions are mainly concentrated in the Gangdise-Himalaya-Ganga and Tarim-Western Kunlun stratigraphic realms. These realms preserve abundant foraminifera, calcareous nannofossils, dinoflagellates, bivalves, and gastropod fossils (Zhang et al., 2010; Hu et al., 2017; Li J G et al., 2020; Xi et al., 2020; Li, 2021). The biostratigraphy and sedimentary ages of these marine strata are closely related to significant scientific questions such as the collision between the Indian and Eurasian plates and the aridification of the Asian interior. Extensive researches have been conducted, and detailed comparisons and summaries have been made with international standards (Figure 4) (Xi et al., 2020; Li G B et al., 2020; Li, 2021). This article does not focus on these topics further. In contrast, the terrestrial strata of the Paleogene within the Qinghai-Tibetan Plateau are primarily composed of fluvial-lacustrine deposits, including red sandstones, conglomerates, and mudstones with interbedded

gray mudstones. Fossils are relatively scarce, with some reports of ostracod, charophyte and bivalve fossils. Mammalian fossils from the Paleogene are also relatively scarce, and they are mainly distributed in the Qaidam-Qilian-Western Qinling stratigraphic realm and the Western Yunnan stratigraphic subrealm on the northeastern and southeastern margins of the Qinghai-Tibetan Plateau. The discovered Paleogene faunas (Figure 1), including the Gemusi fauna (Irdinmanhan), Lijiang fauna (Sharamurunian), Nanpoping fauna (Ulantatalian), Dingdanggou fauna (Tabenbulukian), Yindirte fauna (Tabenbulukian), Jiaozigou fauna (Tabenbulukian), and Xiagou fauna (Tabenbulukian), predominantly represent the Middle Eocene to Late Oligocene fauna assemblages, and detailed studies have been conducted on the paleogeographic patterns (Wang Y Q et al., 2019; Ni et al., 2020). In contrast, the study of plant fossils has made significant progress in the past decade, especially since the second Tibetan Plateau scientific expedition (Zhou et al., 2023). The age of some fossil floras, that were previously considered to be Miocene, have been revised as Late Eocene to Early Oligocene (Zhou et al., 2023). Moreover, several Paleogene fossil floras have been discovered (Zhou et al., 2023). Extensive research on these floras provides a foundation for understanding the role of the Qinghai-Tibetan Plateau in biotic exchange, constraining the timing of the India-Eurasia plates collision, determining stratigraphic ages, and studying paleogeomorphic evolution.

4.1 A new model of flora exchange through the Qinghai-Tibetan region

Over the last decade, there has been a significant increase in the number of Paleogene floras in the Qinghai-Tibetan Plateau. These include the Liuqu, Jianglang, Relu, Dayu, Xiede, Nima, Xiongmei, Menshi, Shuanghe, Markam, Lühe, Huatugou, Dahonggou, Lanzhou, and Kailas floras (Figure 1). Among these, the Liuqu flora in Lazi County is located on the southern side of the Yarlung Zangbo suture zone, while the remaining floras are situated on the northern side. In the past decade, these floras have been extensively investigated, with numerous reported taxa representing the earliest fossil records of their respective families or genera in Asia and even globally (Zhou et al., 2023). Biogeographical studies of these taxa have revealed that the Paleogene Qinghai-Tibetan region served as a crossroad for global biotic exchange and acted as a harbor for the globally floristic migration (Zhou et al., 2023). The dispersal and exchange of biotas in the Qinghai-Tibetan region exhibit four patterns: into Qinghai-Tibetan region, out of the Qinghai-Tibetan region, out of Indian, and into or out of Africa (Zhou et al., 2023). Recent biogeographical studies on some plant taxa have also indicated a certain connection among the Paleogene floras of Qinghai-Tibetan region, Oceania, Antarctica, and South America.

The Liuqu, Relu, and Menshi floras have yielded a large number of fossil leaves, flowers, and fruits of Myrtaceae (Tao, 1981, 1988; Chen et al., 1983). These leaves characterized by leathery texture, entire margins, linear shape, sickle-shaped curvature, and marginal ultimate venation looped (Tao, 1981, 1988; Chen et al., 1983). These leaf fossils have been identified as belonging to the genus "*Eucalyptus*" (Tao, 1981, 1988; Chen et al., 1983). These floras are dated to the early-middle Eocene (Ding et al., 2017c; He et al., 2022; Zhou et al., 2023). *Eucalyptus* is one of the most representative plant genus in Australia, with a distribution spanning most terrestrial environments of the country, excluding extremely arid, alpine, and saline areas (Thornhill et al., 2019). *Eucalyptus* exhibits high diversity in Australia, with 665 described modern species and an estimated total of over 723 species (Thornhill et al., 2019). Some endemic species are found in Indonesia, Philippines, and Papua New Guinea (Thornhill et al., 2019). However, the fossil record of *Eucalyptus* is scarce. Apart from China, there are only limited fossil records in India, Oceania, and South America. Fossil records of *Eucalyptus* in China and India are the only ones found in the Northern Hemisphere. In Australia, the earliest confirmed *Eucalyptus* fossil is the pollen of *Myrtaceidites eucalyptoides* from the Eyre Formation, dating back to the Middle Eocene (Thornhill and Macphail, 2012). Additionally, *Eucalyptus* capsule fossils have been found in plant assemblages of the same age in Australia, although detailed descriptions are lacking (Greenwood et al., 2000; Hermsen et al., 2012). The earliest accurately identified leaf fossil in Australia is *Eucalyptus kitsonii* (Late Oligocene-Early Miocene), and wood fossils from the Early Miocene (~21 Ma) have also been discovered (Hermsen et al., 2012). Pole (1993, 1994) reported *Eucalyptus* leaf and inflorescence fossils from the Eocene and Lower Miocene of New Zealand. Outside of Oceania, there are also some reports that may be related to *Eucalyptus*. In India, wood fossils of Myrtaceae have been reported from the Late Cretaceous-Early Paleocene Deccan volcanic trap and the Lower Eocene (Shukla et al., 2014; Wheeler et al., 2017). These wood fossils display anatomical features consistent with *Eucalyptus*, *Lophostemon*, *Syncarpia*, and *Tristaniopsis* of Myrtaceae (Wheeler et al., 2017). The distribution of the nearest relatives of these wood fossils is mostly limited to Oceania, suggesting that the India plate had ongoing plant exchange with Oceania during its northward drift (Wheeler et al., 2017). Further morphological and anatomical characteristics are needed to determine if these wood fossils belong to the genus *Eucalyptus* (Wheeler et al., 2017). In the Early Eocene Laguna del Hunco flora (~52 Ma) in Argentina, accurately identified leaf, inflorescence, flower, and pollen fossils related to *Eucalyptus* have been found (Gandolfo et al., 2011; Hermsen et al., 2012; Zamaloa et al., 2020). In China, there have been

reports of leaf and capsule fossils that may be related to *Eucalyptus* in the Liuqu flora (~56 Ma), the Relu flora (45–40 Ma), and the Eocene Menshi flora (Tao, 1981, 1988; Chen et al., 1983; Ding et al., 2017c; He et al., 2022; Zhou et al., 2023). However, the identification of these fossils is controversial. While their leaf shape and marginal veins indicate an affinity with Myrtaceae, they are considered most suitable to be classified as the genus *Myrtophyllum* (Guo, 1986; Guo and Chen, 1989). The preservation of the flowers and fruits is poor, with unclear identification features, preventing definitive classification under *Eucalyptus* at present. Nevertheless, based on the fruit fossils described by Chen et al. (1983), some resemblance to modern *Eucalyptus* is apparent. Further excavation and research on these plant assemblages may provide an opportunity to confirm whether their closest relatives are indeed within *Eucalyptus*.

Previous biogeographical studies of the *Eucalyptus* have mainly focused on discussing the floristic exchange between Australia and nearby islands. The discovery of fossil records beyond Oceania has enriched the biogeography research of *Eucalyptus*. Based on the current fossil evidence, there was biotic exchange among the Eurasian continent, Oceania, Antarctica, and South America during the Eocene. This biotic exchange pattern is also supported by other taxa, such as *Castanopsis* (Fagacene), which show a dispersal pattern from South America to Antarctica, Oceania, and Eurasia (Wilf et al., 2019). The discovery of "*Eucalyptus*" fossils in the Qinghai-Tibetan Plateau also contributes to the understanding of the biotic exchange at the crossroads of the Qinghai-Tibetan region during the Paleogene, involving interactions with the flora of Oceania, Antarctica, and South America.

4.2　Plant fossils to constrain the timing of the India-Eurasia collision

The timing of the collision between the India and Eurasia plates has always been a challenging and crucial topic in the research of the Qinghai-Tibetan Plateau. Previous studies have attempted to explore the timing of the collision and the initial location of collision using methods such as the age of the highest marine sedimentary strata, changes in oceanic spreading rates, exchange of materials and provenance shifts in peripheral foreland basins, and paleomagnetic analysis. However, each method has its shortcomings (Wang et al., 2014; Ding et al., 2017b). The disappearance of barriers that previously separated continents promotes the biotic exchange across these regions (Vermeij, 1991). As India approached and collided with Eurasia, there would have been frequent exchange of flora and fauna between the two continents. Biogeographical studies of plant and animal fossils from both continents can provide an opportunity to understand plate collision timing through the lens of biotic ex-

change. However, due to poor studies on animal and plant fossils in the Qinghai-Tibetan region, the role of animal and plant fossils in constraining the timing of plate collision has been overlooked in previous research.

Within the rich Paleogene fossil floras of the Qinghai-Tibetan Plateau, the Liuqu flora is located on the southern side of the Yarlung Zangbo suture zone. The Liuqu flora has yielded abundant fossils of "*Eucalyptus*" and Arecaceae (Coryphoideae, *Sabalites* sp.). These fossil species also occur in the Relu Formation (He et al., 2022), Gongjue Formation (He et al., 1983), and Niubao Formation (Su et al., 2019a) north of the Yarlung Zangbo suture zone. With further in-depth research, the geographic evolution and distribution of these fossil species across the suture zone provide an opportunity to explore the timing of the India-Eurasia plates collision through plant fossils.

During the Paleogene, palm fossils are abundant in the Qinghai-Tibetan Plateau. Researchers have employed climatic factors (mean temperature of the coldest month) that constrain the distribution of modern palm species, along with climate models, to quantitatively reconstruct the geomorphic evolution history of certain regions in the Qinghai-Tibetan Plateau (Su et al., 2019a; Xiong et al., 2020; Spicer et al., 2021). The fossil record of the palm is extensive and distributed globally (Kumar et al., 2022; Song et al., 2022). A review of Arecaceae subfamily Coryphoideae fossils from the Indian subcontinent, Qinghai-Tibetan Plateau, and surrounding regions indicates that the earliest fossil records found on the India plate are leaf fossils from the Deccan volcanic trap, dating back to the Late Cretaceous-Early Paleocene (66–64 Ma) (Kumar et al., 2022). The next significant discovery is palm leaf fossils from the Liuqu flora (Tao, 1988; Ding et al., 2017c). The earliest *Sabalites* sp. discovered in the Eurasian part of the Qinghai-Tibetan Plateau are from the red beds of Gongjue Formation (He et al., 1983), followed by palm fossils from the lacustrine shale of the Niubao Formation in the Lunpola Basin, northern Tibet (Su et al., 2019a). Although the age of the Gongjue Formation remains controversial (Wang L et al., 2022), the volcanic ash of the overlying Ranmugou Formation confirms its deposition prior to 54 Ma (Xiong et al., 2020). Therefore, it can be inferred that *Sabalites* sp. (Coryphoideae) had already spread from the India plate to Eurasia plate across the Yarlung Zangbo suture zone during the Paleocene to Early Eocene period, and the collision of India-Eurasia plates occurred approximately between 65 and 54 Ma. Further refinement of the dating of *Sabalites* sp. from the Gongjue Formation, as well as the discovery of more fossil specimens, can provide more precise constraints on the timing of the collision.

Similar to the *Sabalites*, fossil groups such as "*Eucalyptus*" and *Ailanthus maximus* indicate that the collision of these two plates occurred during the Paleocene to Middle Eocene

(Liu et al., 2019). Studies on the evolution of Paleogene fauna and paleogeographic patterns in Asia have also inferred that the initial formation of the India-Asia animal dispersal corridor took place between 64.8 and 61.3 Ma (Ni et al., 2020), which is close to the geological evidence of the collision between the India and Eurasia plates (Ding et al., 2005; Ding et al., 2017b). The collision between the India and Eurasia plates also greatly facilitated biotic exchange. Research has found evidence of mammalian exchange between India and Asia prior to the Early Eocene (~54.5 Ma) (Rose et al., 2014).

It should be noted that, like other commonly used methods, using plant fossils to constrain the timing of plate collisions also has its limitations. The dispersal of plant seeds is mostly limited to short distances, nonetheless, around 1% of plant species can disperse over long distances through various factors such as animals, water, and airflows (Wu Z Y et al., 2022). When using plant fossils to investigate plate collision timing, further research is needed on the dispersal processes of their extant nearest relatives, as well as the germination characteristics, water tolerance, salt tolerance of seeds. Additionally, plants can also use islands in the ocean as "stepping stones" for long-distance dispersal (Ali and Aitchison, 2008), and direct contact between the two plates is not necessarily required. However, it is foreseeable that as more fossils are unearthed and the absolute ages becomes more refined, biogeographic studies of numerous fossil species across the two plates will better constrain the timing of plate collisions.

4.3 Biostratigraphic implications of some plant fossil species

The distribution of plants is frequently constrained by specific climate and environmental factors, leading to significant regional variation. In particular, the Qinghai-Tibetan Plateau and its surrounding regions have experienced intense tectonic activity, significant geomorphological variations, and diverse climates during the Cenozoic. As a result, in this region, plant fossils from the Cenozoic do not exhibit prominent characteristics for indicating stratigraphic ages and have been rarely utilized in biostratigraphic studies.

In recent years, extensive studies on fossil floras in the Qinghai-Tibetan Plateau and its surrounding regions have revealed the significant stratigraphic implications of certain extinct taxa and newly discovered genera and species (Figures 5 and 6). For example, the extinct genus *Lagokarpos*, although its nearest extant relatives have not been determined, exhibits distinct morphological features, including two elongated wings resembling rabbit ears attached to the top of the fruit (Tang et al., 2019). This genus is exclusively found in the Jianglang flora of the Qinghai-Tibetan Plateau, the Green River flora of the United States, and the Messel

flora of Germany, indicating a Late Paleocene to Early Eocene age (Tang et al., 2019; Su et al., 2020). No such fossils have been found in strata younger than this time period (Tang et al., 2019; Su et al., 2020). Therefore, the presence of *Lagokarpos* can constrain the stratigraphic age to the Ypresian-Lutetian of the Eocene in this region. Fossil species such as *Plibinia*, *Banksia*, and *Comptonia* are predominantly found in the Upper Paleocene to Upper Eocene strata in China (Li, 2002). These taxa have also been reported in the Lijiang Formation, Ninglang Formation, Relu Formation, and Niubao Formation, allowing the stratigraphic age to be constrained to the Late Paleocene to Late Eocene. Taxa like *Cedrelospermum* (Jia et al., 2019), *Limnobiophyllum* (Low et al., 2019), and *Ailanthus maximus* (Liu et al., 2019) first appear in the middle part of the Niubao Formation and are absent in subsequent strata. Based on current research, their stratigraphic age can be limited to the Lutetian to Bartonian stages of the Eocene. Alpine oak fossils from the Markam flora represent the earliest records so far and have been extensively found in the plateau and surrounding flora during the Neogene (Chen et al., 2021). Their pollen fossils can be further distinguished from other evergreen oaks through scanning electron microscopy (Denk and Tekleva, 2014). The appearance of leaves and pollen fossils of alpine oaks can limit the stratigraphic age to the Late Eocene and onwards (since the Priabonian). The Markam flora has also reported several taxa, such as *Elaeagnus tibetensis*, *Hemitrapa alpina*, and *Tsuga asiatica*, which are the earliest records in Asia or globally (Su et al., 2014, 2018; Wu et al., 2020). The appearance of these species can limit the depositional age of the strata since the Eocene-Oligocene transition. Furthermore, while *Betula*, *Alnus*, and *Carpinus* have a long fossil history (Tao and Du, 1987; Xu H et al., 2019), their earliest occurrence in the Qinghai-Tibetan Plateau and its surrounding regions are in the Lawula Formation (Su et al., 2019b; Xu H et al., 2019; Deng W et al., 2020), which can also contribute to the stratigraphic age determination to some extent. Leaf fossils of *Populus* primarily occurs in the Shangganchaigou Formation (Song et al., 2020) and the lower part of the Xianshuihe Formation (Geng et al., 2001) in the northern part of the plateau, as well as in the latest Late Oligocene Kailas flora in the southern part of the plateau (Ai et al., 2019), limiting the stratigraphic age since the Oligocene. *Podocarpium*, an extinct genus of Fabaceae, has a widespread distribution in the northern hemisphere and can be easily identified due to its distinct characteristics (Li et al., 2022). The earliest records are from the Middle Eocene in the Changchang Basin, Hainan (Xu et al., 2015), followed by the Late Eocene Xiongmei flora (Li et al., 2022), Early Oligocene Dahonggou and Huatugou floras (Yan et al., 2018; Han et al., 2020), and Early-Middle Miocene Zeku flora (Li et al., 2021) on the Qinghai-Tibetan Plateau. Recent study of the Middle Eocene Relu flora (He et al., 2022) has also found
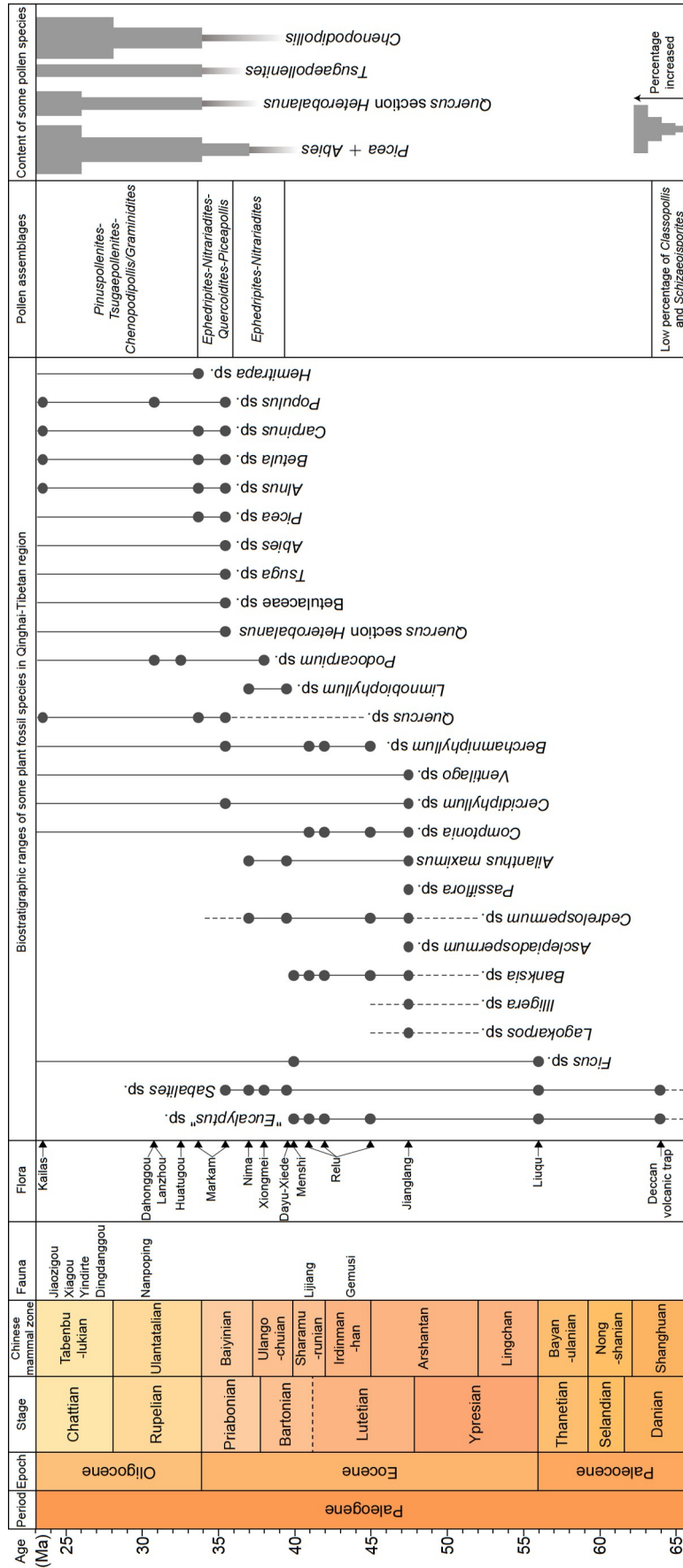
Figure 5 Biostratigraphic ranges of plant fossil species found in the Qinghai-Tibetan Plateau and its surrounding regions, and their implications for depositional age.
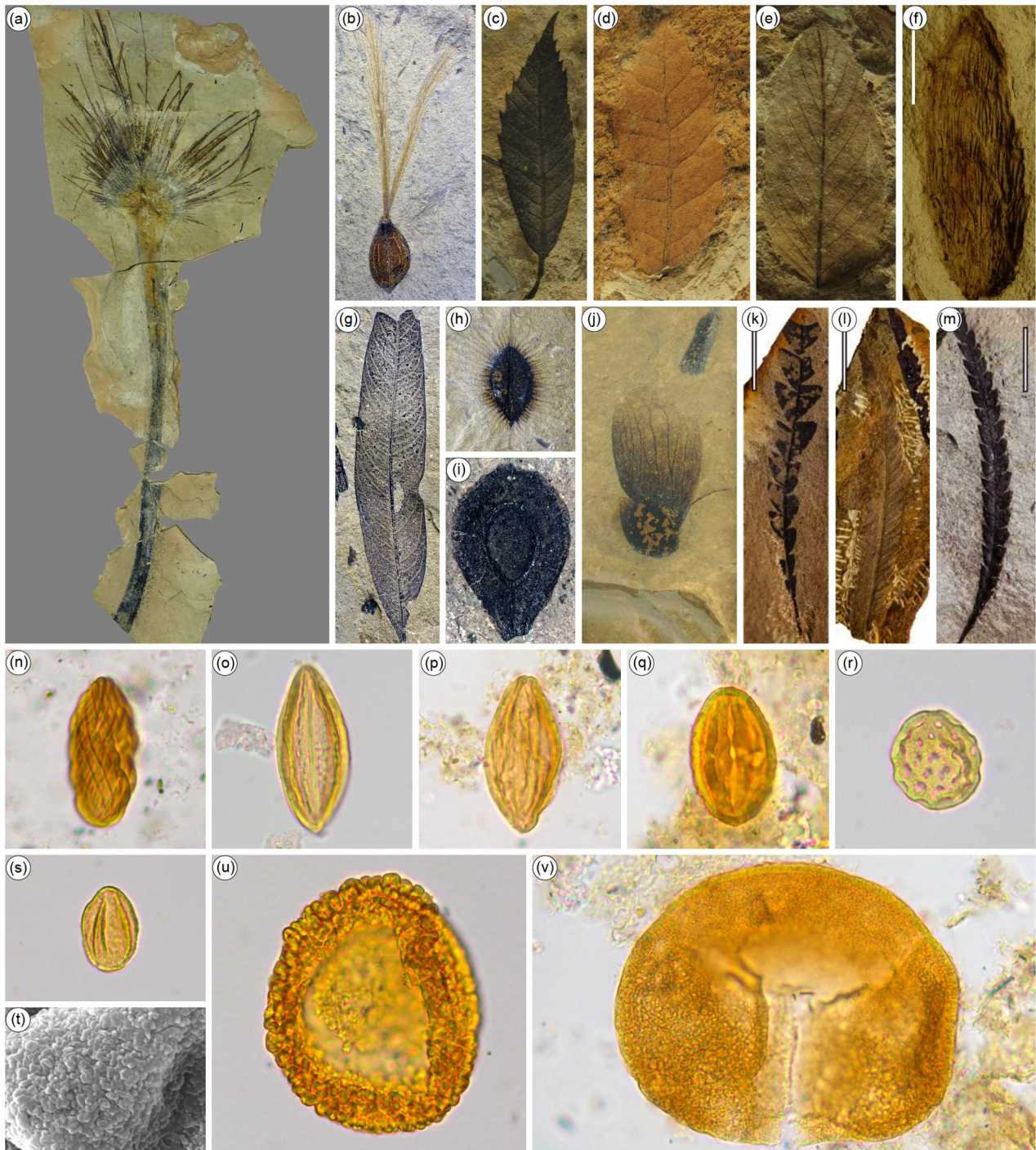
Figure 6 Plant and pollen species with significant biostratigraphic implications from the Paleogene terrestrial strata of the Qinghai-Tibetan Plateau and its surrounding regions. (a) *Sabalites tibetensis* (Dayu flora) (Su et al., 2019a); (b) *Lagokarpos tibetensis* (Jianglang flora) (Tang et al., 2019); (c) *Quercus tibetensis* (Markam flora) (Xu et al., 2016); (d) *Quercus* cf. *presenescens* (Markam flora) (Chen et al., 2021); (e) *Berhamniphyllum junrongiae* (Markam flora) (Zhou et al., 2020); (f) *Tsuga asiatica* (Markam flora) (Wu et al., 2020); (g) Myrtales (Jianglang flora) (Su et al., 2020); (h) *Illigera eocenica* (Jianglang flora) (Wang T X et al., 2021); (i) *Asclepiadospermum marginatum* (Jianglang flora) (Del Rio et al., 2020); (j) *Cedrelospermum tibeticum* (Dayu and Nima floras) (Jia et al., 2019); (k) *Palibinia pinnatifida* (Relu flora) (He et al., 2022); (l) "*Eucalyptus*" *relunensis* (Relu flora) (He et al., 2022); (m) *Banksia puryearemsis* (Relu flora) (He et al., 2022); (n) *Schizaeoisporites* (Yunlong Formation); (o) *Ephedripites* (*Distachyapites*) (Yaxicuo Formation); (p) *Ephedripites* (*Ephedripites*) (Dingqinghu Formation); (q) *Nitrariadites* (Dingqinghu Formation); (r). *Chenopodipollis* (Dingqinghu Formation); (s) (Lawula Formation); (t) Ornamentation of *Quercus* section *Heterobalanus* in Scanning Electron Microscope (Lawula Formation); (u) *Tsugaepollenites* (Lawula Formation); (v) *Piceapollis* (Lawula Formation).

fossil records of *Podocarpium*. Therefore, in the Qinghai-Tibetan Plateau and its surrounding regions, *Podocarpium* can constrain the stratigraphic age to the Middle Eocene and onwards. Fossilized plant thorns and spines, which serve as

physical defense traits against large herbivores, have been discovered in the early Late Eocene Dayu and Xiede floras, with relatively high diversity (Zhang et al., 2022). The absence of these structures in earlier fossil floras in this region (Zhang et al., 2022), indicates that the appearance of fossilized plant thorns and spines can be limited to the early Late Eocene and onwards.

Pollen grains have been widely used in the study of biostratigraphy due to their widespread dispersal and resistance to preserve (Miao et al., 2016; Li et al., 2019; Liu et al., 2021). Pollen grains of *Abies* and *Picea* are commonly found in the pollen assemblages of the Qinghai-Tibetan Plateau and its surrounding regions. *Abies* and *Picea* are characteristic and dominant components of sub-alpine coniferous forests and cold-temperate coniferous forests in the northern hemisphere (Fu et al., 1999; Xiang et al., 2006). The modern distribution ranges of these two genera are very similar, primarily distributed in the subarctic to temperate regions of the northern hemisphere, with some species occurring in subtropical high mountains (Fu et al., 1999; Xiang et al., 2006). In China, the distribution range of *Abies* is similar to that of *Picea*, primarily found in the eastern and southeastern mountainous regions of the Qinghai-Tibetan Plateau (Fu et al., 1999; Xiang et al., 2006). Both *Abies* and *Picea* have a wide vertical distribution range, but in the Qinghai-Tibetan Plateau and its surrounding regions, they are mainly concentrated at elevations ranging from 2500 to 4000 m (Fu et al., 1999; Liu et al., 2002; Xiang et al., 2006). The distribution altitude decreases with increasing latitude, while the presence of the Qinghai-Tibetan Plateau results in a significant increase in elevation on the eastern and southern region (Liu et al., 2002). Studies on the modern distribution of *Abies* and *Picea* in China suggest that western Sichuan and northern Yunnan serve as modern distribution centers for these genera (Liu et al., 2002; Xiang et al., 2006). In the Upper Eocene of northeastern Tibet, the pollen percentage of *Abies* and *Picea* can reach up to 3.8% (Song and Liu, 1982). The pollen of *Abies* and *Picea* is also commonly found in the Upper Eocene of the Qaidam Basin (Song et al., 1983; Wang et al., 1986). In the Upper Eocene of the Jiuquan Basin, the content of *Abies* and *Picea* is relatively high, with some samples having a percentage exceeding 10% for both genera (Miao et al., 2008). In the Upper Eocene of the Xining Basin, there is a sudden increase in the percentage of *Abies* and *Picea* (Dupont-Nivet et al., 2008; Hoorn et al., 2012). During the Oligocene of the Qinghai-Tibetan Plateau and its surrounding regions, the content of *Abies* and *Picea* generally increases (Miao et al., 2013; Sun et al., 2014; Wu et al., 2019; Tang et al., 2020; Xie et al., 2021b). Cenozoic stratigraphic chronology researches from the Xining Basin indicate that the increase in the percentage of *Abies* and *Picea* occurred at 36.6 Ma (Abels et al., 2011). Prior to the Late Eocene, the pollen of *Abies* and *Picea* is generally absent or occasionally

present in the strata (Song and Li, 1982; Song and Liu, 1982; Miao et al., 2016). Fossil floras discovered before the Late Eocene, such as the Liuqu, Jianglang, Dayu, Nima, and Xiongmei floras, are dominated by angiosperms, with no findings of gymnosperms. However, in the Late Eocene MK3 fossil layer of Markam flora, gymnosperm fossils such as *Picea*, *Abies*, and *Tsuga* have been found (Deng W et al., 2020; Wu et al., 2020). Therefore, the increase in percentage of *Abies* and *Picea* within the Qinghai-Tibetan Plateau and its surrounding regions can be used to constrain the stratigraphic age since the Late Eocene. This also indicates the presence of numerous mid to high elevation landforms, supporting the growth of subalpine coniferous forests.

In the Qinghai-Tibetan Plateau and its surrounding regions, *Tsuga* generally forms pure forests or coexists with *Picea* and *Abies* forests in the lower part of the subalpine coniferous forests. In the Late Eocene pollen assemblages of this region, *Tsuga* pollen is occasionally encountered (Hoorn et al., 2012; Miao et al., 2016; Yuan et al., 2020). During the Eocene-Oligocene transition, *Tsuga* plays an important role in the pollen assemblages (Li, 2004; Li et al., 2019). The earliest and most reliable record of *Tsuga* macrofossils is the cone fossils from the late Late Eocene MK3 fossil layer of the Markam flora (Wu et al., 2020). *Tsuga* cone fossils have also been found in the Early Oligocene Lühe flora (Wu et al., 2020).

Additionally, some drought-tolerant plant pollen taxa also hold significant chronostratigraphic implications (Figure 6). For example, the pollen genus *Classopollis* was mainly abundant during the Mesozoic and persisted into the early Paleogene, such as the Aertashi Formation and Talake Formation in the Tarim Basin (Wang et al., 1986), as well as the Yunlong Formation and Mengyejing Formation in Western Margin of Yangtze stratigraphic realm (Song et al., 1976). The pollen genus *Schizaeoisporites*, which is abundant in the Late Cretaceous, becomes less common in the lower Paleogene strata of the Qinghai-Tibetan Plateau and its surrounding regions (Song et al., 1976; Sun et al., 1980). The monolete of this genus is often not prominent or difficult to observe, and this type of pollen may be related to Ephedraceae. Prior to the Eocene, drought-tolerant plants in the Qinghai-Tibetan Plateau and its surrounding regions were mainly represented by the genera *Ephedripites* and *Nitrariadites* (Li et al., 2019; Barbolini et al., 2020). Conversely, since the Oligocene, shrubs dominated by *Chenopodipollis* have rapidly expanded in the central and northern parts of the plateau (Li et al., 2019).

4.4   Geomorphic evolution of the Qinghai-Tibetan region during the Paleogene

The quantitative reconstruction of paleoelevation stands as a central focus and challenge in the study of the formation and

evolution of the Qinghai-Tibetan Plateau (Spicer et al., 2021; Ding et al., 2022; Zhou et al., 2023). Plant fossils play an irreplaceable role in these studies. In recent years, as many as 15 Paleogene floras have been newly discovered or age revised in the Qinghai-Tibetan Plateau (Figure 1). Researchers generally rely on the distribution of nearest relatives (Xu et al., 2016; Ai et al., 2019; Su et al., 2019a; Xie et al., 2021b), or use the leaf characteristics of fossil floras to reconstruct paleoelevations (Ding et al., 2017c; Su et al., 2019b, 2020; Song et al., 2020; He et al., 2022; Wu M X et al., 2022). Furthermore, the results of paleoelevation reconstruction based on plant fossils are supported by other geochemical reconstructions (Xu et al., 2018; Xiong et al., 2022).

The central valley, stretching along the Bangong-Nujiang suture zone in the northern part of the Lhasa terrane, was flanked by the towering Central Watershed Mountains and the Gangdise Mountains during the Paleogene (Su et al., 2019a, 2020; Spicer et al., 2021; Ding et al., 2022; Xiong et al., 2022). This valley experienced a remarkable uplift from the Middle Eocene (~1500 m) to the early Late Eocene (~2850 m) (Su et al., 2019a, 2020; Spicer et al., 2021; Ding et al., 2022; Xiong et al., 2022). It further uplifted to its present elevation during the Oligocene or Neogene (Liu et al., 2019). The Middle Eocene Jianglang flora within the central valley is characterized by a rich diversity, with nearest modern relatives predominantly distributed in tropical or subtropical regions (Su et al., 2020). Referred to as the "Shangri-La"-like warm and moist ecosystem, it represents an unknown paleoecosystem hosting high biodiversity in the central Qinghai-Tibetan region (Su et al., 2020). The early Late Eocene Dayu and Xiede floras contain abundant plant thorns and spines, exhibiting a high diversity of morphological types (Zhang et al., 2022). These floras also contain a large number of herbaceous plant fossils and their phytoliths, indicating a transition from closed forests to open woodland within the central valley with a warm and relatively dry climate during this period (Zhang et al., 2022). The late Oligocene floras and pollen assemblages indicate further uplift of the central valley, with the dominance of *Abies* and *Picea* indicating the presence of a subalpine coniferous forest (Sun et al., 2014; Wu et al., 2019; Xie et al., 2021a, 2021b). Additionally, arid vegetation dominated by *Chenopodium*, *Ephedra*, and *Nitraria* has increased, accompanied by a generally humid climate and reduced temperature (Sun et al., 2014; Wu et al., 2019; Xie et al., 2021a, 2021b). In the southern part of the Lhasa terrane along the Yarlung Zangbo suture zone, low-elevation basins are distributed. From the Paleocene-Eocene transition Liuqu flora to the late Oligocene Kailas flora and the early Miocene Qiabulin flora, these basins experienced an elevation shift from below 1000 m to approximately 2300 m (Ding et al., 2017c; Ai et al., 2019; Ding et al., 2022). Although the Lhasa terrane accreting to the Qiangtang terrane in the Mesozoic and the India plate

attachment with the southern part of the Lhasa terrane in the early Paleogene (Ding et al., 2017a), these low-elevation basins distributed along the suture zone remained stable throughout the Paleogene (Liu et al., 2019). They have served as an ideal corridor for the exchange of fauna and flora between the Qinghai-Tibetan region and the Indian subcontinent (Liu et al., 2019; Deng et al., 2021; Zhou et al., 2023). However, in the late Paleogene or Neogene, as the India plate continued to subduct and compress, these low-elevation basins along the suture zone disappeared (Liu et al., 2019). The establishment of the modern topographic pattern of the Qinghai-Tibetan Plateau created a barrier for the exchange of low-elevation biota with the surrounding regions (Liu et al., 2019). The Himalaya orogeny in the southern part of the plateau lacks Paleogene floras. However, based on the Liuqu, Menshi, Kailas, and Qiabulin floras in its northern part, as well as their warm and humid paleoenvironment, it can be inferred that the elevation of the Himalaya orogeny was relatively low at least before the Middle Miocene, without significant barriers to the northward penetration of Indian Ocean moisture. The Hengduan Mountain in the southeastern margin of the plateau, on the other hand, formed their modern topographic pattern during the late Eocene to early Oligocene. Evidence from the Relu, Markam, and Lühe floras suggests that the Relu flora already harbored a small number of plant taxa that still exist in the Hengduan Mountain today, while most other taxa have become extinct (Chen et al., 1983; Guo, 1986; He et al., 2022). The main components of the Markam and Lühe floras are consistent with the vegetation types currently distributed in the Hengduan Mountain, indicating that the modernized vegetation of the Hengduan Mountain had already formed during the Eocene-Oligocene transition (Linnemann et al., 2018; Su et al., 2019b; Wu M X et al., 2022). In the northern part of the plateau, paleoelevation reconstruction based on the Dahonggou flora in the Qaidam Basin indicates that the area had already reached its present-day elevation during the early Oligocene (Song et al., 2020). However, recent paleoelevation reconstructions based on multiple pollen assemblages and the Huaitoutala flora suggest that the Qaidam Basin underwent a significant uplift from an elevation lower than 1400 m to its current elevation during the middle to late Miocene (Miao et al., 2022).

5. Limitations and prospects

In recent years, significant achievements have been made in the study of the Paleogene stratigraphy, paleobiology, and biogeography in the Qinghai-Tibetan Plateau and its surrounding regions. Absolute dating and magnetostratigraphic researches have provided a comparative framework for understanding sedimentary chronology across different strati-

graphic realms (e.g., Ding et al., 2017c; Su et al., 2019b, 2020; Fang et al., 2021). The discovery of numerous fossil species have indicated the Qinghai-Tibetan region as an importance hub for biotic exchange during the Paleogene (e. g., Deng T et al., 2020; Deng et al., 2021; Zhou et al., 2023).

Based on current research, the marine sediments in the Tarim-Western Kunlun and Gangdise-Himalaya-Ganga realms are rich in fossils and relatively continuous. Fossil studies in these areas have reached a high level, and biostratigraphic framework has been established for fossil correlation with international standards (Xi et al., 2020; Li J G et al., 2020; Li, 2021). In comparison, the study of terrestrial sediments is relatively limited. The Paleogene terrestrial deposits in the plateau and its surrounding regions are mainly composed of red coarse clastic sediments, where the preservation of plant and animal fossils is poor. Currently, rich collections of plant and animal fossils have only been found in a few sandstone layers or interbedded in gray mudstone, siltstone, and oil shale (e.g., Ai et al., 2019; Su et al., 2019a, 2020; Deng W et al., 2020; He et al., 2022; Ni et al., 2023). Given the vast expanse of the Qinghai-Tibetan Plateau, the existing Paleogene paleontological records remain insufficient to reveal the complete picture of paleogeographic evolution in this region (Zhou et al., 2023).

This study attempts to use plant fossils to constrain the age of the strata, the timing of the India-Eurasia plate collision, and the biogeographic evolution of some important groups. These efforts are based on the current research of various stratigraphic realms and paleobiota. The fossil record is characterized by discontinuity and incompleteness, and as further research on paleobiology and chronology in the plateau and its surrounding regions progresses, some of the conclusions obtained so far will be further refined and revised. The integration of biostratigraphy, magnetostratigraphy, isotope dating, and cyclostratigraphy, among other research approaches, will contribute to the establishment of a comprehensive biostratigraphic framework for the Qinghai-Tibetan Plateau and its surrounding regions (Xi et al., 2020; Zhou et al., 2023).

6. Conclusion

The Paleogene period is a crucial time for the formation of the modern geomorphic pattern, monsoon climate, and modern flora in the plateau. Based on previous research findings and recent studies on biostratigraphy, isotope dating, magnetostratigraphy, and sedimentary stratigraphy, this paper focuses on reviewing terrestrial stratigraphic units and their ages in different stratigraphic realms of the plateau and explores the paleobiota and their paleogeographic evolution. Since the initiation of the second Tibetan Plateau scientific expedition, there has been a continuous enrichment of Pa-

leogene floras in the plateau and its surrounding regions. The extensive research conducted on these floras provides a foundation for understanding the role of the plateau in biotic exchange, determining the timing of the India-Eurasia plate collision, and constraining stratigraphic ages. The geobiogeographic evolution of plant fossils, such as the "*Eucalyptus*", provides a new model for biotic exchange between the Paleogene Qinghai-Tibetan region and the Gondwana flora. The evolutionary history of important taxa in fossil floras on both sides of the Yarlung Zangbo suture zone can constrain the timing of the India-Eurasia collision to the range of 65–54 Ma. The significance of extinct or newly appearing species in the Paleogene floras for stratigraphic ages is discussed. The paleoelevation reconstruction based on pollen assemblages and plant fossils indicates that the Hengduan Mountain had already formed its current geomorphological pattern before the Early Oligocene; The Paleogene lowland environments in the vicinity of major suture zones provided warm and humid conditions, serving as significant corridors for biotic exchange through the Qinghai-Tibetan region; The Himalaya orogeny had relatively lower elevation before the Neogene and did not effectively hinder the northward moisture transport from the Indian Ocean.

Conflict of interest   The authors declare that they have no conflict of interest.

References

Abels H A, Dupont-Nivet G, Xiao G, Bosboom R, Krijgsman W. 2011. Step-wise change of Asian interior climate preceding the Eocene-Oligocene Transition (EOT). Palaeogeogr Palaeoclimatol Palaeoecol, 299: 399–412

Acharyya S K. 2007. Evolution of the Himalayan Paleogene foreland basin, influence of its litho-packet on the formation of thrust-related domes and windows in the Eastern Himalayas—A review. J Asian Earth Sci, 31: 1–17

Ai K, Shi G, Zhang K, Ji J, Song B, Shen T, Guo S. 2019. The uppermost Oligocene Kailas flora from southern Tibetan Plateau and its implications for the uplift history of the southern Lhasa terrane. Palaeogeogr Palaeoclimatol Palaeoecol, 515: 143–151

Ali J R, Aitchison J C. 2008. Gondwana to Asia: Plate tectonics, paleogeography and the biological connectivity of the Indian sub-continent from the Middle Jurassic through latest Eocene (166–35 Ma). Earth-Sci Rev, 88: 145–166

Bai B. 2023. Reappraisal of some perissodacyl fossils from the Middle Eocene of the Lijiang Basin, Yunnan, China with a revision of tapiroid

Diplolophodon (in Chinese). Vertebr Palasiat, 61: 26–42

Bai P R, Zeng Y R, Li Y S, Huang J G, Liao Z M, Ma D S, Fu H B, Mo C H, Guo H, Fan H F. 2017. Discovery and Its Significance of the Eocene Plant Fossils in the Kongnongla Area from the Southeast Margin Bangor Basin in Northern Tibet (in Chinese). Guizhou Geol, 34: 301–305

Baig M S, Munir M. 2007. Foraminiferal biostratigraphy of Yadgar area, Muzaffarabad Azad Kashmir, Pakistan. J Himal Earth Sci, 40: 33–43

Barbolini N, Woutersen A, Dupont-Nivet G, Silvestro D, Tardif D, Coster P M C, Meijer N, Chang C, Zhang H X, Licht A, Rydin C, Koutsodendris A, Han F, Rohrmann A, Liu X J, Zhang Y, Donnadieu Y, Fluteau F, Ladant J B, Le Hir G, Hoorn C. 2020. Cenozoic evolution of the steppe-desert biome in Central Asia. Sci Adv, 6: eabb8227

Beck R A, Burbank D W, Sercombe W J, Riley G W, Barndt J K, Berry J R, Afzal J, Khan A M, Jurgen H, Metje J, Cheema A, Shafique N A, Lawrence R D, Khan M A. 1995. Stratigraphic evidence for an early collision between northwest India and Asia. Nature, 373: 55–58

Benton M J, Wilf P, Sauquet H. 2022. The Angiosperm Terrestrial Revolution and the origins of modern biodiversity. New Phytol, 233: 2017–2035

Bhatia S B, Bhargava O N. 2006. Biochronological continuity of the Paleogene sediments of the Himalayan Foreland Basin: Paleontological and other evidences. J Asian Earth Sci, 26: 477–487

Bosboom R E, Dupont-Nivet G, Houben A J P, Brinkhuis H, Villa G, Mandic O, Stoica M, Zachariasse W J, Guo Z J, Li C X, Krijgsman W. 2011. Late Eocene sea retreat from the Tarim Basin (west China) and concomitant Asian paleoenvironmental change. Palaeogeogr Palaeoclimatol Palaeoecol, 299: 385–398

Bosboom R, Dupont-Nivet G, Grothe A, Brinkhuis H, Villa G, Mandic O, Stoica M, Kouwenhoven T, Huang W, Yang W, Guo Z J. 2014a. Timing, cause and impact of the late Eocene stepwise sea retreat from the Tarim Basin (west China). Palaeogeogr Palaeoclimatol Palaeoecol, 403: 101–118

Bosboom R, Dupont-Nivet G, Grothe A, Brinkhuis H, Villa G, Mandic O, Stoica M, Huang W, Yang W, Guo Z, Krijgsman W. 2014b. Linking Tarim Basin sea retreat (west China) and Asian aridification in the late Eocene. Basin Res, 26: 621–640

Cai C, Huang D Y, Wu F X, Zhao M, Wang N. 2019. Tertiary water striders (Hemiptera, Gerromorpha, Gerridae) from the central Tibetan Plateau and their palaeobiogeographic implications. J Asian Earth Sci, 175: 121–127

Cai X Y, Fu J H. 2003. Paleocene and Eocene Palaeobiocoenotic feature in the Dazhuoma section at Gangni village of Qiangtang Basin (in Chinese). J Northwest Univ-Nat Sci Ed, 33: 443–448

Cao W, Xi D, Melinte-Dobrinescu M C, Jiang T, Wise Jr. S W, Wan X. 2018. Calcareous nannofossil changes linked to climate deterioration during the Paleocene-Eocene thermal maximum in Tarim Basin, NW China. Geosci Front, 9: 1465–1478

Carvalho M R, Jaramillo C, de la Parra F, Caballero-Rodríguez D, Herrera F, Wing S, Turner B L, D'Apolito C, Romero-Báez M, Narváez P, Martínez C, Gutierrez M, Labandeira C, Bayona G, Rueda M, Paez-Reyes M, Cárdenas D, Duque Á, Crowley J L, Santos C, Silvestro D. 2021. Extinction at the end-Cretaceous and the origin of modern Neotropical rainforests. Science, 372: 63–68

Chen L L, Deng W Y D, Su T, Li S F, Zhou Z K. 2021. Late Eocene sclerophyllous oak from Markam Basin, Tibet, and its biogeographic implications. Sci China Earth Sci, 64: 1969–1981

Chen M H, Kong Z C, Chen Y. 1983. On the discovery of paleogene flora from the western Sichuan Plateau and its significance in phytogeography (in Chinese). Acta Botan Sin, 25: 482–491

Chen P R, Del Rio C, Huang J, Liu J, Zhao J G, Spicer R A, Li S F, Wang T X, Zhou Z K, Su T. 2022. Fossil capsular valves of *Koelreuteria* (Sapindaceae) from the Eocene of central Tibetan Plateau and their biogeographic implications. Int J Plant Sci, 183: 307–319

Dai J G, Fox M, Shuster D L, Hourigan J, Han X, Li Y L, Wang C S. 2020. Burial and exhumation of the Hoh Xil Basin, northern Tibetan Plateau: Constraints from detrital (U-Th)/He ages. Basin Res, 32: 894–915

Dai J G, Li Y L, Ge Y K. 2013. Detrital zircon U-Pb age and Hf isotopic composition, and detrital apatite (U-Th)/He age from the Paleogene sediments of Changsha-Gongma Basin, the Songpan-Ganzi block and their geological significance (in Chinese). Acta Petrol Sin, 29: 1003–1016

Dai S, Fang X, Dupont-Nivet G, Song C, Gao J, Krijgsman W, Langereis C, Zhang W. 2006. Magnetostratigraphy of Cenozoic sediments from the Xining Basin: Tectonic implications for the northeastern Tibetan Plateau. J Geophys Res, 111: B11102

Dai S, Fang X, Song C, Gao J, Gao D, Li J. 2005. Early tectonic uplift of the northern Tibetan Plateau. Chin Sci Bull, 50: 1642

DeCelles P G, Kapp P, Gehrels G E, Ding L. 2014. Paleocene-Eocene foreland basin evolution in the Himalaya of southern Tibet and Nepal: Implications for the age of initial India-Asia collision. Tectonics, 33: 824–849

DeCelles P G, Quade J, Kapp P, Fan M, Dettman D L, Ding L. 2007. High and dry in central Tibet during the Late Oligocene. Earth Planet Sci Lett, 253: 389–401

DeCelles P G, Gehrels G E, Najman Y, Martin A J, Carter A, Garzanti E. 2004. Detrital geochronology and geochemistry of Cretaceous-Early Miocene strata of Nepal: implications for timing and diachroneity of initial Himalayan orogenesis. Earth Planet Sci Lett, 227: 313–330

Del Rio C, Wang T X, Liu J, Liang S Q, Spicer R A, Wu F X, Zhou Z K, Su T. 2020. Asclepiadospermum gen. nov., the earliest fossil record of Asclepiadoideae (Apocynaceae) from the early Eocene of central Qinghai-Tibetan Plateau, and its biogeographic implications. Am J Bot, 107: 126–138

Del Rio C, Wang T X, Li S F, Jia L B, Chen P R, Spicer R A, Wu F X, Zhou Z K, Su T. 2022. Fruits of *Firmiana* and *Craigia* (Malvaceae) from the Eocene of the Central Tibetan Plateau with emphasis on biogeographic history. J Sytematics Evol, 60: 1440–1452

Deng T, Ding L. 2015. Paleoaltimetry reconstructions of the Tibetan Plateau: Progress and contradictions. Natl Sci Rev, 2: 417–437

Deng T, Lu X, Wang S, Flynn L J, Sun D, He W, Chen S. 2021. An Oligocene giant rhino provides insights into *Paraceratherium* evolution. Commun Biol, 4: 639

Deng T, Wu F, Zhou Z, Su T. 2020. Tibetan Plateau: An evolutionary junction for the history of modern biodiversity. Sci China Earth Sci, 63: 172–187

Deng T. 2004. Evolution of the late Cenozoic mammalian faunas in the Linxia Basin and its background relevant to the uplift of the Qinghai-Xizang Plateau (in Chinese). Quat Sci, 24: 413–420

Deng W, De Franceschi D, Xu X, Del Rio C, Low S L, Zhou Z, Spicer R A, Ren L, Yang R, Tian Y, Wu M, Yang J, Liang S, Wappler T, Su T. 2022. Plant-insect and -fungal interactions in *Taxodium*-like wood fossils from the Oligocene of southwestern China. Rev Palaeobot Palynol, 302: 104669

Deng W, Su T, Wappler T, Liu J, Li S, Huang J, Tang H, Low S L, Wang T, Xu H, Xu X, Liu P, Zhou Z. 2020. Sharp changes in plant diversity and plant-herbivore interactions during the Eocene-Oligocene transition on the southeastern Qinghai-Tibetan Plateau. Glob Planet Change, 194: 103293

Deng W, Sun H, Zhang Y. 1999. Cenozoic K-Ar ages of volcanic rocks in the Nangqian Basin, Qinghai (in Chinese). Chin Sci Bull, 44: 2554–2558

Denk T, Tekleva M V. 2014. Pollen morphology and ultrastructure of *Quercus* with focus on Group Ilex (=*Quercus* subgenus *Heterobalanus* (Oerst.) Menitsky): Implications for oak systematics and evolution. Grana, 53: 255–282

Ding L, Kapp P, Cai F, Garzione C N, Xiong Z, Wang H, Wang C. 2022. Timing and mechanisms of Tibetan Plateau uplift. Nat Rev Earth Environ, 3: 652–667

Ding L, Kapp P, Wan X. 2005. Paleocene-Eocene record of ophiolite obduction and initial India-Asia collision, south central Tibet. Tectonics, 24: TC3001

Ding L, Li Z Y, Song P P. 2017a. Core fragments of Tibetan Plateau from Gondwanaland united in Northern Hemisphere (in Chinese). Proc Chin

Acad Sci, 32: 945–950

Ding L, Maksatbek S, Cai F L, Wang H Q, Song P P, Ji W Q, Xu Q, Zhang L Y, Muhammad Q, Upendra B. 2017b. Processes of initial collision and suturing between India and Asia. Sci China Earth Sci, 60: 635–651

Ding L, Qasim M, Jadoon I A K, Khan M A, Xu Q, Cai F, Wang H, Baral U, Yue Y. 2016. The India-Asia collision in north Pakistan: Insight from the U-Pb detrital zircon provenance of Cenozoic foreland basin. Earth Planet Sci Lett, 455: 49–61

Ding L, Spicer R A, Yang J, Xu Q, Cai F, Li S, Lai Q, Wang H, Spicer T E V, Yue Y, Shukla A, Srivastava G, Khan M A, Bera S, Mehrotra R. 2017c. Quantifying the rise of the Himalaya orogen and implications for the South Asian monsoon. Geology, 45: 215–218

Ding L, Zhou Y, Zhang J, Deng W. 2000. Geologic relationships and geochronology of the Cenozoic volcanoes and interbedded weathered mantles of Yulinshan in Qiangtang, North Tibet. Chin Sci Bull, 45: 2214–2220

Ding W N, Huang J, Su T, Xing Y W, Zhou Z K. 2018a. An early Oligocene occurrence of the palaeoendemic genus *Dipteronia* (Sapindaceae) from Southwest China. Rev Palaeobot Palynol, 249: 16–23

Ding W N, Kunzmann L, Su T, Huang J, Zhou Z K. 2018b. A new fossil species of *Cryptomeria* (Cupressaceae) from the Rupelian of the Lühe Basin, Yunnan, East Asia: Implications for palaeobiogeography and palaeoecology. Rev Palaeobot Palynol, 248: 41–51

Duan Q F, Zhang K X, Wang J X, Yao H Z, Bu J J. 2007. Sporopollen assemblage from the Totohe formation and its stratigraphic significance in the Tanggula Mountains, Northern Tibet (in Chinese). Earth Sci—J China Univ Geosci, 32: 629–637

Duan Q F, Zhang K X, Wang J X, Yao H Z, Niu Z J. 2008. Oligocene palynoflora, paleovegetation and paleoclimate in the Tanggula Mountains, nortnern Tibet (in Chinese). Acta Micropal Sin, 25: 185–195

Dupont-Nivet G, Hoorn C, Konert M. 2008. Tibetan uplift prior to the Eocene-Oligocene climate transition: Evidence from pollen analysis of the Xining Basin. Geology, 36: 987–990

Fan X P. 2018. The Paleogene foraminiferal biostratigraphy of the Keliyang section in the western Tarim Basin (in Chinese). Dissertation for Master's Degree. Beijing: China University of Geosciences. 1–72

Fang A M, Yan Z, Liu X H, Tao J R, Li J L, Pan Y S. 2005. The flora of the Liuqu Formation in south Tibet and its climatic implications (in Chinese). Acta Palaeontol Sin, 44: 435–445

Fang X M, Li J J, Zhu J J, Chen H L, Cao J X. 1997. Absolute age determination and subdivision of the Cenozoic stratigraphy in the Linxia Basin, Gansu (in Chinese). Chin Sci Bull, 42: 1457–1471

Fang X, Dupont-Nivet G, Wang C, Song C, Meng Q, Zhang W, Nie J, Zhang T, Mao Z, Chen Y. 2020. Revised chronology of central Tibet uplift (Lunpola Basin). Sci Adv, 6: eaba7298

Fang X, Fang Y, Zan J, Zhang W, Song C, Appel E, Meng Q, Miao Y, Dai S, Lu Y, Zhang T. 2019. Cenozoic magnetostratigraphy of the Xining Basin, NE Tibetan Plateau, and its constraints on paleontological, sedimentological and tectonomorphological evolution. Earth-Sci Rev, 190: 460–485

Fang X, Garzione C, Van der Voo R, Li J J, Fan M J. 2003. Flexural subsidence by 29 Ma on the NE edge of Tibet from the magnetostratigraphy of Linxia Basin, China. Earth Planet Sci Lett, 210: 545–560

Fang X, Wang J, Zhang W, Zan J, Song C, Yan M, Appel E, Zhang T, Wu F, Yang Y, Lu Y. 2016. Tectonosedimentary evolution model of an intracontinental flexural (foreland) basin for paleoclimatic research. Glob Planet Change, 145: 78–97

Fang X, Yan M, Zhang W, Nie J, Han W, Wu F, Song C, Zhang T, Zan J, Yang Y. 2021. Paleogeography control of Indian monsoon intensification and expansion at 41 Ma. Sci Bull, 66: 2320–2328

Feng Z, Zhang W, Fang X, Zan J, Zhang T, Song C, Yan M. 2022. Eocene deformation of the NE Tibetan Plateau: Indications from magnetostratigraphic constraints on the oldest sedimentary sequence in the Linxia Basin. Gondwana Res, 101: 77–93

Fu L K, Li N, Thomas S E. 1999. Flora of China vol.14. Missouri: Missouri Botanical Garden

Gandolfo M A, Hermsen E J, Zamaloa M C, Nixon K C, González C C,

Wilf P, Cúneo N R, Johnson K R. 2011. Oldest known *Eucalyptus* macrofossils are from South America. PLoS One, 6: e21084

Gao B T, Zhang Q H, Ding L, Zhang H J, Fang P Y. 2023. Age of the latest marine sedimentation in the western Kunlun area constrained by planktic foraminifera. Palaeoworld, 32: 490–508

Geng B Y, Tao J R, Xie G P. 2001. Early Tertiary fossil plants and paleoclimate of Lanzhou Basin (in Chinese). Acta Phytotax Sin, 39: 105–115

Gourbet L, Leloup P H, Paquette J L, Sorrel P, Maheo G, Wang G C, Yadong X, Cao K, Antoine P O, Eymard I, Liu W, Lu H, Replumaz A, Chevalier M L, Kexin Z, Jing W, Shen T. 2017. Reappraisal of the Jianchuan Cenozoic basin stratigraphy and its implications on the SE Tibetan plateau evolution. Tectonophysics, 700-701: 162–179

Greenwood D, Vadala A, Douglas J. 2000. Victorian Paleogene and Neogene macrofloras: A conspectus. Proc-R Soc Victoria, 112: 65–92

Guo S X, Chen J L. 1989. Cenozoic floras and coal-accumulating environment in Himalays and Hengduan Mountains areas (in Chinese). Acta Palaeontol Sin, 28: 512–521

Guo S X. 1986. An Eocene flora from the Relu Formation in Litang county of Sichuan and the history of *Eucalyptus*. In: Sun H, ed. Studies in Qinghai-Xizang (Tibet) Plateau special issue of Hengduan Mountains scientific expedition II. Beijng: Beijing Publishing House of Science and Technology. 66–70

Han F, Yang T, Zhang K, Hou Y, Song B. 2020. Early Oligocene *Podocarpium* (Leguminosae) from Qaidam Basin and its paleoecological and biogeographical implications. Rev Palaeobot Palynol, 282: 104309

Han Z, Sinclair H D, Li Y, Wang C, Tao Z, Qian X, Ning Z, Zhang J, Wen Y, Lin J, Zhang B, Xu M, Dai J, Zhou A, Liang H, Cao S. 2019. Internal drainage has sustained low-relief Tibetan landscapes since the early Miocene. Geophys Res Lett, 46: 8741–8752

Hanif M, Ali F, Afridi B Z. 2013. Depositional environment of the Patala Formation in biostratigraphic and sequence stratigraphic context from Kali Dilli Section, Kala Chitta Range, Pakistan. J Himal Earth Sci, 46: 55–65

Hanif M, Imraz M, Ali F, Haneef M, Saboor A, Iqbal S, Ahmad Jr S. 2014. The inner ramp facies of the Thanetian Lockhart Formation, western Salt Range, Indus Basin, Pakistan. Arab J Geosci, 7: 4911–4926

Hao Y C, Guo X P, Ye L S. 2001. The Boundary between the Marine Cretaceous and Tertiary in the Southwest Tarim Basin (in Chinese). Beijing: Geological Publishing House

Hao Y C, Wan X Q. 1985. The marine Cretaceous and Tertiary strata of Tingri, Xizang (Tibet). Contrib Geol Qinghai-Xizang (Tibet) Plateau, 17: 227–232

Hao Y C, Zeng X L, Li H M. 1982. Cretaceous–Paleogene stratigraphy and foraminifera of the western Tarim Basin (in Chinese). Earth Sci—J China Univ Geosci, 2: 1–161

Hao Y C, Zeng X L. 1984. On the evolution of the west Tarim Gulf from Mesozoic to Cenozoic in terms of characteritics of foraminiferal fauna (in Chinese). Acta Micropalaeontol Sin, 1: 1–18

He S Y, Tian Y H, Chen K G, Chen Q Y, Wen H C. 1983. Paleogene Gonjo Red Beds in east Xizang (Tibet) (in Chinese). Contrib Geol Qinghai-Xizang (Tibet) Plateau, 15: 233–242

He S, Ding L, Xiong Z, Spicer R A, Farnsworth A, Valdes P J, Wang C, Cai F, Wang H, Sun Y, Zeng D, Xie J, Yue Y, Zhao C, Song P, Wu C. 2022. A distinctive Eocene Asian monsoon and modern biodiversity resulted from the rise of eastern Tibet. Sci Bull, 67: 2245–2258

Hermsen E J, Gandolfo M A, Zamaloa M D C. 2012. The fossil record of *Eucalyptus* in Patagonia. Am J Bot, 99: 1356–1374

Hoorn C, Straathof J, Abels H A, Xu Y, Utescher T, Dupont-Nivet G. 2012. A late Eocene palynological record of climate change and Tibetan Plateau uplift (Xining Basin, China). Palaeogeogr Palaeoclimatol Palaeoecol, 344-345: 16–38

Horton B K, Yin A, Spurlin M S, Zhou J, Wang J. 2002. Paleocene-Eocene syncontractional sedimentation in narrow, lacustrine-dominated basins of east-central Tibet. GSA Bull, 114: 771–786

Hu X M, Li J, An W, Wang J G. 2017. The redefinition of Cretaceous-Paleogene lithostratigraphic units and tectonostratigraphic division in

southern Tibet (in Chinese). Earth Sci Front, 24: 174–194

Ji J, Zhang K, Clift P D, Zhuang G, Song B, Ke X, Xu Y. 2017. High-resolution magnetostratigraphic study of the Paleogene-Neogene strata in the Northern Qaidam Basin: Implications for the growth of the Northeastern Tibetan Plateau. Gondwana Res, 46: 141–155

Jia L, Su T, Huang Y J, Wu F X, Deng T, Zhou Z K. 2019. First fossil record of *Cedrelospermum* (Ulmaceae) from the Qinghai-Tibetan Plateau: Implications for morphological evolution and biogeography. J Sytematics Evol, 57: 94–104

Jiang G L, Yuan A H, Zhang K X. 2014. The ostracod fauna and its geological significance from the late Eocene Kangtuo Formation, Gaize Basin, southern Tibet Plateau, China (in Chinese). Acta Micropalaeontol Sin, 31: 405–419

Jiang H, Su T, Wong W O, Wu F, Huang J, Shi G. 2019. Oligocene *Koelreuteria* (Sapindaceae) from the Lunpola Basin in central Tibet and its implication for early diversification of the genus. J Asian Earth Sci, 175: 99–108

Jiang L, Deng B, Liu S G, Wang Z J, Zhou Z, Luo Q, He Y, Lai D. 2018. Differential uplift and fragmentation of Upper Yangtze Basin in Cenozoic. Earth Sci—J China Univ Geosci, 43: 1872–1886

Jiang T, Wan X, Aitchison J C, Xi D, Cao W. 2018. Foraminiferal response to the PETM recorded in the SW Tarim Basin, central Asia. Palaeogeogr Palaeoclimatol Palaeoecol, 506: 217–225

Jiang Z F, Cui X Z, Wu H, Zhuo J W. 2014. Detrital zircon LA-ICP-MS U-Pb ages of the Paleogene Leidashu Formation in Huili, Sichuan Province and their geological significance (in Chinese). Geol Bull China, 33: 788–803

Jin C, Liu Q, Liang W, Roberts A P, Sun J, Hu P, Zhao X, Su Y, Jiang Z, Liu Z, Duan Z, Yang H, Yuan S. 2018. Magnetostratigraphy of the Fenghuoshan Group in the Hoh Xil Basin and its tectonic implications for India-Eurasia collision and Tibetan Plateau deformation. Earth Planet Sci Lett, 486: 41–53

Kumar S, Hazra T, Spicer R A, Hazra M, Spicer T E V, Bera S, Khan M A. 2022. Coryphoid palms from the K-Pg boundary of central India and their biogeographical implications: Evidence from megafossil remains. Plant Diversity, 45: 80–97

Lakshami K, Sudheer Kumar M, Bhalla M, Rao G. 2000. Magnetostratigraphy of Himalayan sediments from Himachal Pradesh. J Indian Geophys U, 4: 147–154

Lan X, Wei J M. 1995. Late Cretaceous-Early Tertiary Marine Bivalve Fauna from the Western Tarim Basin (in Chinese). Beijing: Chinese Science Publishing House

Lease R O, Burbank D W, Hough B, Wang Z, Yuan D. 2012. Pulsed Miocene range growth in northeastern Tibet: Insights from Xunhua Basin magnetostratigraphy and provenance. GSA Bull, 124: 657–677

Li B Y, Yuan L S. 1990. Palynological assemblages of Fenghuoshan Group and its significance (in Chinese). Northwest Geology, 4: 7–9

Li C K, Qiu Z D, Wang S J. 1980. Discussion on Miocene stratigraphy and mammals from Xining Basin, Qinghai (in Chinese). Vertebr Palasiat, 18: 198–214

Li G B, Wang T Y, Li X F, Niu X L, Zhang W Y, Xie D, Li Y W, Yao Y J, Li Q, Ma X S, Li X P, Xiu D, Han Z C, Zhao S N, Han Y, Xue S, Reng R, Jia Z X. 2020. A review on marine Cretaceous Paleogene biostratigraphy of and major geological events in Tibet-Tethyan Himalaya (in Chinese). Earth Sci Front, 27: 144–164

Li H M. 2002. *Palibinia* from the Eocene of Jiangxi, China—With remarks on the dry climate mechanism of northern Hemisphere in Paleogene (in Chinese). Acta Palaeontol Sin, 41: 119–129

Li J G, Lin M, Wu Y, Luo H, Peng J, Mu L, Xu B, Zhang C. 2020. New biostratigraphic framework for the Triassic-Paleogene in the Neo-Tethys realm of southern Xizang (Tibet), China. J Asian Earth Sci, 202: 104369

Li J G, Peng J, Batten D J. 2015. Palynomorph assemblages from the Fenghuoshan Group, southern Qinghai, China: Their age and palaeoenvironmental significance. Sci Bull, 60: 470–476

Li J G, Wu Y, Batten D J, Lin M. 2019. Vegetation and climate of the central and northern Qinghai-Xizang Plateau from the Middle Jurassic

to the end of the Paleogene inferred from palynology. J Asian Earth Sci, 175: 35–48

Li J G. 2004. Discovery and prelminary study on palynofossils from the Cenozoic Qiuwu Formation of Xizang (Tibet) (in Chinese). Acta Micropalaeontol Sin, 21: 216–221

Li J G. 2015. A primary investigation on the palynoassemblages of the Cenozoic Yaxicuo and Wudaoliang Formations, Hoh Xil (in Chinese). Quat Sci, 35: 787–790

Li J G. 2021. Integrated biostratigraphy of Mesozoic and Paleogene strata in southern Xizang, China and some notes on regional stratigraphy (in Chinese). J Stratigr, 45: 493–505

Li J X, Yue L P, Roberts A P, Hirt A M, Pan F, Guo L, Xu Y, Xi R G, Guo L, Qiang X K, Gai C C, Jiang Z X, Sun Z M, Liu Q S. 2018. Global cooling and enhanced Eocene Asian mid-latitude interior aridity. Nat Commun, 9: 3026

Li L, Garzione C N, Pullen A, Zhang P, Li Y. 2018. Late Cretaceous-Cenozoic basin evolution and topographic growth of the Hoh Xil Basin, central Tibetan Plateau. GSA Bull, 130: 499–521

Li Q, Zhou X, Ni X, Fu B, Deng T. 2020. Latest Middle Miocene fauna and flora from Kumkol Basin of northern Qinghai-Xizang Plateau and paleoenvironment. Sci China Earth Sci, 63: 188–201

Li S, Su T, Spicer R A, Xu C, Sherlock S, Halton A, Hoke G, Tian Y, Zhang S, Zhou Z, Deng C, Zhu R. 2020a. Oligocene deformation of the Chuandian terrane in the SE margin of the Tibetan Plateau related to the extrusion of Indochina. Tectonics, 39: e2019TC005974

Li S, van Hinsbergen D J J, Najman Y, Liu-Zeng J, Deng C, Zhu R. 2020b. Does pulsed Tibetan deformation correlate with Indian plate motion changes? Earth Planet Sci Lett, 536: 116144

Li W C, Huang J, Chen L L, Spicer R A, Li S F, Liu J, Gao Y, Wu F X, Farnsworth A, Valdes P J, Zhou Z K, Su T. 2022. *Podocarpium* (Fabaceae) from the late Eocene of central Tibetan Plateau and its biogeographic implication. Rev Palaeobot Palynol, 305: 104745

Li X C, Manchester S R, Wang Q, Xiao L, Qi T L, Yao Y Z, Ren D, Yang Q. 2021. A unique record of *Cercis* from the late early Miocene of interior Asia and its significance for paleoenvironments and paleophytogeography. J Sytematics Evol, 59: 1321–1338

Li Y L, Wang C S, Zhu L D, Wang L C, Yang W G. 2010. Discovery of oil shale in the Nima basin, Tibet, China and its significance (in Chinese). Geol Bull China, 29: 1872–1874

Licht A, Dupont-Nivet G, Pullen A, Kapp P, Abels H A, Lai Z, Guo Z, Abell J, Giesler D. 2016. Resilience of the Asian atmospheric circulation shown by Paleogene dust provenance. Nat Commun, 7: 12390

Lin J, Dai J G, Zhuang G, Jia G, Zhang L, Ning Z, Li Y, Wang C. 2020. Late Eocene-Oligocene high relief paleotopography in the North Central Tibetan Plateau: Insights from detrital zircon U-Pb geochronology and leaf wax hydrogen isotope studies. Tectonics, 39: e2019TC005815

Linnemann U, Su T, Kunzmann L, Spicer R A, Ding W N, Spicer T E V, Zieger J, Hofmann M, Moraweck K, Gärtner A, Gerdes A, Marko L, Zhang S T, Li S F, Tang H, Huang J, Mulch A, Mosbrugger V, Zhou Z K. 2018. New U-Pb dates show a Paleogene origin for the modern Asian biodiversity hot spots. Geology, 46: 3–6

Liu J, Su T, Spicer R A, Tang H, Deng W Y D, Wu F X, Srivastava G, Spicer T, Van Do T, Deng T, Zhou Z K. 2019. Biotic interchange through lowlands of Tibetan Plateau suture zones during Paleogene. Palaeogeogr Palaeoclimatol Palaeoecol, 524: 33–40

Liu J, Wang T X, Zhang X W, Song A, Li S F, Huang J, Spicer T, Spicer R A, Wu F X, Su T, Zhou Z K. 2021. Snapshot of the Pliocene environment of West Kunlun region, Northwest China. Palaeobio Palaeoenv, 101: 163–176

Liu S. 2019. Study on palaeoenvironment restoration and tectonic evolution of late Paleogene in Luhe Basin, Nanhua County, Yunnan Province (in Chinese). Dissertation for Master's Degree. Kunming: Kunming University of Science and Technology. 1–152

Liu Z L, Fang J Y, Piao S L. 2002. Geographical distribution of species in genera *Abies*, *Picea* and *Larix* in China (in Chinese). Acta Geo Sin, 57: 577–586

Low S L, Su T, Spicer T E V, Wu F X, Deng T, Xing Y W, Zhou Z K.

2019. Oligocene *Limnobiophyllum* (Araceae) from the central Tibetan Plateau and its evolutionary and palaeoenvironmental implications. J Systat Palaeontol, 18: 415–431

Lu J F, Song B W, Chen R M, Zhang J Y, Ye H. 2010. Palynological assemblage of Eocene-Oligocene pollen and their biostratigraphic correlation in Dahonggou, Daqaidam Area, Qaidam Basin (in Chinese). Earth Sci—J China Univ Geosci, 35: 839–848

Lu Y, Kerrich R, Cawood P A, McCuaig T C, Hart C J R, Li Z, Hou Z, Bagas L. 2012. Zircon SHRIMP U-Pb geochronology of potassic felsic intrusions in western Yunnan, SW China: Constraints on the relationship of magmatism to the Jinsha suture. Gondwana Res, 22: 737–747

Luo M S, Zhang K X, Lin Q X, Zhang J X, Chen F N, Xu Y D, Chen R M. 2010. Cenozoic sedimentary paleogeography evolution of Xunhua-Hualong Area, Northwestern Qinghai-Tibetan Plateau (in Chinese). Geol Sci Tech Inform, 29: 23–31

Lyle M, Barron J, Bralower T J, Huber M, Olivarez Lyle A, Ravelo A C, Rea D K, Wilson P A. 2008. Pacific Ocean and Cenozoic evolution of climate. Rev Geophys, 46: 10.1029–2005RG000190

Lyson T R, Miller I M, Bercovici A D, Weissenburger K, Fuentes A J, Clyde W C, Hagadorn J W, Butrim M J, Johnson K R, Fleming R F, Barclay R S, Maccracken S A, Lloyd B, Wilson G P, Krause D W, Chester S G B. 2019. Exceptional continental record of biotic recovery after the Cretaceous-Paleogene mass extinction. Science, 366: 977–983

Ma C W, Ye Z Y, Cao Y, Wang C. 2021. Formation and evolution of Cenozoic basin in Ninglang of Yunnan Province (in Chinese). Geol Survey China, 8: 80–88

Ma H J, Zhang S T, Lin N, Cheng X F, Zhang L. 2016. LA-ICP-MS zircon U-Pb dating of the trachyte and its significance in Mangkang Basin, Tibet (in Chinese). Sci Technol Eng, 16: 9–14

Ma H J, Zhang S T, Su T, Wang L, Sui S G. 2012. New materials of *Equisetum* from the Upper Miocene of Mangkang, Eastern Xizang and its ecological implications (in Chinese). J Jilin Univ-Earth Sci Ed, 42: 189–195

Ma J Q. 1993. The Tertiary sporopollen assemblage in the Jiuquan Basin and the Palaeoenvironment (in Chinese). Experiment Petrol Geol, 15: 423–435

Ma P F, Wang L C, Ran B. 2013. Subsidence analysis of the Cenozoic Lunpola basin, central Qinghai-Tibetan Plateau (in Chinese). Acta Petrol Sin, 29: 990–1002

Ma X M. 2014. Study on Cenozoic Charophyta & Paleoecological Characteristics and Paleoclimatic Conditions in Dongping, Qaidam Basin (in Chinese). Dissertation for Master's Degree. Beijing: China University of Geosciences. 1–65

Ma Y Z, Li J J, Fang X M. 1998. Pollen assemblage in 30.6–5.0 Ma redbeds of Linxia region and climate evolution (in Chinese). Chin Sci Bull. 43: 301–304

Meng J, Coe R S, Wang C, Gilder S A, Zhao X, Liu H, Li Y, Ma P, Shi K, Li S. 2017. Reduced convergence within the Tibetan Plateau by 26 Ma? Geophys Res Lett, 44: 6624–6632

Miao Y F, Fang X M, Song Z C, Wu F L, Han W X, Dai S, Song C H. 2008. Late Eocene pollen records and palaeoenvironmental changes in northern Tibetan Plateau. Sci China Ser D-Earth Sci, 51: 1089–1098

Miao Y, Fang X, Sun J, Xiao W, Yang Y, Wang X, Farnsworth A, Huang K, Ren Y, Wu F, Qiao Q, Zhang W, Meng Q, Yan X, Zheng Z, Song C, Utescher T. 2022. A new biologic paleoaltimetry indicating Late Miocene rapid uplift of northern Tibet Plateau. Science, 378: 1074–1079

Miao Y, Wu F L, Chang H, Fang X M, Deng T, Sun J M, Jin C S. 2016. A Late-Eocene palynological record from the Hoh Xil Basin, northern Tibetan Plateau, and its implications for stratigraphic age, paleoclimate and paleoelevation. Gondwana Res, 31: 241–252

Miao Y, Wu F L, Herrmann M, Yan X L, Meng Q Q. 2013. Late early Oligocene East Asian summer monsoon in the NE Tibetan Plateau: Evidence from a palynological record from the Lanzhou Basin, China. J Asian Earth Sci, 75: 46–57

Molnar P, Tapponnier P. 1975. Cenozoic tectonics of Asia: Effects of a continental collision: Features of recent continental tectonics in Asia

can be interpreted as results of the India-Eurasia collision. Science, 189: 419–426

Najman Y, Carter A, Oliver G, Garzanti E. 2005. Provenance of Eocene foreland basin sediments, Nepal: Constraints to the timing and diachroneity of early Himalayan orogenesis. Geology, 33: 309–312

Najman Y, Pringle M, Godin L, Oliver G. 2001. Dating of the oldest continental sediments from the Himalayan foreland basin. Nature, 410: 194–197

Ni X, Li Q, Deng T, Zhang L, Gong H, Qin C, Shi J, Shi F, Fu S. 2023. New *Yuomys* rodents from southeastern Qinghai-Tibetan Plateau indicate low elevation during the Middle Eocene. Front Earth Sci, 10: 1018675

Ni X, Li Q, Li L, Beard K C. 2016. Oligocene primates from China reveal divergence between African and Asian primate evolution. Science, 352: 673–677

Ni X, Li Q, Zhang C, Samiullah K, Zhang L, Yang Y, Cao W. 2020. Paleogene mammalian fauna exchanges and the paleogeographic pattern in Asia. Sci China Earth Sci, 63: 202–211

Nie J, Ren X, Saylor J E, Su Q, Horton B K, Bush M A, Chen W, Pfaff K. 2020. Magnetic polarity stratigraphy, provenance, and paleoclimate analysis of Cenozoic strata in the Qaidam Basin, NE Tibetan Plateau. GSA Bull, 132: 310–320

Ojha T P, Butler R F, DeCelles P G, Quade J. 2009. Magnetic polarity stratigraphy of the Neogene foreland basin deposits of Nepal. Basin Res, 21: 61–90

Pole M. 1993. Early Miocene flora of the Manuherikia Group, New Zealand. 7. Myrtaceae, including *Eucalyptus*. J R Soc New Zealand, 23: 313–328

Pole M. 1994. An Eocene macroflora from the Taratu Formation at Livingstone, North Otago, New Zealand. Aust J Bot, 42: 341–367

Pradhan U M S, Sharma S R. 2003. Palynological study of pre-Siwalik sediments in Sub-Himalaya of central Nepal. J Nepal Geol Soc, 28: 63–67

Qiu Z D, Wang B Y, Li L. 2023. Middle Cenozoic micromammals from Linxia Basin, Gansu Province, China, and their implications for biostratigraphy and palaeoecology. Palaeogeogr Palaeoclimatol Palaeoecol, 616: 111467

Qiu Z X, Wang B Y, Deng T. 2004. Mammal fossils from Yagou, Linxia Basin, Gansu, and related stratigraphic problems (in Chinese). Vertebr Palasiat, 42: 276–296

Qiu Z X, Wang B Y. 1999. *Allacerops* (Rhinocerotoidea, Perissodactyla), its discovery in China and its systematic position (in Chinese). Vertebr Palasiat, 37: 48–61

Raup D M, Sepkoski Jr J J. 1982. Mass extinctions in the marine fossil record. Science, 215: 1501–1503

Rose K D, Holbrook L T, Rana R S, Kumar K, Jones K E, Ahrens H E, Missiaen P, Sahni A, Smith T. 2014. Early Eocene fossils suggest that the mammalian order Perissodactyla originated in India. Nat Commun, 5: 5570

Scher H D, Whittaker J M, Williams S E, Latimer J C, Kordesch W E C, Delaney M L. 2015. Onset of Antarctic circumpolar current 30 million years ago as Tasmanian Gateway aligned with westerlies. Nature, 523: 580–583

Shah S. 2009. Stratigraphy of Pakistan. Ministry of Petroleum and Natural Resources. Geological Survey of Pakistan

Shen L J. 2020. Sedimentary evolution of the Suonahu Formation in North Qiangtang Basin and its response to the uplift of Tibetan Plateau (in Chinese). Dissertation for Doctoral Degree. Chengdu: Chengdu University of Technology, 1–127

Shen Q Q, Cao K, Wang G C, Xu Y D, Zhang K X. 2017. Paleogene sedimentary and structural evolution of the Jianchuan-Lanping Basins, Western Yunnan and its regional tectonic implications (in Chinese). Geotect Metall, 41: 23–41

Shukla A, Mehrotra R C, Guleria J S. 2014. Palaeophytogeography of *Eucalyptus* L'H'erit: New fossil evidences. J Geol Soc India, 84: 693–700

Song A, Liu J, Liang S Q, Van Do T, Nguyen H B, Deng W Y D, Jia L B,

Del Rio C, Srivastava G, Feng Z, Zhou Z K, Huang J, Su T. 2022. Leaf fossils of *Sabalites* (Arecaceae) from the Oligocene of northern Vietnam and their paleoclimatic implications. Plant Diversity, 44: 406–416

Song B W, Liu Z Y, Wei Y, Ai K K, Xu Y D, Hou Y F, Zhang K X. 2019. Ostracod fauna from the Yaxicuo Formation in the Hoh Xil Basin, Qinghai Province and its strtigraphic significance (in Chinese). Acta Palaeontol Sin, 58: 388–401

Song B, Spicer R A, Zhang K, Ji J, Farnsworth A, Hughes A C, Yang Y, Han F, Xu Y, Spicer T, Shen T, Lunt D J, Shi G. 2020. Qaidam Basin leaf fossils show northeastern Tibet was high, wet and cool in the early Oligocene. Earth Planet Sci Lett, 537: 116175

Song C H. 2006. Tectonic uplift and Cenozoic sedimentary evolution in the northern margin of the Tibetan Plateau (in Chinese). Dissertation for Doctoral Degree. Lanzhou: Lanzhou University. 1–341

Song Z C, Li M Y, Li W B. 1976. Some Mesozoic and Early Tertiary spore-pollen assemblages from Yunnan, China. In: Nanjing Institute of Geology and Palaeontology, Chinese Academy of Sciences, eds. Fossils of Yunnan Mesozoic (Vol. I) (in Chinese). Beijing: Science Press. 1–64

Song Z C, Li M Y. 1982. Eocene palynological assemblage from Gonjo Formation in eastern Xizang. In: Survey Team of Sichuan Geological Bureau, Nanjing Insititute of Geology and Palaeontology, Academia Sinica, eds. Stratigraphy and Palaeontology of West Sichuan and East Xizang (II) (in Chinese). Chengdu: Sichuan People's Publishing House. 7–28

Song Z C, Li W B, He C Q. 1983. Cretaceous and Palaeogene palynofloras and distribution of organic (in Chinese). Sci Sin Ser-B, 13: 168–176

Song Z C, Liu G W. 1982. Early Tertiary palynoflora and its significance of palaeogeography from northern and eastern Xizang (in Chinese). In: Integrative Scientific Expedition Team to the Qinghai-Xizang plateau, Academia Sinica, ed. Palaeontology of Xizang. Book V. Beijing: Science Press. 165–190

Speijer R P, Pälike H, Hollis C J, Hooker J J, Ogg J G. 2020. Chapter 28—The Paleogene Period. In: Gradstein F M, Ogg J G, Schmitz M D, Ogg G M, eds. Geologic Time Scale 2020. Amsterdam: Elsevier. 1087–1140

Spicer R A, Su T, Valdes P J, Farnsworth A, Wu F X, Shi G, Spicer T E V, Zhou Z. 2021. Why 'the uplift of the Tibetan Plateau' is a myth. Natl Sci Rev, 8: Nwaa091

Srivastava G, Srivastava R, Mehrotra R C. 2011. *Ficus palaeoracemosa* sp. nov.—A new fossil leaf from the Kasauli Formation of Himachal Pradesh and its palaeoclimatic significance. J Earth Syst Sci, 120: 253–262

Srivastava P, Patel S, Singh N, Jamir T, Kumar N, Aruche M, Patel R C. 2013. Early Oligocene paleosols of the Dagshai Formation, India: A record of the oldest tropical weathering in the Himalayan foreland. Sediment Geol, 294: 142–156

Staisch L M, Niemi N A, Hong C, Clark M K, Rowley D B, Currie B. 2014. A Cretaceous-Eocene depositional age for the Fenghuoshan Group, Hoh Xil Basin: Implications for the tectonic evolution of the northern Tibet Plateau. Tectonics, 33: 281–301

Studnicki-Gizbert C, Burchfiel B C, Li Z, Chen Z. 2008. Early Tertiary Gonjo basin, eastern Tibet: Sedimentary and structural record of the early history of India-Asia collision. Geosphere, 4: 713–735

Su T, Farnsworth A, Spicer R A, Huang J, Wu F X, Liu J, Li S F, Xing Y W, Huang Y J, Deng W Y D, Tang H, Xu C L, Zhao F, Srivastava G, Valdes P J, Deng T, Zhou Z K. 2019a. No high Tibetan Plateau until the Neogene. Sci Adv, 5: eaav2189

Su T, Li S F, Tang H, Huang Y J, Li S H, Deng C L, Zhou Z K. 2018. *Hemitrapa* Miki (Lythraceae) from the earliest Oligocene of south-eastern Qinghai-Tibetan Plateau and its phytogeographic implications. Rev Palaeobot Palynol, 257: 57–63

Su T, Spicer R A, Li S H, Xu H, Huang J, Sherlock S, Huang Y J, Li S F, Wang L, Jia L B, Deng W Y D, Liu J, Deng C L, Zhang S T, Valdes P J, Zhou Z K. 2019b. Uplift, climate and biotic changes at the Eocene-Oligocene transition in south-eastern Tibet. Natl Sci Rev, 6: 495–504

Su T, Spicer R A, Wu F X, Farnsworth A, Huang J, Del Rio C, Deng T, Ding L, Deng W Y D, Huang Y J, Hughes A, Jia L B, Jin J H, Li S F, Liang S Q, Liu J, Liu X Y, Sherlock S, Spicer T, Srivastava G, Tang H, Valdes P, Wang T X, Widdowson M, Wu M X, Xing Y W, Xu C L,

Yang J, Zhang C, Zhang S T, Zhang X W, Zhao F, Zhou Z K. 2020. A Middle Eocene lowland humid subtropical "Shangri-La" ecosystem in central Tibet. Proc Natl Acad Sci USA, 117: 32989–32995

Su T, Wilf P, Xu H, Zhou Z K. 2014. Miocene leaves of *Elaeagnus* (Elaeagnaceae) from the Qinghai-Tibetan Plateau, its modern center of diversity and endemism. Am J Bot, 101: 1350–1361

Sun J, Windley B F, Zhang Z L, Fu B H, Li S H. 2016. Diachronous seawater retreat from the southwestern margin of the Tarim Basin in the late Eocene. J Asian Earth Sci, 116: 222–231

Sun J, Xu Q H, Liu W M, Zhang Z Q, Xue L, Zhao P. 2014. Palynological evidence for the latest Oligocene-early Miocene paleoelevation estimate in the Lunpola Basin, central Tibet. Palaeogeogr Palaeoclimatol Palaeoecol, 399: 21–30

Sun L, Deng C, Deng T, Kong Y, Wu B, Liu S, Li Q, Liu G. 2023. Magnetostratigraphy of the Oligocene and Miocene of the Linxia Basin, northwestern China. Palaeogeogr Palaeoclimatol Palaeoecol, 613: 111404

Sun X Y, Zhao Y N, He Z S. 1980. Characteristics of Late Cretaceous-Paleogene spore-pollen assemblages, stratigraphic age, paleovegetation, and Paleoclimate in the Xining-Minhe Basin (in Chinese). Experi Petrol Geol, 2: 44–52

Sun Z, Feng X, Li D, Yang F, Qu Y, Wang H. 1999. Cenozoic Ostracoda and palaeoenvironments of the northeastern Tarim Basin, western China. Palaeogeogr Palaeoclimatol Palaeoecol, 148: 37–50

Sun Z, Yang Z, Pei J, Ge X, Wang X, Yang T, Li W, Yuan S. 2005. Magnetostratigraphy of Paleogene sediments from northern Qaidam Basin, China: Implications for tectonic uplift and block rotation in northern Tibetan Plateau. Earth Planet Sci Lett, 237: 635–646

Tang H, Li S F, Su T, Spicer R A, Zhang S T, Li S H, Liu J, Lauretano V, Witkowski C R, Spicer T E V, Deng W Y D, Wu M X, Ding W N, Zhou Z K. 2020. Early Oligocene vegetation and climate of southwestern China inferred from palynology. Palaeogeogr Palaeoclimatol Palaeoecol, 560: 109988

Tang H, Liu J, Wu F X, Spicer T, Spicer R A, Deng W, Xu C L, Zhao F, Huang J, Li S F, Su T, Zhou Z K. 2019. Extinct genus *Lagokarpos* reveals a biogeographic connection between Tibet and other regions in the Northern Hemisphere during the Paleogene. J Sytematics Evol, 57: 670–677

Tang M Y. 2015. Reconstruction of the paleoelevation in the Gonjo basin in the southeastern Tibetan Plateau during the Paleocene-Eocene and its implications (in Chinese). Dissertation for Master's Degree. Beijing: Institute of Geology, China Earthquake Administration. 1–86

Tao J R, Du N Q. 1987. Miocene flora from Markam County and fossil record of Betulaceae (in Chinese). Acta Botan Sin, 29: 649–655

Tao J R. 1981. Succession of the floras in Xizang during Upper Cretaceous-Paleogene and Neogene (in Chinese). Acta Botan Sin, 23: 140–145

Tao J R. 1988. Plant fossils from Liuqu formation in Lhaze County, Xizang and their palaeoclimatological significances (in Chinese). Acad Sin Geol Inst Memoir, 3: 223–238

Thornhill A H, Crisp M D, Külheim C, Lam K E, Nelson L A, Yeates D K, Miller J T. 2019. A dated molecular perspective of eucalypt taxonomy, evolution and diversification. Aust Syst Bot, 32: 29–48

Thornhill A H, Macphail M. 2012. Fossil myrtaceous pollen as evidence for the evolutionary history of Myrtaceae: A review of fossil *Myrtaceidites* species. Rev Palaeobot Palynol, 176-177: 1–23

Tibet Autonomous Region Geological Survey Institute. 2003. Report of regional geological survey of Shiquan River area, 1: 250,000 (in Chinese)

Vermeij G J. 1991. When biotas meet: Understanding biotic interchange. Science, 253: 1099–1104

Wang B Y, Qiu Z X, Wang X M, Xie G P, Xie J Y, Qiu Z D, Deng T. 2003. Cenozoic stratigraphy in Danghe area, Gansu Province, and uplift of Tibetan Palteau (in Chinese). Vertebr Palasiat, 41: 66–75

Wang C, Dai J, Zhao X, Li Y, Graham S A, He D, Ran B, Meng J. 2014. Outward-growth of the Tibetan Plateau during the Cenozoic: A review. Tectonophysics, 621: 1–43

Wang D N, Sun X Y, Zhao Y N. 1986. Palnoflora from late Cretaceous to

Tertiary in Qinghai and Xinjiang (in Chinese). Bull Chin Acad of Geol Sci, 15: 152–165

Wang J X, Niu Z J, Tang Z Y, Bai Y S, Duan Q F. 2003. Palaeogene bivalve fossils form Meidutang area, the source of Yangtze River (in Chinese). Geol Bull China, 22: 216–217

Wang J, Zeng S Q, Fu X G, Chen W B, Dai J, Ren J. 2019. New evidence for deposition age of the Suonahu Formation in the Qiangtang Basin (in Chinese). Geol Bull China, 38: 1256–1258

Wang L, Yuan Q, Shen L, Ding L. 2022. Middle Eocene paleoenvironmental reconstruction in the Gonjo Basin, eastern Tibetan Plateau: Evidence from palynological and evaporite records. Front Earth Sci, 10: 818418

Wang N, Wu F X. 2015. New Oligocene cyprinid in the central Tibetan Plateau documents the pre-uplift tropical lowlands. Ichthyol Res, 62: 274–285

Wang Q W, Kan Z Z, Liang B, Zeng Y J. 2006. Stratigraphic division and correlation of the continental Meso-Cenozoic Group in Ya'an, west Sichuan Basin (in Chinese). Acta Geo Sichuan, 26: 65–69

Wang S B, Jiang F C, Tian G Q, Fu J L, Li C Z. 2020. New insights into Neogene stratigraphic age in the Jianchuan Basin, northwest Yunnan and its tectonic significance (in Chinese). Quat Sci, 40: 28–39

Wang T X, Del R C, Manchester S R, Liu J, Wu F X, Deng W Y D, Su T, Zhou Z K. 2021. Fossil fruits of *Illigera* (Hernandiaceae) from the Eocene of central Tibetan Plateau. J Sytematics Evol, 59: 1276–1286

Wang W, Zhang P, Garzione C N, Liu C, Zhang Z, Pang J, Wang Y, Zheng D, Zheng W, Zhang H. 2022. Pulsed rise and growth of the Tibetan Plateau to its northern margin since ca. 30 Ma. Proc Natl Acad Sci USA, 119: e2120364119

Wang X H. 2022. Magnetic stratigraphy and tectonic evolution of Cenozoic Seru formation in Leiwuqi area, Eastern Tibet (in Chinese). Dissertation for Master's Degree. Lanzhou: Lanzhou University. 1–76

Wang X, Qiu Z D, Li Q, Wang B Y, Qiu Z X, Downs W R, Xie G P, Xie J Y, Deng T, Takeuchi G T, Tseng Z J, Chang M, Liu J, Wang Y, Biasatti D, Sun Z C, Fang X M, Meng Q Q. 2007. Vertebrate paleontology, biostratigraphy, geochronology, and paleoenvironment of Qaidam Basin in northern Tibetan Plateau. Palaeogeogr Palaeoclimatol Palaeoecol, 254: 363–385

Wang Y Q, Li Q, Bai B, Jin X, Mao F, Meng J. 2019. Paleogene integrative stratigraphy and timescale of China. Sci China Earth Sci, 62: 287–309

Wang Y Q, Li Q, Bai B, Zhang Z Q, Xu R C, Wang X Y, Zhang X Y. 2021. Lithostratigraphic subdivision and correlation of the Paleogene in China (in Chinese). J Stratigr, 45: 402–425

Wei L J, Liu X H, Yan F H, Mai X S, Li G W, Liu X B, Zhou X J. 2011. Palynological evidence sheds new light on the age of the Liuqu Conglomerates in Tibet and its geological significance. Sci China Earth Sci, 54: 901–911

Wei M. 1985. Eocene ostracods from Nangqen in Qinghai (in Chinese). Contrib Geol Qinghai-Xizang (Tibet) Plateau, 17: 313–325

Wei Y F, Luo S L. 2005. The discovery of the Eocene sporomorphs in the Sharmu Basin, Serxu, western Sichuan (in Chinese). Sediment Geol Tethyan Geol, 25: 42–45

Wei Y, Zhang K, Garzione C N, Xu Y, Song B, Ji J. 2016. Low palaeoelevation of the northern Lhasa terrane during late Eocene: Fossil foraminifera and stable isotope evidence from the Gerze Basin. Sci Rep, 6: 27508

Westerhold T, Marwan N, Drury A J, Liebrand D, Agnini C, Anagnostou E, Barnet J S K, Bohaty S M, De Vleeschouwer D, Florindo F, Frederichs T, Hodell D A, Holbourn A E, Kroon D, Lauretano V, Littler K, Lourens L J, Lyle M, Pälike H, Röhl U, Tian J, Wilkens R H, Wilson P A, Zachos J C. 2020. An astronomically dated record of Earth's climate and its predictability over the last 66 million years. Science, 369: 1383–1387

Wheeler E A, Srivastava R, Manchester S R, Baas P, Wiemann M. 2017. Surprisingly modern Latest Cretaceous-earliest Paleocene woods of India. IAWA J, 38: 456–542

Wilf P, Nixon K C, Gandolfo M A, Cúneo N R. 2019. Eocene Fagaceae from Patagonia and Gondwanan legacy in Asian rainforests. Science,

364: eaaw5139

Writing Group of Cenozoic Plant of China. 1978. Fossil Plants of China. Vol. 3: Cenozoic Plants from China (in Chinese). Beijing: Science Press

Wu F, Fang X, Yang Y, Dupont-Nivet G, Nie J, Fluteau F, Zhang T, Han W. 2022. Reorganization of Asian climate in relation to Tibetan Plateau uplift. Nat Rev Earth Environ, 3: 684–700

Wu F, Miao D, Chang M-m, Shi G, Wang N. 2017. Fossil climbing perch and associated plant megafossils indicate a warm and wet central Tibet during the late Oligocene. Sci Rep, 7: 878

Wu F, Miao Y, Meng Q, Fang X, Sun J. 2019. Late Oligocene Tibetan Plateau warming and humidity: Evidence from a sporopollen record. Geochem Geophys Geosyst, 20: 434–441

Wu M X, Huang J, Manchester S R, Tang H, Gao Y, Wang T, Zhou Z, Su T. 2023. A new fossil record of *Palaeosinomenium* (Menispermaceae) from the Upper Eocene in the southeastern margin of the Tibetan Plateau and its biogeographic and paleoenvironmental implications. Rev Palaeobot Palynol, 310: 104827

Wu M X, Huang J, Spicer R A, Li S, Zhao J, Deng W, Ding W, Tang H, Xing Y, Tian Y, Zhou Z, Su T. 2022. The early Oligocene establishment of modern topography and plant diversity on the southeastern margin of the Tibetan Plateau. Glob Planet Change, 214: 103856

Wu M X, Huang J, Su T, Leng Q, Zhou Z K. 2020. *Tsuga* seed cones from the late Paleogene of southwestern China and their biogeographical and paleoenvironmental implications. Palaeoworld, 29: 617–628

Wu M X, Huang J, Su T, Zhou Z K, Xing Y W. 2021. *Fraxinus* L. (Oleaceae) fruits from the early Oligocene of Southwest China and their biogeographic implications. Fossil Imprint, 77: 287–298

Wu Z Y, Milne R I, Liu J, Nathan R, Corlett R T, Li D Z. 2022. The establishment of plants following long-distance dispersal. Trends Ecol Evol, 38: 289–300

Xi D P, Tang Z H, Wang X J, Qin Z H, Cao W X, Jiang Q, Wu B X, Li Y H, Zhang Y Y, Jiang W B, Kamran M, Fang X M, Wan X Q. 2020. The Cretaceous Paleogene marine stratigraphic framework that records significant geological events in the western Tarim Basin (in Chinese). Earth Sci Front, 27: 165–198

Xi D, Cao W, Cheng Y, Jiang T, Jia J, Li Y, Wan X. 2016. Late Cretaceous biostratigraphy and sea-level change in the southwest Tarim Basin. Palaeogeogr Palaeoclimatol Palaeoecol, 441: 516–527

Xia W G. 1982. Ostracoda fauna from Lunpola group in Xizang (Tibet) and its geological age. In: Chinese Geology Bureau Tibetan Plateau Proceeding Editorial Committee, ed. (in Chinese). Contribution to the Geology of the Qinghai-Xizang (Tibet) Plateau, 4: 149–207

Xia W G. 1986. Charophytes from the Lunpola group in Bangor County, Tibet. In: Chengdu Institute of Geology and Mineral Resources, ed. Bulletin of the Chengdu Institute of Geology and Mineral Resources, Chinese Academy of Geological Sciences (Vol. 7) (in Chinese). Beijing: Geological Publishing House. 64–71

Xiang X G, Cao M, Zhou Z K. 2006. Fossil history and modern distribution of the genus *Abies* (Pinaceae) (in Chinese). Acta Botan Yunnan, 28: 439–452

Xiao A F, Li D M, Zhang H J, Li X L. 2003. Climate evolution and compositional features of sporopollen in the Oligocene-Pliocene series of the Kumukuli Basin in Xinjiang (in Chinese). Geol Shaanxi, 21: 36–44

Xiao R, Zheng Y, Liu X, Yang Q, Liu G, Xia L, Bian Z, Guan J, Feng P, Xu H, Clift P D, Qiang X, Zhang Y, Zheng H. 2021. Synchronous sedimentation in Gonjo Basin, Southeast Tibet in response to India-Asia collision constrained by magnetostratigraphy. Geochem Geophys Geosyst, 22: e2020GC009411

Xie G P. 2004. The Teritiary and local mammalian faunas in Lanzhou Basin, Gansu (in Chinese). J Stratigr, 28: 67–80

Xie G, Li J F, Wang S Q, Yao Y F, Sun B, Ferguson D K, Li C S, Deng T, Liu X D, Wang Y F. 2021a. Bridging the knowledge gap on the evolution of the Asian monsoon during 26–16 Ma. Innovation, 2: 100110

Xie G, Sun B, Li J F, Wang S Q, Yao Y F, Li M, Zhang X C, Ferguson D K, Li C S, Liu X D, Deng T, Wang Y F. 2021b. Fossil evidence reveals uplift of the central Tibetan Plateau and differentiated ecosystems during the Late Oligocene. Sci Bull, 66: 1164–1167

Xinjiang Uygur Autonomous Region Regional Stratigraphic Compilation Group. 1981. Regional Stratigraphic Chart of Northwest China: Xinjiang Uygur Autonomous Region Volume (in Chinese). Beijing: Geological Publishing House. 1–496

Xiong X. 2019. Paleogene bivalves biostratigraphy and paleoecological environment in Western Tarim basin: evidence from Smhana and Bashbulak sections. Dissertation for Master's Degree (in Chinese). Beijing: China University of Geosciences. 1–73

Xiong Z, Ding L, Spicer R A, Farnsworth A, Wang X, Valdes P J, Su T, Zhang Q, Zhang L, Cai F, Wang H, Li Z, Song P, Guo X, Yue Y. 2020. The early Eocene rise of the Gonjo Basin, SE Tibet: From low desert to high forest. Earth Planet Sci Lett, 543: 116312

Xiong Z, Liu X, Ding L, Farnsworth A, Spicer R A, Xu Q, Valdes P, He S, Zeng D, Wang C, Li Z, Guo X, Su T, Zhao C, Wang H, Yue Y. 2022. The rise and demise of the Paleogene Central Tibetan Valley. Sci Adv, 8: eabj0944

Xu C, Su T, Huang J, Huang Y, Li S, Zhao Y, Zhou Z. 2019. Occurrence of *Christella* (Thelypteridaceae) in Southwest China and its indications of the paleoenvironment of the Qinghai-Tibetan Plateau and adjacent areas. J Sytematics Evol, 57: 169–179

Xu H, Su T, Zhang S T, Deng M, Zhou Z K. 2016. The first fossil record of ring-cupped oak (*Quercus* L. subgenus *Cyclobalanopsis* (Oersted) Schneider) in Tibet and its paleoenvironmental implications. Palaeogeogr Palaeoclimatol Palaeoecol, 442: 61–71

Xu H, Su T, Zhou Z. 2019. Leaf and infructescence fossils of *Alnus* (Betulaceae) from the late Eocene of the southeastern Qinghai-Tibetan Plateau. J Sytematics Evol, 57: 105–113

Xu Q, Ding L, Spicer R A, Liu X, Li S, Wang H. 2018. Stable isotopes reveal southward growth of the Himalayan-Tibetan Plateau since the Paleocene. Gondwana Res, 54: 50–61

Xu Q Q, Qiu J, Zhou Z K, Jin J H. 2015. Eocene *Podocarpium* (Leguminosae) from South China and its biogeographic implications. Front Plant Sci, 6: 938

Xu X T, Szwedo J, Huang D Y, Deng W Y D, Obroślak M, Wu F X, Su T. 2022. A new genus of *Spittlebugs* (Hemiptera, Cercopidae) from the Eocene of Central Tibetan Plateau. Insects, 13: 770

Xu Z L. 2015. Oligocene-Miocene pollen records in Xunhua Basin, northern Tibetan Plateau and its implications for evolution of the East Asian monsoon. Dissertation for Doctoral Degree (in Chinese). Wuhan: China University of Geosciences, 1–125

Yan D F, Zhang L, Han L, Yang T, Chen Y Q. 2018. *Podocarpium* from the Oligocene of NW Qaidam Basin, China and its implications. Rev Palaeobot Palynol, 259: 1–9

Yan M, Zhang D, Fang X, Zhang W, Song C, Liu C, Zan J, Shen M. 2021. New insights on the age of the Mengyejing Formation in the Simao Basin, SE Tethyan domain and its geological implications. Sci China Earth Sci, 64: 231–252

Yang G L, Wang Z X, Chen J W, Yan D F, Sun B N. 2016. *Equisetum* cf. *oppositum* (Equisetaceae) from the Paleocene-Eocene of Tibet in southwestern China and its paleoenvironmental implications. Arab J Geosci, 9: 749

Yang H, Jiang X, Lin S. 1995. Late Cretaceous-Early Tertiary Ostracod: Fauna from Western Tarim Basin, S. Xinjiang, China (in Chinese). Beijing: Science Press

Yang T, Jia J, Chen H, Zhang Y, Wang Y, Wang H, Bao L, Zhang L, Li W, Xie S, Yan D. 2021a. Oligocene *Ailanthus* from northwestern Qaidam Basin, northern Tibetan Plateau, China and its implications. Geol J, 56: 616–627

Yang T, Liang W, Cai J, Gu H, Han L, Chen H, Wang H, Bao L, Yan D. 2021b. A new cyprinid from the Oligocene of Qaidam Basin, northeastern Tibetan Plateau, and its implications. J Systat Palaeontol, 19: 1161–1182

Yong T S, Shan J B, Wei J M. 1989. Lithofacies and Paleogeography of the Tarim Paleobay in the Northern Branch of Paleo-Tethys Sea (in Chinese). Beijing: Science Press

Yuan Q, Barbolini N, Rydin C, Gao D L, Wei H C, Fan Q S, Qin Z J, Du Y S, Shan J J, Shan F S, Vajda V. 2020. Aridification signatures from fossil pollen indicate a drying climate in east-central Tibet during the late Eocene. Clim Past, 16: 2255–2273

Yue L, Heller F, Qiu Z, Zhang L, Xie G, Qiu Z, Zhang Y. 2001. Magnetostratigraphy and pavleo-environmental record of Tertiary deposits of Lanzhou Basin. Chin Sci Bull, 46: 770–773

Yue L, Mou S Y, Zeng C X, Yi C X. 2006. Age of the Kangtog Formation in the Dinggo-Gyaco area, Qiangtang, northern Tibet, China (in Chinese). Geol Bull China, 25: 229–232

Zamaloa M C, Gandolfo M A, Nixon K C. 2020. 52 million years old *Eucalyptus* flower sheds more than pollen grains. Am J Bot, 107: 1763–1771

Zhang H, He H, Wang J, Xie G. 2005. $^{40}Ar/^{39}Ar$ chronology and geochemistry of high-K volcanic rocks in the Mangkang basin, Tibet. Sci China Ser D-Earth Sci, 48: 1–12

Zhang K X, Wang G C, Ji J L, Luo M S, Kou X H, Wang Y M, Xu Y D, Chen F N, Chen R M, Song B W, Zhang J Y, Liang Y P. 2010. Paleogene-Neogene stratigraphic realm and sedimentary sequence of the Qinghai-Tibetan Plateau and their response to uplift of the plateau. Sci China Earth Sci, 53: 1271–1294

Zhang P, Ao H, Dekkers M J, An Z, Wang L, Li Y, Liu S, Qiang X, Chang H, Zhao H. 2018. Magnetochronology of the Oligocene mammalian faunas in the Lanzhou Basin, Northwest China. J Asian Earth Sci, 159: 24–33

Zhang P, Ao H, Dekkers M J, Li Y, An Z. 2016. Late Oligocene-Early Miocene magnetochronology of the mammalian faunas in the Lanzhou Basin-environmental changes in the NE margin of the Tibetan Plateau. Sci Rep, 6: 38023

Zhang Q. 2017. The sea retreat from the west Tarim Basin: Evidence from Late Eocene to early Oligocene ostracod form the Bashibulake Section (in Chinese). Dissertation for Master's Degree. Beijing: China University of Geosciences. 1–78

Zhang Q. 2021. Framework of Cenozoic in the Qaidam Basin—Based on Cyclostratigraphy (in Chinese). Dissertation for Master's Degree. Xian: Northwest University. 1–73

Zhang S, Hu X, Han Z, Li J, Garzanti E. 2018. Climatic and tectonic controls on Cretaceous-Palaeogene sea-level changes recorded in the Tarim epicontinental sea. Palaeogeogr Palaeoclimatol Palaeoecol, 501: 92–110

Zhang W, Fang X, Zhang T, Song C, Yan M. 2020. Eocene rotation of the northeastern central Tibetan Plateau indicating stepwise compressions and eastward extrusions. Geophys Res Lett, 47: e2020GL088989

Zhang X, Gélin U, Spicer R A, Wu F, Farnsworth A, Chen P, Del Rio C, Li S, Liu J, Huang J, Spicer T E V, Tomlinson K W, Valdes P J, Xu X, Zhang S, Deng T, Zhou Z, Su T. 2022. Rapid Eocene diversification of spiny plants in subtropical woodlands of central Tibet. Nat Commun, 13: 3787

Zhang Y X, Che Z C, Liu L, Luo J L. 1996. Tertiary in the Kumkol Basin, Xinjiang (in Chinese). Regional Geol China, 4: 311–316

Zhang Y Y, Li J G. 2000. The Tertiary Chronostratigraphic Researches and Tertiary Chronostratigraphic Chart of China (in Chinese). J Stratigr, 24: 120–125

Zhang Y Z, Wang G C, Wang A, Zhang K X. 2013. Coupling Processes of Xunhua-Hualong Basin-Orogenic Belt Since Late Cretaceous: Evidence from Apatite Fision Track Geochronology and Source Analysis (in Chinese). Earth Sci—J China Univ Geosci, 38: 725–744

Zhao H. 2011. Study on Sdimentary System and Sequence Stratigraphy of Early Teriary-Late Teriary in Kuche Depression, Tarim Basin (in Chinese). Dissertation for Master's Degree. Chengdu: Chengdu University of Technology, 1–92

Zhao Z, Wu Z H, Yang Y Z, Ji C J. 2020. Establishing the chronostratigraphic framework of the continental red beds in Central Qiangtang Basin: Constrained by zircon U-Pb ages (in Chinese). Geol Rev, 66: 1155–1171

Zheng H, Yang Q, Cao S, Clift P D, He M, Kano A, Sakuma A, Xu H, Tada R, Jourdan F. 2022. From desert to monsoon: irreversible climatic transition at ~36 Ma in southeastern Tibetan Plateau. Progr Earth Planet Sci, 9: 1–4

Zheng Y, Qiu Z, Qiu Z, Li L, Wei X, Zhang R, Yue L, Deng T. 2023. Revised magnetostratigraphy of the Linxia Basin in the northeast Tibetan Plateau, constrained by micromammalian fossils. Palaeogeogr Palaeoclimatol Palaeoecol, 623: 111620

Zhou K K. 2007. The lacustrine carbonates in the Cenozoic Hoh Xil Basin and paleoenvironment change (in Chinese). Dissertation for Master's Degree. Chengdu: Chengdu University of Technology.1–97

Zhou Z K, Liu J, Chen L L, Spicer R A, Li S F, Huang J, Zhang S T, Huang Y J, Jia L B, Hu J J, Su T. 2023. Cenozoic plants from Tibet: An extraordinary decade of discovery, understanding and implications. Sci China Earth Sci, 66: 205–226

Zhou Z K, Wang T X, Huang J, Liu J, Deng W Y D, Li S H, Deng C L, Su T. 2020. Fossil leaves of *Berhamniphyllum* (Rhamnaceae) from Markam, Tibet and their biogeographic implications. Sci China Earth Sci, 63: 224–234

Zhou Z K. 1996. Studies on *Dryophyllum* complex from China and its geological and systematic implications (in Chinese). Acta Botan Sin, 38: 666–671

Zhu C Y. 2022. Cenozoic southeastern progressive growth of Sichuan-Yunnan block, southeastern Tibet Plateau: Constraint from structure analysis and low-temperature thermochronology (in Chinese). Dissertation for Doctoral Degree. Wuhan: China University of Geosciences. 1–125

Zhu Z J, Jiang Y B, Guo F S, Hou Z Q, Yang T N, Xue C D. 2011. Palaeogene sedimentary facies types and sedimentary environment evolution in Lanping basin (in Chinese). Acta Petrol Mineral, 30: 409–418

Zong G F, Chen W Y, Huang X S. 1996. Cenozoic Mammals and Environment of Hengduan Mountains Region (in Chinese). Beijing: Ocean Press

Zong G F. 1987. Note on some mammalian fossils of Yunnan, Sichuan (in Chinese). Vertebr Palasiat, 25: 137–145

(Editorial handling: Tao DENG)